Mathematical and numerical analysis of the wrinkling of graphene

Laila Taourirte

Thèse de Doctorat

Mention Mathématiques

Présentée à ***l'Ecole Doctorale en Sciences Technologie et Santé (ED 585)*** **de**
l'Université de Picardie Jules Verne
et
à la Faculté des Sciences et Techniques
de l'Université Cadi Ayyad - Marrakech

par

Laila TAOURIRTE

Pour obtenir le grade de Docteur de l'Université de Picardie Jules Verne

Mathematical and Numerical Analysis of the Wrinkling of Graphene

Soutenue le 19 décembre 2020, après avis des rapporteurs, devant le jury d'examen :

M. A. H, Bentbib, Professeur, Université Cadi Ayyad	**Président**
M. M, Grinfeld, Professeur, Université de Strathclyde	**Rapporteur**
M. M, Pierre, Maître de Conférences HDR, Université de Poitiers	**Rapporteur**
M. M, Asch, Professeur, Université de Picardie Jules Verne	**Examinateur**
M. D, Meskine, Professeur, Université Cadi Ayyad	**Examinateur**
M. C, Misbah, Directeur de Recherche, CNRS Grenoble	**Examinateur**
M. M, Guedda, Professeur, Université de Picardie Jules Verne	**Directeur de thèse**
M. N, Alaa, Professeur, Université Cadi Ayyad	**Co-directeur**

Acknowledgments

First and foremost, praises and thanks to Allah, for his help and blessings throughout the research work to complete my thesis successfully.

I would like to express my deep and sincere gratitude to my two research supervisors, Professor Nour Eddine Alaa, of University Cadi Ayyad and Professor Mohammed Guedda of University Picardie Jules Verne (Amiens, France), for giving me the opportunity to do research and providing continuous support and guidance throughout all these years of research. Their dynamism, vision and motivation have deeply inspired me. They have taught me the methodology to carry out the research and to present the results as clearly and pertinent as possible. It was a great privilege to study under their guidance.

I am extending my thanks to the rest of my thesis committee: Pr. Abdeslam Bentbib, Pr. Morgan Pierre, Pr. Michael Grinfeld, Pr. Driss Meskine, Pr. Chaouqi Misbah and Pr. Mark Asch, for generously offering their time, support and good will throughout the preparation and the review of this document.

Part of my thesis was carried out during my stay at the laboratory of Fundamental and Applied mathematics of Amiens (LAMFA), as part of my cotutelle thesis between Marrakesh and Amiens (France). It was a very enriching experience on the scientific and the human level. On this occasion, i would like to thank the International Affairs Department (DAI) of the Picardie Jules Verne University for making my stay in good conditions easier.

My thesis was also able to benefit from the financial support of the French-German University programme ÓLiving FluidsÓ (grant CFDA-Q1-14), managed by Pr. Christian Wagner and Pr. Chaouqi Misbah. I thank them very warmly.

I would also like to thank Pr. Misbah for his hostage in the interdisciplinary laboratory LIPHY in Grenoble. I really enjoyed my visit to this laboratory where I met an amazing and available team .
During my stay in France, I also had the opportunity to work with Pr. Gabriella Bognár, Pr. Robert Kersner and Pr. Krisztián Hriczó in the French-Hungarian Scientific Cooperation Project PHC-Balaton (grant 41897UF), managed by Pr. Guedda and Pr. Bognár.

Last but certainly not least, I am extremely grateful to my parents for their unconditional love, prayers, caring and sacrifices for educating and preparing me for my future. I would never be where I am today without them. I am very thankful to all my other special family members for their love, understanding, patience, prayers and continuous support to complete my dissertation. I can never thank them enough. This book is dedicated to them.
My thanks also go to my colleagues and friends either in Morocco or in France, for all the help they might have provided and especially the fun moments we shared during these last years. I wish the best of luck to each one of them.

Contents

List of Figures

List of Algorithms

0.1 Résumé Substantiel

Cette thèse s'inscrit dans le vaste champ multidisciplinaire de recherche réunissant la science de couches minces, l'analyse mathématique et le calcul scientifique des équations aux dérivées partielles non linéaires. L'objectif est de développer des méthodes mathématiques et numériques nouvelles qui permettent d'apporter des explications et de comprendre la dynamique des nanostructures et leur autoorganisation sur des surfaces de films minces. La morphologie d'une surface correspond à des réarrangements qui abaissent l'énergie totale du système, mais augmentent l'énergie de déformation élastique. Pour relaxer l'énergie correspondante, le film a la possibilité de modifier la forme de sa surface libre, de façon à se placer dans une configuration d'énergie plus favorable.

Ces phénomènes de déformation sont observés dans la vie de tous les jours à toutes les échelles, allant de la déformation à micro-échelle (rides sur la peau humaine) à la déformation à macro-échelle (formations de crêtes de montagne). Ils ont été et restent un défi pour différentes disciplines. En effet, la nature est très élégante. Ses formes sont à la fois fonctionnelles et esthétiques. En regardant profondément dans la nature, de nombreuses théories ont été apportées à l'architecture et au design. L'une des formes naturelles les plus fascinantes est la forme caténaire ou chaînette. La caténaire est la courbe obtenue lorsqu'une chaîne de densité uniforme est suspendue entre deux points. Cette forme se produit naturellement dans un œuf ou les fils suspendus d'une toile d'araignée. En effet, l'architecte finno-américain Eero Saarinen a adopté cette forme dans l'emblématique Gateway Arch de Saint-Louis en 1963, représentée sur la Figure 2 . Un autre architecte qui a étudié et incorporé la forme caténaire dans son travail est le célèbre architecte catalan Antoni Gaudi. Son bâtiment Casa Mila à Barcelone, Espagne (voir Figure 3) était le modèle répétitif de la caténaire inversée.

En fait, le problème de la chaînette et de l'arc est l'un des problèmes les plus anciens qui a été résolu en utilisant le calcul des variations. La question était de trouver la forme exacte d'une chaînette suspendue ou un cordon flexible. Galileo (1602) a été le premier à poser le problème. Ne pas avoir les bons outils mathématiques (calcul de variation), Galilée a répondu à tort que la courbe résultante était une parabole. Pour les arcs, c'est Robert Hooke (1675) qui fait le lien entre la forme idéale d'un arc et celle d'une chaîne suspendue. La géométrie d'un arc est considérée comme un miroir de celle d'une chaîne suspendue. C'est probablement l'une des (les plus anciennes) raisons pour lesquelles les termes utilisés

pour décrire le populaire St. Louis Gateway Arch sont souvent une caténaire ou une parabole.

A l'échelle nanométrique, différentes morphologies ou déformations, y compris chaînette et arc, sont obtenues et/ou observées dans des surfaces élastiques minces. Ce problème, qui a une longue histoire, est un sujet classique de la mécanique des milieux continus. La question a été étudiée sous différents points de vue et différents types de déformations ou d'instabilités de surface et une possible transition continue / discontinue entre elles ont été prédites (conditions critiques). La plupart des déformations (délamination-flambage, plissement, fissuration ou fracture, ...) sont considérées comme des minimiseurs (locaux) d'une énergie élastique appropriée. Cependant, en raison de la complexité des équations (équations aux dérivées partielles du quatrième ordre, couche mince, conditions aux frontières libres, ...) qui décrivent les morphologies de surface, des preuves rigoureuses sont dans la plupart des cas difficiles à réaliser, et comme des solutions explicites sont difficiles à obtenir sauf dans certains cas, les traitements numériques sont souvent inévitables.

On sait depuis longtemps que l'instabilité d'une couche mince élastique peut se manifester par la formation des arêtes étroites. En particulier, les lois d'échelle pour un les arêtes ont d'abord été dérivées par Written et Li [192]. Les auteurs ont prédit qu'une arête de longueur χ dans une feuille d'épaisseur h a une largeur $w \sim h^{1/3}\ chi^{2/3}$. Dans [110], Lobkovsky a confirmé ce résultat dans le cadre des équations de Von Karman pour une couche mince utilisant à la fois des simulations numériques et une analyse asymptotique.

En effet, en physique, la forme caténaire apparaît naturellement dans un matériau appelé graphène. Le graphène est une feuille d'un atome d'épaisseur composée d'atomes de carbone disposés dans une structure en nid d'abeille faite d'hexagones, et peut être considérée comme des cycles benzéniques extraits de leurs atomes d'hydrogène comme le montre Figure 4.
Pour les rides d'une couche de graphène, (voir détails ci-dessous), l'approche analytique élastique de Yamamoto et al. suppose que la ride créée entre deux nanoparticules de diamètres d séparés par χ, suit un profil sous forme de chaînette (comme dans Figure 5 où ζ est la déviation et $\zeta_0 = \zeta(0)$ est la déviation maximale), qui ressemble à un morceau de papier froissé, ou à une chaîne suspendue à la Robert Hooke, avec une densité uniforme ou à un arc inversé.

De plus, au-delà des processus de déformation, les caractéristiques géométriques du froissement et du délaminage peuvent être utilisées pour étudier l'adhésion des couches de graphène [89], ou autres propriétés mécaniques des couches minces [168]. Par conséquent, il est important de savoir si la couche de graphène adhère ou pas d'une manière conforme au substrat, et de construire un modèle théorique pour prédire comment une couche de graphène suspendue se déforme en réponse à l'interaction entre les forces d'étirement et de flexion.

Il y a près de 70 ans, ce cristal a été manipulé par Wallace pour mieux comprendre les propriétés électroniques et chimiques des empilements de couches de graphène faiblement couplées par les forces de Van der Waals, appelées graphite. En effet, lorsqu'un crayon est pressé contre un morceau de papier, des couches de graphène sont en fait produites, et quelque part entre ces couches, il pourrait y avoir des couches de graphène individuelles. Cependant, malgré la production présumée de graphène à chaque utilisation d'un crayon sur une feuille de papier, il n'a été extrait que 440 ans après son invention, par les deux scientifiques de l'Université de Manchester: Andrei Geim et Kosty Novoselov, qui ont obtenu un prix Nobel pour cette découverte en 2010. La méthode utilisée consistait à coller et à décoller à plusieurs reprises le scotch d'une couche de graphite. Cela a fait une énorme révolution dans la physique bidimensionnelle car personne ne s'attendait à ce que le graphène existe réellement à l'état libre.

Le carbone est un matériau indispensable à la vie et à la base de toute chimie organique. Par conséquent, comme tous les systèmes à base de carbone, le graphène a montré une utilité considérable dans les études fondamentales, les applications industrielles et électroniques, allant de la nanoélectronique à la biologie, grâce à ses propriétés électroniques, mécaniques et chimiques notables, [6]. De plus, le graphène a ouvert de nouvelles possibilités pour le stockage de plus d'ions lithium, ce qui conduit à l'augmentation de la capacité de la batterie [69].

Il est indéniable que les membranes minces réagissent fortement aux forces extérieures et aux contraintes géométriques complexes. Le graphène étant parmi les membranes les plus minces et les plus rigides, et en raison de sa rigidité en flexion extrêmement faible, il a souvent tendance à se froisser [69]. En fait, le dépôt chimique en phase vapeur (CVD) est un moyen de faire croître des couches continues de graphène de grande taille. Mais pour pouvoir manipuler le graphène issu de CVD, il doit être transféré sur d'autres substrats, principalement un substrat de silicium. Lors de ce transfert, de nombreuses rides

peuvent être induites en raison de la dilatation thermique différente des substrats en plus du processus de transfert lui-même et des interactions de type Van der Waals créées entre le graphène et son substrat sous-jacent. D'une part, comme ces ondulations formées sont principalement liées à des fluctuations thermiques, elles sont appelées «rides intrinsèques». D'autre part, la structure bidimensionnelle du graphène est également affectée par d'autres facteurs qui ne sont pas encore totalement compris, mais qui sont généralement considérés comme le résultat de contraintes de compression ou de forces d'étirement et de flexion. Les rides résultantes dans ce cas sont appelées "rides extrinsèques". Nous renvoyons le lecteur à [198] pour une étude physique détaillée.

En particulier, la formation de plis dans le graphène a été très étudiée par les physiciens au cours des dernières années, car elle modifie la structure bidimensionnelle de la planéité totale à la formation des rides, ce qui peut avoir un effet remarquable sur les propriétés physiques du graphène, comme le support mobilité, conductivité thermique, transmittance optique et mouillabilité [69]. Cette déformation affecte également les propriétés électroniques du graphène, cela peut être facilement remarqué lorsqu'une couche de graphène est pliée à une certaine courbure, la partie localement courbée est semi-conductrice tandis que le graphène plat est hautement conducteur [211].

Puisque la morphologie du graphène influence fortement ses caractéristiques physiques, la formation de plis aléatoires conduit à des propriétés imprévisibles du graphène [198]. Ce changement aléatoire doit être évité dans les nanoélectroniques dans lesquels un contrôle précis est essentiel. Pour cela, des modèles théoriques doivent être construits afin de prédire la réponse du graphène à différents types de déformations, principalement les forces d'étirement et de flexion.

En 2012, Yamamoto et al. ([198]) ont fourni un rapport sur les observations expérimentales de la formation de rides dans une couche de graphène supportée sur un substrat de silicium ($Si0_2$) avec des perturbations topographiques placées aléatoirement produites par les nanoparticules de $Si0_2$ avec une densité de dispersion ρ_{np}, [197]. Cette étude a montré que ρ_{np} a un effet direct sur le froissement du graphène. Plus précisément, dans un premier temps (à $\rho_{np} = 11\mu m^{-2}$), le graphène adhère de manière conforme au substrat ([87], [179] et [82]) et au fur et à mesure que la densité des nanoparticule augmente (à $\rho_{np} = 22\mu m^{-2}$), les rides reliant les nanoparticules prolifèrent, et enfin un réseau de rides s'étend sur l'ensemble de l'échantillon.

Ces observations indiquent qu'il existe une distance critique χ_c entre deux nanoparticules, au-delà de laquelle on perd le profil chaînette de la ride et une délamination totale se produit.

La détermination de χ_c a été l'objectif principal de nombreux travaux à commencer par Lobkovsky et al. dans [111] qui ont fourni un modèle élastique continu vu ci-dessous sur Figure 1 pour une monocouche de graphène déposée sur un substrat de silicium décoré de nanoparticules de silicium. Ils ont supposé que chacune des rides formées entre deux nanoparticules de diamètre d séparées par une distance χ, suit un profil de type caternaire. Le profil de ride est alors paramétré par une déviation $\zeta(x)$ et une déviation maximale $\zeta_0 = \zeta(0), 0 < \zeta_0 \leq d$.

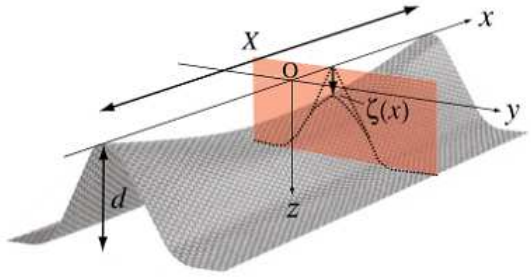

Figure 1: Deformation of graphene membrane between two nanoparticles with diameters d.

On suppose que la longueur maximale notée χ_c que peut avoir la ride est atteinte où la déviation maximale $\zeta_0 := \zeta(0)$ de la ride atteint le diamètre d de la nanoparticule, soit $\zeta_0 = d$. Expérimentalement, cette longueur de ride est d'ordre 200 *nm*. Cependant, en théorie, cette valeur n'a jamais été atteinte. Cette incapacité à atteindre la valeur observée lors des expérimentations est la principale motivation des travaux réalisés dans cette thèse.

La thèse est divisée en deux parties. Le but de la première partie est de: a) développer une méthode numérique originale pour optimiser l'énergie associée au modèle ce qui nous a permis de déterminer la distance critique entre les deux nanoparticules du silicium ayant la même taille en dessous de la quelle la ride est conservée, b) développer un autre modèle mathématique du graphène entre deux nanoparticules ayant différentes tailles cette fois-ci, une analyse analytique a été menée d'une manière rigoureuse pour déterminer là aussi la distance critique mais le résultat obtenu est loin des résultats expérimentaux. La deuxième partie porte sur l'étude de deux EDP génériques. Ces équations sont utilisées pour analyser

les instabilités qui sont à l'origine des ondulations des marches. Pour la première équation, on a obtenu une classification complète de solutions via une analyse de solutions stationnaires. La deuxième partie du chapitre est dévouée à l'étude du comportement asymptotique de la période des solutions. Cette partie est principalement consacrée à l'analyse des solutions périodiques autosimilaires. Ensuite, on propose d'approfondir l'analyse théorique et numérique présentées au chapitres précédents. Le but de cette partie est de minimiser une énergie plus générale sous des contraintes sur la taille, et on montre que cette énergie peut être minimisée sous des conditions sur l'exposant critique et on obtient ensuite une caractérisation du diamètre critique de la nanoparticule. On s'est aussi intéressé à l'analyse mathématique d'une équation singulière quasi linéaire elliptique avec donnée mesure de Radon, on obtient l'existence, la non-existence et l'unicité des solutions faibles. A cet effet, on obtient diverses conditions nécessaires ou suffisantes sur les données du problème. L'ingrédient principal est l'inégalité isopérimétrique. En outre, une partie de cette thèse est consacrée à l'analyse mathématique d'une équation avec non linéarité singulière et un terme gradient non linéaire à droite de l'équation et sans second membre. On montre l'existence et l'unicité d'une solution faible en utilisant un changement de variable adéquat. En dernier lieu, on s'intéresse à l'analyse mathématique d'un système d'équation aux dérivée partielles capable de décrire les phénomènes de chimiotaxique biologique. Le modèle proposé est une modification du modèle classique de Keller Segel et de ses développements ultérieurs, qui, dans de nombreux cas, ont été développés pour obtenir des modèles qui empêchent l'explosion non physique des solutions. On obtient l'existence de solution faible sous une condition d'exposant critique qui apparait dans le modèle.

Les grandes lignes de la thèse

Plus en détail, cette thèse est structurée comme suit:

Chapitre 1: Algorithme GWO amélioré pour la détermination de la longueur critique des rides du graphène.

Dans ce chapitre, un effort est fait pour fournir un algorithme numérique qui détermine la longueur critique χ_c des rides en dessous de laquelle le froissement est induit dans une couche de graphène déposée sur un substrat de silicium décoré de nanoparticules de silicium de même taille, (c'est-à-dire pour une taille de nanoparticule donnée la membrane de graphène se déforme si la distance entre deux nanoparticules n'est pas supérieure à χ_c). En effet, comme mentionné précédemment, la longueur maximale d'une ride sera déterminée sous la contrainte $\zeta(0) = d$, où ζ est le minimum de la fonctionnelle énergétique

suivante

$$\begin{cases} \mathscr{J}(\zeta) = \varepsilon_1(\theta)\int_{|x|<\frac{\chi}{2}} \zeta\,(\zeta_x)^4 + \varepsilon_2(\theta)\int_{|x|<\frac{\chi}{2}} \zeta^{-1} + 2\Gamma\chi d\tan\left(\dfrac{\theta}{2}\right) \\ \\ \text{subject to } \zeta(\pm\frac{\chi}{2}) = 0. \end{cases}$$

dans laquelle ε_1, ε_2, θ et Γ sont des paramètres physiques qui seront détaillés dans le chapitre correspondant.

Cette fonctionnelle peut être réécrite en utilisant le changement de variable $v = \zeta^{\frac{5}{4}}$; comme suit;

$$\begin{cases} \mathscr{J}(v) = \left(\frac{4}{5}\right)^4 \varepsilon_1(\theta)\int_{|x|<\frac{\chi}{2}} (v_x)^4 + \varepsilon_2(\theta)\int_{|x|<\frac{\chi}{2}} v^{-\frac{4}{5}} + 2\Gamma\chi d\tan\left(\dfrac{\theta}{2}\right) \\ \\ \text{subject to } v(\pm\frac{\chi}{2}) = 0. \end{cases} \tag{0.1}$$

L'algorithme numérique est utilisé pour minimiser la fonction coût suivante $\mathscr{F}$, et le problème d'optimisation est alors exprimé comme suit:

$$\begin{cases} \textit{Minimiser} \quad \mathscr{F}(\chi,\theta) = \mid v(0) - d^{5/4} \mid^2, \\ \quad \text{où } v \text{ est le minimum de (0.1).} \end{cases}$$

L'algorithme que nous utiliserons est le Grey Wolf Optimizer (GWO) qui est une méta-heuristique basée sur le comportement de chasse des loups gris dans la nature (Canis-Lupus), modélisée mathématiquement par Mirjalili et al. dans [117]. Les résultats obtenus montrent que l'approche proposée donne de bons résultats en comparaison avec les résultats de la littérature. Cependant, la longueur maximale des rides observée est encore sous-estimée.

Ce travail est publié dans Annals of the University of Craiova, Mathematics and Computer Science Series [174].

A ce stade, une question se pose: quelles peuvent être les causes de cet écart entre la théorie et les expériences? En fait, Yamamoto a mentionné dans son article [198] que les deux nanoparticules de silicium n'ont pas nécessairement le même diamètre, ce qui signifie que la ride ne s'affaissera pas nécessairement au milieu. Nous avons suivi cette voie, et étudié le cas où les deux nanoparticules ont des tailles différentes dans le chapitre suivant.

Chapitre 2: Analytical results for the wrinkling of graphene on nanoparticles with different diam-

eters.

Suite aux points mentionnés ci-dessus, le but de ce chapitre est de présenter une étude mathématique du froissement du graphène entre deux nanoparticules de hauteurs différentes d et $d-\delta$, pour $\delta > 0$ et $\frac{\delta}{d} << 1$, séparés par une distance χ^δ, en examinant l'énergie élastique associée qui est différente de l'énergie (0.5) puisque la différence de taille δ doit être prise en compte.

Dans ce cas, le problème est de minimiser l'énergie $\mathscr{J}$ définie par:

$$\begin{cases} \mathscr{J}(\zeta) = \varepsilon_1 \displaystyle\int_{\frac{\chi_-^\delta}{2}}^{\frac{\chi_+^\delta}{2}} \zeta\,(\zeta_x)^4 + \varepsilon_2 \int_{\frac{\chi_-^\delta}{2}}^{\frac{\chi_+^\delta}{2}} \zeta^{-1} + 2\Gamma\chi^\delta \left(d - \frac{\delta}{2}\right) \tan\left(\frac{\theta}{2}\right) \\ \\ \text{subject to } \zeta\left(\frac{\chi_-^\delta}{2}\right) = 0 \text{ and } \zeta\left(\frac{\chi_+^\delta}{2}\right) = \delta, \end{cases}$$

telle que ε_1, ε_2, Γ et θ sont des paramètres physiques qui seront détaillés dans le chapitre correspondant, et χ_-^δ, χ_+^δ sont à déterminer, avec $\chi_-^\delta < 0$ et $\chi_+^\delta > 0$. Nous confirmons que la ride s'affaisse de manière asymétrique vers la nanoparticule de plus petite hauteur. Cependant, la longueur maximale des rides dans ce cas est inférieure à la longueur maximale des rides obtenue lorsque les deux nanoparticules ont la même taille. On peut alors en conclure qu'on ne peut pas espérer atteindre théoriquement la longueur maximale observée de 200 *nm*, puisque cette différence peut être simplement due au fait que physiquement, le substrat n'est presque jamais plat à cause des impuretés à sa surface, ou car il pourrait s'agir d'une surface vicinale composée d'une succession de terrasses séparées par des gradins. Du fait de ces étapes, même si les nanoparticules ont la même taille, la hauteur de la marche sera la différence entre les nanoparticules. Cela nous amène au chapitre suivant dans lequel nous réexaminons les équations singulières généralisées pour discuter le mûrissement des interfaces croissantes.

Ce travail est soumis au journal Surface Science.

Chapitre 3: An obstacle problem for a graphene wrinkle model-type.

Dans ce chapitre, nous présentons une approche analytique modifiée pour étudier une classe d'équations de type modèle graphène. En particulier, nous nous intéresserons à un algorithme de résolution de cette classe de problèmes qui peut être formulé comme un problème d'obstacles. Le présent chapitre est motivé par le désir de trouver une solution numérique approximative décrivant la configuration d'équilibre de la déformation interfaciale de la membrane de graphène (considérée ici). Comme nous l'avons vu au

chapitre 2, du point de vue mathématique, l'énergie du graphène déformé peut souffrir du phénomène du GAP. Donc, une question importante est de développer un algorithme pour résoudre le problème physique. L'idée est de transformer le problème du froissement du graphène en problème d'obstacle qui permet de calculer simultanément l'énergie et la déviation du graphène. Le problème d'optimisation écrit:

Soient $p > 1$ et $1 < \gamma < \frac{2p-1}{p-1}$,

$$\begin{cases} \text{Minimize} \quad \mathscr{J}(v) = \frac{1}{p}\int_{-1}^{1} \mid v_x \mid^p + \dfrac{1}{\gamma-1}\int_{-1}^{1} v^{1-\gamma}, \\ \\ \qquad \text{subject to } v(\pm 1) = 0 \text{ and } v(0) = d > 0. \end{cases} \tag{0.2}$$

Minimiser cette énergie conduit à un problème singulier unidimensionnel impliquant le p-laplacien ou l'opérateur p-Laplace écrit comme $\Delta_p v := \left(|v_x|^{p-2}v_x\right)_x$, et souffrant d'une non-linéarité singulière et d'une masse de Dirac à l'origine. Nous montrerons que l'existence d'un minimum pour (0.2) dans un espace approprié K que nous introduirons en utilisant la sous-solution de l'équation et la première fonction propre du p-Laplacien, dépend de l'existence d'une valeur notée d^* au-delà de laquelle le minimum existe. Enfin, des études numériques sont menées pour déterminer le profil du minimum.

Ce travail est soumis au journal Mathematical Modeling and Computing.

Chapitre 4: Instabilities and scaling properties in certain one-dimensional singular interfacial equation.

Dans la première section de ce chapitre, nous réexaminons une équation singulière généralisée pour discuter du mûrissement des interfaces croissantes, en présence de la barrière Ehrlich – Schwoebel – Villain qui induit une structure pyramidale. L'objectif principal de cette partie est la prédiction et le contrôle de ces surfaces. En particulier, nous étudierons la dynamique unidimensionnelle d'une croissance MBE dans laquelle les monticules augmentent à la fois en hauteur et en taille latérale. On constate que la hauteur interfaciale continue dans un cas unidimensionnel obéit à l'équation générale d'évolution phénoménologique suivante [155],

$$\partial_t h = -a\partial_x\left(\frac{\partial_x h}{\left(1+|\partial_x h|^2\right)^n}\right) - b\partial_x^4 h, \tag{0.3}$$

où a et b sont des constantes physiques positives et $n \geqslant 1$. La fonction lisse inconnue h mesure l'épaisseur du film au-dessus d'un point du substrat x et au temps t. Le but de cette section est de rapporter une justification analytique des solutions au modèle, qui prédisent le processus de grossissement. En fait, nous nous intéressons principalement aux solutions stationnaires, qui sont utilisées avec succès pour décrire les principales caractéristiques du processus de grossissement dans une large classe de phénomènes de croissance de surface.

La deuxième section de ce chapitre est consacrée à l'étude de la similitude solutions du modèle phénoménologique généralisé

$$\partial_t h = -\partial_x \left(a\,(\partial_x h)^{1-2\nu} + b\partial_{xxx} h \right), \tag{0.4}$$

qui est proposé pour $\nu \geq 1$, pour discuter le mûrissement des interfaces croissantes. On montre que les solutions de similarité résultantes ont un régime périodique pour tout $\nu > \frac{1}{2}$. Notre contribution fournit une justification mathématique rigoureuse de l'existence de solutions de similitude périodique spatiale à l'équation interfaciale singulière et présente les propriétés géométriques des fonctions d'échelle. Le présent travail fournit un support pour des solutions avec des $\partial_{xx} h$ divergents aux points où $\partial_x h = 0$ pour $\nu \geq 1$.

La première section de ce chapitre est publiée dans le journal Physica Scripta [38] et la seconde section est en préparation pour être soumise.

Chapitre 5: On singular quasilinear elliptic equations with data measures.

Dans ce chapitre, nous restreignons notre attention à l'étude d'une classe d'un problème elliptique quasilinéaire avec une non-linéarité singulière et une mesure de données à savoir

$$(P_\lambda) \begin{cases} -\Delta u = \dfrac{a(x)}{u^\gamma} + b(x)|\nabla u|^p + \lambda f \quad \textit{dans} \quad \Omega, \\ u > 0 \qquad\qquad\qquad\qquad\qquad\quad \textit{dans} \quad \Omega, \\ u = 0 \qquad\qquad\qquad\qquad\qquad\quad \textit{sur} \quad \partial\Omega. \end{cases}$$

Ω est un sous-ensemble ouvert et borné de $\mathbb{R}^N$ pour $N \geq 2$, avec une frontière lisse $\partial\Omega$, $f : \Omega \to [0, +\infty[$ est un étant donné une mesure de Radon non négative finie, $\gamma > 0$, $\lambda > 0$, et a et b sont des fonctions non négatives dans $L^1(\Omega)$. Nous commençons par identifier les conditions nécessaires sur les données

afin d'obtenir l'existence de solutions faibles dans (P_λ). Ensuite, en utilisant l'inégalité isopérimétrique, nous montrons l'existence de solutions pour le problème sublinéaire non singulier et le problème sublinéaire singulier, pour toute mesure de Radon non négative dépendant de la valeur de γ: Si $0 < \gamma \leq 1$ et $b \in L^{N+\eta}(\Omega)$, $\eta > 0$, alors pour toute mesure finie f et $\lambda \in \mathbb{R}$, le problème (P_λ) a une solution u dans $W_0^{1,q}(\Omega)$ pour tout $1 \leq q < \dfrac{N}{N-1}$. Sinon, si $\gamma > 1$ et $b \in L^{N+\eta}(\Omega)$, le problème (P_λ) admet une solution u dans $W_{loc}^{1,q}(\Omega)$ pour tout $1 \leq q < \dfrac{N}{N-1}$ et $T_k(u)^{\frac{\gamma+1}{2}} \in H_0^1(\Omega)$, où $T_k(u)$ représente la troncature de u.

Ce travail est accepté dans le journal Advances in Nonlinear Analysis.

Chapitre 6: Mathematical Analysis of a quasilinear elliptic equation with singular non-linearity.

Dans ce chapitre, on se concentre sur l'étude mathématique de l'équation suivante:

$$(Q)\begin{cases} -\Delta u + |\nabla u|^2 = u^{-\gamma} & dans\ \ \Omega, \\ u = 0 \quad sur\ \ \partial\Omega. \end{cases}$$

en utilisant une approximation de Yosida et quelques techniques très intéressantes, on montre l'existence d'une solution $u \in W_{loc}^{2,p}(\Omega)$, pour tout $p \in [1, +\infty[$.
En outre, on prouve que $u^{\gamma+1} \in W_0^{1,q}(\Omega)$, pour tout $1 \leq q \leq \frac{N}{N-1}$ et $e^{-\frac{\gamma+1}{2}u} \in H_0^1(\Omega)$.

Chapitre 7: On the Existence of Global Weak Solutions to a Generalized Keller Segel Model with Growth and Nonlinear Signal Production.

Dans ce dernier chapitre, le modèle proposé est une modification du modèle classique de Keller Segel et de ses développements ultérieurs qui, dans de nombreux cas, ont été développés pour obtenir des modèles qui empêchent le blow up non physique des solutions. Nous nous intéressons principalement à l'existence globale dans $L^2(\Omega)$ de solutions globales faibles à une classe de systèmes de chemotaxis parabolique-elliptique englobant le prototype:

$$\begin{aligned} u_t - \bigtriangledown.(\bigtriangledown u + \chi u \bigtriangledown v) &= f(u) \quad ,x \in \Omega, t > 0, \\ -\Delta v + v &= u^\gamma \quad ,x \in \Omega, t > 0, \end{aligned}$$

avec condition initiale non négative pour u et sans conditions au bord du flux dans un domaine borné $\Omega \subset \mathbb{R}^n$ $(n \geqslant 2)$, où $\chi > 0$, $0 < \gamma < 1$ et $f \in C^1(\mathbb{R})$ tels que , $f(0) = 0$ et

$$f(s) \leqslant 0, \quad s \geqslant 0.$$

Il est démontré dans ces conditions que le problème admet des solutions faibles dans $L^2(\Omega)$. Afin de développer l'analyse mathématique de notre modèle, nous définissons un schéma approximatif avec des conditions initiales plus régulières, puis nous faisons quelques estimations qui nous permettront de prouver que la solution du système approché converge vers la solution de notre problème.

Ce travail est publié dans Annals of the University of Craiova, Mathematics and Computer Science Series [104].

Chapitre 8: Conclusion and Perspectives. Dans ce chapitre, nous présentons une conclusion de la thèse, discutons des contributions de nos travaux et esquissons les travaux futurs liés à cette recherche.

Introduction and Thesis Overview

0.2 Statement of the problem

The main objective of the present thesis is to focus on few aspects of the surface instabilities. These phenomena are observed in everyday life across a wide range of length scales, ranging from micro-scale deformation (wrinkles on human skin) to macro-scale deformation (mountain ridge formations). They have been and remain a challenge for different disciplines.

Nature is very elegant. Its forms are both functional and aesthetic. Looking deep into nature, many theories were brought in architecture and design. One of the most fascinating natural forms is the catenary-form. Catenary is the curve obtained when a chain of uniform density is hung from two points. This form occurs naturally in an egg or the hanging threads of a spider's web. Indeed, the finnish-american architect, Eero Saarinen adopted this form into the iconic Gateway Arch in St. Louis in 1963, depicted in Figure 2. Another architect who studied and incorporated the catenary form in his work is the famous catalan architect Antoni Gaudi. His Casa Mila building in Barcelona, Spain (see Figure 3) was the repetitive pattern of the inverted Catenary.

In fact, the problem of catenary and arch is one of the oldest problems that have been solved by using the calculus of variations. The question was to find the exact shape formed by a hanging chain, or flexible cord. Galileo (1602) was the first to pose the problem. Not having calculus (at that time), Galileo answered incorrectly that the resulting curve was a parabola. For arches, it was Robert Hooke (1675) who made a connection between the ideal shape of an arch and that of a hanging chain. The geometry of an arch is seen as a mirror of that of a hanging chain. Probably, this is one of the (oldest) reasons that the terms used in describing the popular St. Louis Gateway Arch is often a catenary or a parabola.

Figure 2: The Gateway Arch on the west bank of the Mississippi River in St. Louis, Missouri, U.S.

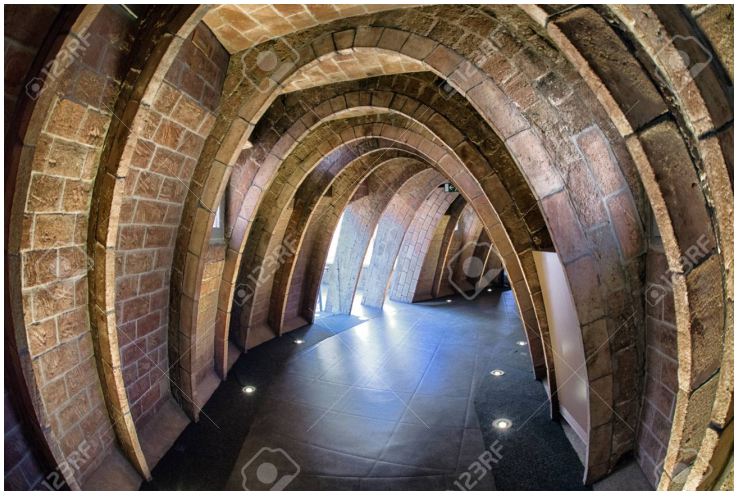

Figure 3: Interior of Casa Mila also known La Pedrera - house designed by Antoni Gaudi in Barcelona, Spain.

At nanoscale, different morphologies or deformations, including catenary and arch-type, are obtained and/or observed in elastic sheet thins. This problem, which has a long history, is a classical subject of continuum mechanics. The question has been studied from different points of view and different types of deformations or surface instabilities and a possible continuously/discontinuously transition between them have been predicted (critical conditions). Most deformations (buckle-delamination, wrinkling, cracking or fracture,...) are viewed as (local) minimizers of a suitable elastic energy. However, due to the complexity of the equations (fourth-order partial differential equations, boundary layer, free boundary conditions,

...) that describe surface morphologies, rigorous proofs are in most cases difficult to achieve and since explicit solutions exist only in a few cases, numerical treatments are inevitable.

It has long been known that a thin elastic plate can be mediated by the formation of narrow ridges. More importantly, scaling laws for a ridge were first derived by Written and Li [192]. The authors predicted that a ridge of length χ in a sheet of thickness h has a width $w \sim h^{1/3}\chi^{2/3}$. In [110], Lobkovsky confirmed this result in the framework of the von Karman equations for a thin plate using both numerical simulations and an asymptotic analysis.

For wrinkling graphene (see details below), the elastic analytical approach of Yamamoto *et al.* supposes that the ridge running along the wrinkle between two nanoparticles with diameters d separated by χ, follows a catenary-like profile (see Figure 5), with a deflection ζ (from the original ridge line) and a maximum deflection $\zeta_0 = \zeta(0)$ that looks similar to a crumpled piece of paper, or to a hanging chain à la Robert Hooke, with uniform density or to an inverted arch.

The catenary-like profile was used by Lobkosvky *el al.* [111] to find the scaling energy properties of a crumpled elastic sheet. This approach allowed an analytical treatment of the wrinkling graphene. In particular, an equilibrium equation has been derived (see below) and an exact expression of the deflection ζ has been proposed to describe characteristic features of wrinkling graphene.

In addition, beyond deformation processes, geometrical characteristics of the wrinkling and delamination can be used to probe the adhesion energy of graphene sheets [89], or other mechanical properties of thin sheets [168]. Therefore, it is important to know whether or not the graphene sheet can conform to the subtrate, and to build a theoretical model to predict how a suspended graphene sheet deforms in response to the interplay between stretching and bending forces. As a matter of fact, in physics, the catenary form appears naturally in a material called graphene. Graphene is a one-atom-thick sheet composed of carbon-atoms arranged in honeycomb structure made out of hexagons, and can be thought as benzene rings stripped out from their hydrogen atoms as seen in Figure 4.

Almost 70 years ago, this crystal was manipulated by Wallace to get a better understanding of the electronic and chemical properties of stacks of graphene layers weakly coupled by Van der Waals forces, known as Graphite. Indeed, when a pencil is pressed against a piece of paper, graphene stacks are ac-

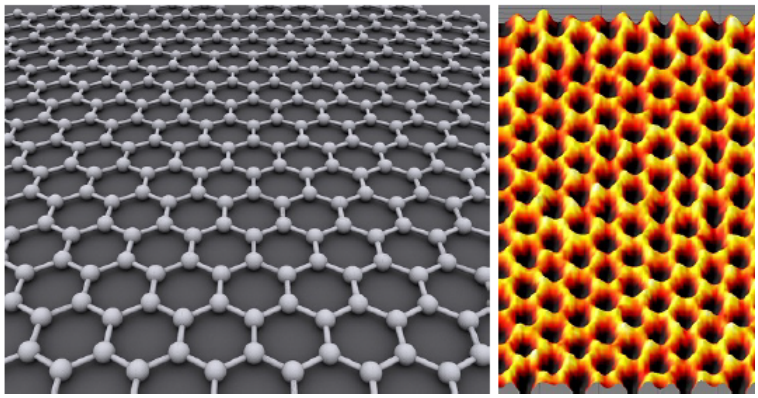

Figure 4: The ideal crystalline structure of graphene is a hexagonal grid (right) and a Scanning probe microscopy image of graphene (left).

tually being produced, and somewhere between these stacks, there could be individual graphene layers. However, despite the presumed production of graphene at every use of a pencil on a sheet of paper, it was only extracted 440 years after its invention, by the two scientists of Manchester University: Andrei Geim and Kosty Novoselov, who got a Nobel prize for it in 2010. The method they used was to repeatedly stick and peel back the scotch tape off of a graphite layer. This made a huge revolution in two-dimensional physics as no one expected graphene to actually exist in the free state.

Carbon is an indispensable material for life and the basis of the background of all organic chemistry. Consequently, like all carbon-based systems, graphene has shown tremendous utility in fundamental studies, industrial and electronic applications, ranging from nanoelectronics to biology, thanks to its notable electronic, mechanical and chemical properties, [6]. Furthermore, graphene has opened new possibilities for the storage of more lithium ions which leads to the increase of the battery's capacity [69].

It is undeniable that thin membranes strongly react to external forces and complex geometrical constraints. As graphene is among the thinnest and most rigid known membranes, and because of its extremely low bending rigidity, it often tends to wrinkle [69]. In fact, one way to grow continuous large-size layers of graphene is the chemical vapor deposition (CVD). But in order to be able to manipulate the CVD-grown graphene, it has to be transferred to other substrates, mainly a silicium substrate. During this transfer, many wrinkles can be induced because of the different thermal expansion of the substrates besides the transfer process itself and the Van der Waals type interactions created between graphene and its underlying substrate. On one hand, since these formed ripples are mainly related to thermal fluctuations,

they are referred to as "intrinsic wrinkles". On the other hand, the two dimensional structure of graphene is also affected by other factors which are not yet fully understood, but usually considered to be a result of compressive stresses or stretching and bending forces. The resulted wrinkles in this case are referred to as "extrinsic wrinkles". We refer the reader to [198] for detailed physical study .

In particular, the wrinkling formation in graphene has been highly studied by physicists in the last decade, as it modifies the two-dimensional structure from total planarity to wavy sheet, which can have a remarkable effect on the physical properties of graphene, such as carrier mobility, thermal conductivity, optical transmittance and wettability [69]. This deformation also affects the electronic properties of graphene, this can easily be noticed when it is bent to a certain curvature, a band gap is generated and that locally curved portion is semiconducting while the flat graphene is highly conductive [211].

Since the morphology of graphene strongly influences its physical characteristics, random wrinkling formation leads to unpredictable graphene properties [198]. This random change must be avoided in nanoelectronic devices in which precise control is key. For this purpose, theoretical models need to be built in order to predict graphene's response to different kinds of deformations mainly stretching and bending forces.

In 2012, Yamamoto et al.([198]) provided a report on experimental observations of the formation of wrinkles in a graphene layer supported on $Si0_2$ substrates with randomly placed topographic perturbations produced by $Si0_2$ nanoparticles with a dispersion density ρ_{np}, [197]. This study showed that ρ_{np} has a direct effect on the wrinkling of graphene. More precisely, at first (at $\rho_{np} = 11\mu m^{-2}$), graphene adheres conformally to the substrate ([87], [179] and [82]) and as the nanoparticle's density increases (at $\rho_{np} = 22\mu m^{-2}$), the wrinkles connecting the protrusions proliferate, and finally a network of wrinkles extends over the entire sample.
These observations indicate that there exists a critical distance χ_c between two nano-particles, beyond which we lose the caternary-like profile of the wrinkle and a total delamination occurs.

The determination of χ_c was the main aim of many works starting with Lobkovsky et al. in [111] in which the authors provided a continuum elastic model seen below in Figure 5 for a graphene mono-layer deposited on a silica substrate decorated with silica nano-particles. They presumed that each formed

wrinkle between two nano-particles with diameter d separated by a distance χ, follows a Caternary-like profile. The wrinkle profile is then parametrised by a deflection $\zeta(x)$ and a maximum deflection $\zeta_0 = \zeta(0), 0 < \zeta_0 \leq d$.

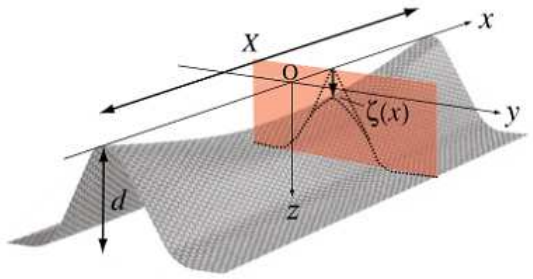

Figure 5: Deformation of graphene membrane between two nanoparticles with diameters d.

It is assumed that the maximum length denoted χ_c which the wrinkle can have is attained where the maximum deviation $\zeta_0 := \zeta(0)$ of the wrinkle attains the nanoparticle's diameter d, i.e. $\zeta_0 = d$. Experimentally, this wrinkle length is of order of 200 nm. However, theoretically, this value has never been reached. This inability to reach the value observed during the experiments is the main motivation behind the works realised in this thesis.

This thesis is divided into three parts. The first part is devoted to the investigation of the reasons behind the discrepancy between the experimental and theoretical results. The second part of the thesis is composed of one rich chapter in which two partial differential equations are studied. These equations are used to analyze the instabilities which deal with the steps in the surfaces. We note that the presence of the stairs in a surface will have the same effect as the presence of a difference in the size of silica nanoparticles. The third part presents the mathematical study and numerical simulations of quasilinear equations with singular non-linearities and data measure.

0.3 Outlines of the thesis

More in details, this thesis is structured as follows:

Chapter 1: Improved GWO algorithm for the determination of the critical wrinkle length of Graphene.

In this chapter, an effort is made to provide a numerical algorithm that determines the critical ridge length χ_c below which wrinkling is induced in a graphene layer put on a silica substrate decorated with silica nanoparticles that have the same size, (i.e. for a given nanoparticle size the graphene membrane wrinkles if the distance between two nanoparticles is not larger than χ_c) . Indeed, as mentioned before, the maximum length of a wrinkle will be determined under the constraint $\zeta(0) = d$, where ζ is the minimum of the following energy functional

$$\begin{cases} \mathscr{J}(\zeta) = \varepsilon_1(\theta)\displaystyle\int_{|x|<\frac{\chi}{2}} \zeta\,(\zeta_x)^4 + \varepsilon_2(\theta)\int_{|x|<\frac{\chi}{2}} \zeta^{-1} + 2\Gamma\chi d\tan\left(\frac{\theta}{2}\right) \\ \\ \text{subject to } \zeta(\pm\frac{\chi}{2}) = 0. \end{cases} \tag{0.5}$$

in which ε_1, ε_2, θ and Γ are physical parameters to be detailed in the chapter.
The functional defined above can be rewritten using a change of variable $v = \zeta^{\frac{5}{4}}$:

$$\begin{cases} \mathscr{J}(v) = \left(\frac{4}{5}\right)^4 \varepsilon_1(\theta)\displaystyle\int_{|x|<\frac{\chi}{2}} (v_x)^4 + \varepsilon_2(\theta)\int_{|x|<\frac{\chi}{2}} v^{-\frac{4}{5}} + 2\Gamma\chi d\tan\left(\frac{\theta}{2}\right) \\ \\ \text{subject to } v(\pm\frac{\chi}{2}) = 0. \end{cases} \tag{0.6}$$

The numerical algorithm is used to minimize the following cost function $\mathscr{F}$, and the optimization problem is then expressed as follows:

$$\begin{cases} \textit{Minimize} \quad \mathscr{F}(\chi,\theta) = \mid v(0) - d^{5/4} \mid^2, \\ \quad \text{where } v \text{ is the minimum of (0.6).} \end{cases} \tag{0.7}$$

The algorithm we will use is the Grey Wolf Optimizer (GWO) which is a swarm-based-meta-heuristic based on the social leadership and hunting behavior of grey wolves in nature (Canis-Lupus), mathematically modeled by Mirjalili et al. in [117]. The obtained results show that the proposed approach provides good results in comparison with the results in the literature. However, the observed maximum wrinkle length is still underestimated.

This work is published in Annals of the University of Craiova, Mathematics and Computer Science Series [174].

At this stage, a question arises: What may be the causes behind this discrepancy between the theory

and the experiments? In fact, Yamamoto mentioned in his paper [198] that the two silica nano-particles don't necessarily have the same diameter which means that the wrinkle won't necessarily sag in the middle. We followed this path, and studied the case where the two nanoparticles have different sizes in the following chapter.

Chapter 2: Analytical results for the wrinkling of graphene on nanoparticles with different diameters.

Regarding the aforementioned points, the purpose of this chapter is to present a mathematical study of the wrinkling of graphene between two nanoparticles with different heights d and $d-\delta$, for $\delta > 0$ and $\frac{\delta}{d} << 1$, separated by a distance χ^δ, by examining the associated elastic energy which is different from the energy (0.5) since the size's difference δ has to be taken into account.

In this case, the problem is to minimize the energy $\mathscr{J}$ defined by :

$$\begin{cases} \mathscr{J}(\zeta) = \varepsilon_1 \displaystyle\int_{\frac{\chi_-^\delta}{2}}^{\frac{\chi_+^\delta}{2}} \zeta\,(\zeta_x)^4 + \varepsilon_2 \int_{\frac{\chi_-^\delta}{2}}^{\frac{\chi_+^\delta}{2}} \zeta^{-1} + 2\Gamma\chi^\delta \left(d - \frac{\delta}{2}\right) \tan\left(\frac{\theta}{2}\right) \\ \\ \text{subject to } \zeta\left(\frac{\chi_-^\delta}{2}\right) = 0 \text{ and } \zeta\left(\frac{\chi_+^\delta}{2}\right) = \delta, \end{cases} \tag{0.8}$$

in which ε_1, ε_2, Γ and θ are physical parameters that are detailed in the chapter, and χ_-^δ, χ_+^δ are to be determined later on, where $\chi_-^\delta < 0$ and $\chi_+^\delta > 0$. We confirm that the wrinkle sags asymmetrically toward the nanoparticle of smaller height. However, the maximum wrinkle length in this case is lower than the maximum wrinkle length obtained when the two nanoparticles have the same size. We may then conclude that we can't expect to theoretically attain the observed maximum length of 200 nm, since this difference may be simply due to the fact that physically, the substrate is almost never flat because of the impurities at its surface, or because it might be a vicinal surface composed of a succession of terraces separated by steps. Because of these steps, even if the nanoparticles have the same size, the height of the step will be the difference between the nanoparticles. This leads us to the next chapter in which we re-examine generalized singular equations to discuss the coarsening of growing interfaces.

This work is submitted to the Journal Surface Science.

Chapter 3: An obstacle problem for a graphene wrinkle model-type.

In this chapter we present a modified analytical approach to study a class of equations of the graphene model-type. In particular, we shall be interested in an algorithm for solving this class of problems which can be formulated as an obstacle problem. The present chapter is motivated by the desire to find an approximate numerical solution describing the equilibrium configuration of out of plane deformation of the graphene membrane (under consideration here). As we have seen in Chapter 2, from the mathematical point of view, the energy of the deformed graphene may suffer from the GAP phenomenon. So, an important question is to develop an algorithm to solve the physical problem. The idea is to transform the wrinkling of graphene problem into an obstacle problem which enables to compute the energy and the graphene deflection simultaneously. The optimization problem writes:

Let $p > 1$ and $1 < \gamma < \frac{2p-1}{p-1}$,

$$\begin{cases} \text{Minimize} \quad \mathscr{J}(v) = \frac{1}{p}\displaystyle\int_{-1}^{1} \mid v_x \mid^p + \frac{1}{\gamma-1}\int_{-1}^{1} v^{1-\gamma}, \\ \\ \qquad \text{subject to } v(\pm 1) = 0 \text{ and } v(0) = d > 0. \end{cases} \tag{0.9}$$

Minimizing this energy leads to a one-dimensional singular problem involving the p-Laplacian or the p-Laplace operator written as $\Delta_p v := \left(|v_x|^{p-2}v_x\right)_x$, and suffering from a singular non-linearity and a Dirac mass at the origin. We will show that the existence of a minimum for (0.9) in a suitable space K that we will introduce using the sub-solution of the equation and the first eigenfunction of the p-Laplacian, depends on the existence of a value denoted d^* beyond which the minimum exists. Finally, numerical investigations are carried out to determine the profile of the minimum.

This work is submitted to Mathematical Modeling and Computing.

Chapter 4: Instabilities and scaling properties in certain one-dimensional singular interfacial equation.

In the first section of this chapter, we re-examine a generalized singular equation to discuss the coarsening of growing interfaces, in the presence of Ehrlich–Schwoebel–Villain barrier that induces a pyramidal or mound-type structure without slope selection. The main goal of this part is the prediction and control of these surfaces. In particular, we will study the one-dimentional dynamics of a MBE growth in which the mounds increase in both height and lateral size. The continuous interfacial height in one-dimensional case , is found to obey the following general phenomenological evolution equation [155],

$$\partial_t h = -a\partial_x \left(\frac{\partial_x h}{\left(1+|\partial_x h|^2\right)^n} \right) - b\partial_x^4 h, \tag{0.10}$$

where a and b are physical positive constants and $n \geqslant 1$. The unknown smooth function h measures the film thickness above a substrate point x and at time t. The purpose of this section is to report an analytical justification of solutions to the model, which predict the coarsening process. In fact, we are mainly concerned with stationary solutions, which are successfully used to describe the major features of the process of coarsening in a wide class of surface growth phenomena.

The second section of this chapter is devoted to the investigation of the similarity solutions of the generalized phenomenological model

$$\partial_t h = -\partial_x \left(a\,(\partial_x h)^{1-2\nu} + b\partial_{xxx} h \right), \tag{0.11}$$

which is proposed for $\nu \geq 1$, to discuss the coarsening of growing interfaces. The resulting similarity solutions are shown to have a periodic regime for any $\nu > \frac{1}{2}$. Our contribution provides a rigorous mathematical justification for the existence of spacial periodic similarity solutions to the singular interfacial equation and exhibits geometrical properties of the scaling functions. The present work provides support for solutions with diverging $\partial_{xx} h$ at points where $\partial_x h = 0$ for $\nu \geq 1$.

The first section of this chapter is published in the journal Physica Scripta [38] and the second section is in preparation to be submitted.

Chapter 5: On singular quasilinear elliptic equations with data measures.

In this chapter, we restrict our attention to the study of a class of a quasilinear elliptic problem with a singular non-linearity and data measure namely

$$(P_\lambda) \begin{cases} -\Delta u = \dfrac{a(x)}{u^\gamma} + b(x)|\nabla u|^p + \lambda f \ \ in \ \ \Omega, \\ u > 0 \quad in \quad \Omega, \\ u = 0 \ \ on \ \ \partial\Omega. \end{cases}$$

Ω is an open bounded subset of $\mathbb{R}^N$ for $N \geq 2$, with smooth boundary $\partial\Omega$, $f : \Omega \to [0, +\infty[$ is a given finite nonnegative Radon measure, $\gamma > 0$, $\lambda > 0$, and a and b are nonnegative functions in $L^1(\Omega)$. We

start by identifying the necessary conditions on the data in order to get existence of weak solutions in (P_λ). Then, using the isoperimetric inequality, we show the existence of solutions for the non-singular sublinear problem and the singular sublinear problem, for every nonnegative Radon measure depending on the value of γ : If $0 < \gamma \leq 1$ and $b \in L^{N+\eta}(\Omega)$, $\eta > 0$, then for all finite measure f and $\lambda \in \mathbb{R}$, the problem (P_λ) has a solution u in $W_0^{1,q}(\Omega)$ for every $1 \leq q < \frac{N}{N-1}$. Otherwise, if $\gamma > 1$ and $b \in L^{N+\eta}(\Omega)$, the problem (P_λ) has a solution u in $W_{loc}^{1,q}(\Omega)$ for every $1 \leq q < \frac{N}{N-1}$ and $T_k(u)^{\frac{\gamma+1}{2}} \in H_0^1(\Omega)$, where $T_k(u)$ represents the truncated function of u.

This work is accepted in the journal Advances in Nonlinear Analysis.

Chapter 6: Mathematical Analysis of a quasilinear elliptic equation with singular non-linearity.

In this chapter, we focus on the mathematical study of the following equation:

$$(Q)\begin{cases} -\Delta u + |\nabla u|^2 = u^{-\gamma} & in\ \ \Omega, \\ u = 0 \quad on\ \partial\Omega. \end{cases}$$

Using the Yosida approximation and very interesting techniques, we show the existence of a solution $u \in W_{loc}^{2,p}(\Omega)$, for all $p \in [1, +\infty[$.

Furthermore, we prove that $u^{\gamma+1} \in W_0^{1,q}(\Omega)$, for all $1 \leq q \leq \frac{N}{N-1}$ and $e^{-\frac{\gamma+1}{2}u} \in H_0^1(\Omega)$.

Chapter 7: On the Existence of Global Weak Solutions to a Generalized Keller Segel Model with Growth and Nonlinear Signal Production.

In this last chapter, the proposed model is a modification of the classical Keller Segel model and its subsequent developments which, in many cases, have been developed to obtain models that prevent the non-physical blow up of solutions. We are mainly concerned with the global existence in $L^2(\Omega)$ of weak global solutions to a class of parabolic-elliptic chemotaxis systems encompassing the prototype:

$$\begin{aligned} u_t - \bigtriangledown.(\bigtriangledown u + \chi u \bigtriangledown v) &= f(u) \quad ,x \in \Omega, t > 0, \\ -\Delta v + v &= u^\gamma \quad ,x \in \Omega, t > 0, \end{aligned}$$

with non-negative initial condition for u and no flux boundary conditions in a bounded domain $\Omega \subset \mathbb{R}^n$ $(n \geqslant 2)$, where $\chi > 0$, $0 < \gamma < 1$ and $f \in C^1(\mathbb{R})$ satisfying, $f(0) = 0$ and

$$f(s) \leqslant 0, \quad s \geqslant 0.$$

It is shown under those conditions that the problem admits weak solutions in $L^2(\Omega)$. In order to develop the mathematical analysis of our model, we define an approximating scheme with more regular initial conditions, then we make some estimates that will allow us to prove that the solution of the approximated system converge to the solution of our problem.

This work is published in Annals of the University of Craiova, Mathematics and Computer Science Series [104].

Chapter 8: Conclusion and Perspectives. In this chapter, We present a conclusion of the thesis, discuss the contributions of our work, and outline future work related to this research.

Chapter 1

Improved GWO algorithm for the determination of the critical wrinkle length of Graphene

This chapter is adapted from "Improved GWO algorithm for the determination of the critical wrinkle length of Graphene" by Taourirte Laila, Alaa Nour Eddine and Khalfi Hamza, published in Annals of the University of Craiova- Mathematics and Computer Science series, Volume 46(1), Pages 27-40, 1223-6934, (2019).

1.1 Introduction

The one dimensional energy model derived in [198] states that the actual wrinkle profile is the minimum of an energy obtained by summing both bending and stretching energies, which will be detailed in the next section.

In fact, Yamamoto and co-authors claim that this minimum has an exact expression given by:

$$\zeta(x) = \left(\frac{27\varepsilon_2}{4\varepsilon_1}\right)^{\frac{1}{6}} \left(\frac{\chi}{2} - |x|\right)^{\frac{2}{3}}, \tag{1.1}$$

where ε_i for $i = 1, 2$ are physical constants.

From this solution, many characteristics were deduced, such as the critical length χ_c of the wrinkle below which wrinkling is induced, and the pseudo-magnetic field created in the middle of the wrinkle which is of order 10 T for $\chi = 100$nm [198]. However the given solution suffers from slope discontinuity at $x = 0$, as mentioned by Yamamoto et al., which means it may not follow a Catenary-like profile, and the expression of this proposed minimizer could be incorrect and as a matter of a fact leads to imprecise approximations of the desired morphological characteristics of the wrinkling.
Furthermore, it is not verified if this singular solution is the minimizer of the energy, nor that the associated ridge length is the critical distance between the two nanoparticles, knowing that this latter is in rough agreement with the observed maximum wrinkle length of approximately 200nm.

For all these reasons and in order to improve the results, Guedda et al. [69] presented a mathematical study of the same problem based on the phase-plane analysis, and identified a C^1-smooth minimizer deflection of the elastic energy, in terms of the inverse of an incomplete normalized beta function which kind of corrects the singularity from which Yamamoto's solution suffers. It is stated that Graphene is deflected in a smooth manner, and the maximum wrinkle length is explicitly given by:

$$\chi_c = 2\, C\, d^{\frac{3}{2}}\, \beta\left(\frac{3}{2}, \frac{3}{4}\right), \tag{1.2}$$

where C is a physical constant, d is the nanoparticle's size and β is the complete beta function.
This obtained critical wrinkle length using this smooth deflection improved compared to the previous results, however is still underestimated ([69]).

On the other hand, Zhu and Li [211] presented a systematic molecular dynamics study of the wrinkling of graphene put on a silica substrate, and the critical wrinkle length is determined as a second degree polynomial which depends only on the nanoparticle's size d:

$$\chi_c = 2.64d^2 + 0.96d + 9.2. \tag{1.3}$$

By taking $d = 7.4$, the authors obtained a numerical value of χ_c similar to the one obtained by Yamamoto et al. . We might deduce that the results obtained by Zhu and Li overestimate the critical distance.

Our initial aim in this chapter is not to introduce another physical study of the wrinkling of graphene. Rather, an effort is made to provide a numerical algorithm that determines the critical ridge length below which wrinkling is induced, and which can be used in a more general context. The algorithm we'll be using is the Grey Wolf Optimizer (GWO) which is a swarm-based meta-heuristic based on the social leadership and hunting behavior of grey wolves in nature (Canis Lupus), mathematically modeled by Mirjalili et al. in [117]. The obtained results show that the proposed approach provides us with a good wrinkle length in comparison with what's found in previous works.

This chapter is organised as follows: in the next section, we present in details the physical model on which we'll be basing our numerical analysis. The associated Euler-Lagrange equation is presented. The third section is dedicated to the numerical simulation using the classical method that turns out to be very hard to tackle, which will be our motivation behind using the GWO algorithm that will be described in the first subsection of the fourth section and implemented in the second one. Finally, we draw a conclusion from the showcased results.

1.2 Formulation of the Physical Problem of the Wrinkled Graphene in Terms of Optimization

The model on which we will base our numerical analysis on is the one derived by Yamamoto et al., depicted in Figure 1.1.

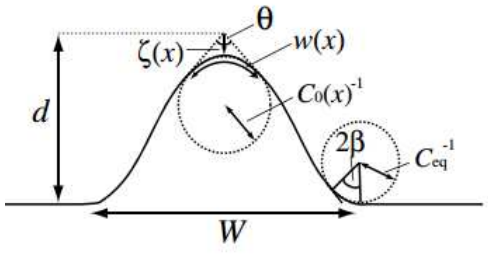

Figure 1.1: The wrinkle profile along the transverse direction.

In the deformed region, or the x projection of the wrinkling region ($i.e.\ |x| < \frac{\chi}{2}$), the elastic energy is expressed as a summation of the stretching energy given by:

$$\boxed{E_s = \frac{\mathrm{E_{2D}}}{2} \int_{|x|<\frac{\chi}{2}} \omega(x)\varepsilon_x^2 dx,} \tag{1.4}$$

and the bending energy given by:

$$\boxed{E_b = \frac{\mathrm{k}}{2} \int_{|x|<\frac{\chi}{2}} \omega(x) C_0^2(x) dx,} \tag{1.5}$$

where $\mathrm{E_{2D}} \approx 2.12 \times 10^3\ ev/nm^2$ is the tensile rigidity [211], $\mathrm{k} \approx 1\ ev$ is the bending rigidity [103], ω is the width of the deformed region, ε_x is the stretching strain which is supposed to be irrelevant in the y-direction, C_0 is the curvature that describes the profile of the ridge along the transverse direction, and θ is the dihedral angle which is assumed to be independant of x as validated in [111].

Now, using the geometrical model given in Figure 1.1, we obtain:

$$\sin\left(\frac{\theta}{2}\right) = \frac{C_0^{-1}(x)}{\zeta(x) + C_0^{-1}(x)}, \tag{1.6}$$

which implies that

$$C_0 = \zeta(x) \left[\frac{1}{\sin(\frac{\theta}{2})} - 1\right]^{-1}. \tag{1.7}$$

Furthermore, we have

$$\omega(x) = (\pi - \theta) C_0^{-1}(x), \tag{1.8}$$

and

$$\varepsilon_x = [1 + (\partial_x \zeta)^2]^{\frac{1}{2}} - 1] \approx \frac{(\partial_x \zeta)^2}{2}. \tag{1.9}$$

As a consequence, by replacing each term in (1.4) and (1.5) by its corresponding expression, the elastic energy is written as:

$$\boxed{E(\zeta) = \varepsilon_1(\theta) \int_{|x|<\frac{\chi}{2}} \zeta\, (\partial_x \zeta)^4 dx + \varepsilon_2(\theta) \int_{|x|<\frac{\chi}{2}} \zeta^{-1} dx,} \tag{1.10}$$

where

$$\begin{cases} \varepsilon_1(\theta) & = \frac{E_{2D}}{8}(\pi-\theta)\left[\frac{1}{\sin(\frac{\theta}{2})}-1\right]^{-1}, \\ \varepsilon_2(\theta) & = \frac{k}{2}(\pi-\theta)\left[\frac{1}{\sin(\frac{\theta}{2})}-1\right]. \end{cases} \tag{1.11}$$

On the other hand, the adhesion energy to the substrate is proportional to the area of the substrate uncovered by the membrane: :

$$E_a = \Gamma \int_{|x|<\frac{\chi}{2}} W dx, \tag{1.12}$$

in which W is the base of the wrinkle profile as depicted in Figure 1.1.

Again, from the geometrical model, we have

$$\tan\left(\frac{\theta}{2}\right) = \frac{W}{2d} \tag{1.13}$$

hence (1.12) becomes

$$\boxed{E_a = 2\Gamma\chi\, d\, \tan\left(\frac{\theta}{2}\right)} \tag{1.14}$$

where Γ is the graphene-SiO_2 adhesion energy per area.

Furthermore, we have a bending and adhesion energies at the foot of the wrinkle, i.e. at the point where graphene touches the substrate. They are given by:

$$\boxed{E_{b'} = \chi\left(\frac{\Gamma k}{2}\right)^{\frac{1}{2}}(\pi-\theta)} \tag{1.15}$$

and

$$\boxed{E_{a'} = \chi\,(2\,\Gamma\,\chi)^{\frac{1}{2}}\tan\left(\frac{\pi-\theta}{4}\right)} \tag{1.16}$$

However, these two energies turn out to be negligible [198].

Finally, the expression of the total energy is given as the sum of all these energies:

$$\mathscr{J}(\zeta) = E(\zeta) + E_a + E_{a'} + E_{b'}. \tag{1.17}$$

As mentioned in the introduction, the authors in [198] claim that (1.1) is the exact expression of the

minimizer of the total energy (1.17). This latter led to a critical wrinkle length given by:

$$\chi_c = d^{\frac{3}{2}} \left(\frac{64 E_{2D}}{27k} \right)^{\frac{1}{4}} \left[\frac{1}{\sin(\frac{\theta}{2})} - 1 \right]^{-\frac{1}{2}} \tag{1.18}$$

However the given solution suffers from slope discontinuity at $x = 0$, which means it doesn't necessarily follow a Catenary-like profile and then the expression (1.18) may be not correct.

On the other hand, in [69], Guedda et al. provided an improved estimate of the critical wrinkle length given by:

$$\chi_c = d^{\frac{3}{2}} \left(\frac{3 E_{2D}}{4k} \right)^{\frac{1}{4}} \left[\frac{1}{\sin(\frac{\theta}{2})} - 1 \right]^{-\frac{1}{2}} \bar{\chi}, \tag{1.19}$$

in which $\bar{\chi}$ is the inverse of an incomplete normalized beta function that corrects the singularity from which Yamamoto's solution suffers. Using this minimizer instead of (1.1) led to better results, however still not sufficiently close to the observed length which attains 200 *nm*.

It is worth mentioning that in the previous works, the dihedral angle θ depicted in Figure 1.1 is usually assumed to vary arbitrarily, which is physically not very accurate since the optimal graphene shape we obtain must have a critical angle that minimizes the total energy (1.17), which becomes $\mathscr{J}(\zeta, \theta)$. For this aim, Guedda et al. injected the expression of the critical wrinkle length given by (1.19) in the expression of the total energy (1.17). However, the expression of the new total energy made the minimization problem impossible to solve analytically. Therefore, for any analytical progress the critical opened angle which minimizes the new total energy will be evaluated in two opposite regimes depending on whether $C_{eq} d >> 1$ (the strong adhesion limit) or $C_{eq} d << 1$ (the weak adhesion limit). For intermediate regimes, the opened angle can only be determined numerically.

In this chapter, we hope to provide a numerical investigation that allows us to identify the critical wrinkle length associated to the critical dihedral angle θ_c that minimizes the energy.

First of all, we set a well posed mathematical formulation by adding a set of constraints. The problem is to minimize the energy $\mathscr{J}$ defined by :

$$\begin{cases} \mathscr{J}(\zeta) = \varepsilon_1(\theta) \displaystyle\int_{|x|<\frac{\chi}{2}} \zeta \, (\zeta_x)^4 + \varepsilon_2(\theta) \int_{|x|<\frac{\chi}{2}} \zeta^{-1} + 2\Gamma \chi d \tan\left(\frac{\theta}{2}\right) \\ \\ \text{subject to } \zeta(\pm\frac{\chi}{2}) = 0. \end{cases} \tag{1.20}$$

The functional defined above can be rewritten using a change of variable $v = \zeta^{\frac{5}{4}}$:

$$\begin{cases} \mathscr{J}(v) = \left(\frac{4}{5}\right)^4 \varepsilon_1(\theta) \int_{|x|<\frac{\chi}{2}} (v_x)^4 + \varepsilon_2(\theta) \int_{|x|<\frac{\chi}{2}} v^{-\frac{4}{5}} + 2\Gamma\chi d \tan\left(\frac{\theta}{2}\right) \\ \\ \text{subject to } v(\pm\frac{\chi}{2}) = 0. \end{cases} \tag{1.21}$$

One should proceed carefully when tackling this minimization problem since the functional $\mathscr{J}$ is a sum of two opposing terms. Finding a minimum translates to finding a balance between the competing integrals. To illustrate this we consider $\zeta(x) = (1-|x|)$, the integral $\int_{|x|<\frac{\chi}{2}} \zeta\,(\zeta_x)^4$ is almost minimal but the other integral is actually divergent.

Now, let χ be fixed.

We start by insuring the existence of a suitable minimum for (2.22).

Theorem 1

The functional $\mathscr{J}$ admits a local minimum v in K that satisfies the associated Euler-lagrange equation:

$$\begin{cases} -\varepsilon_1(\theta)(v_x^3)_x = \frac{5^3}{4^4}\varepsilon_2(\theta) v^{\frac{-9}{5}} \qquad \mathscr{D}'(]-\frac{\chi}{2},\frac{\chi}{2}[) \\ \qquad\qquad\qquad v(\pm\frac{\chi}{2}) = 0, \end{cases} \tag{1.22}$$

where:

$$K = \left\{ v \in W^{1,4}_{loc}(]-\frac{\chi}{2},\frac{\chi}{2}[) / v^{-\frac{4}{5}} \in L^1(]-\frac{\chi}{2},\frac{\chi}{2}[) \text{ and } v^{\frac{6}{5}} \in W^{1,4}_0(]-\frac{\chi}{2},\frac{\chi}{2}[) \right\}.$$

Proof.

Let us consider the functional :

$$\begin{array}{rccc} \Phi & : & L^2(]-\frac{\chi}{2},\frac{\chi}{2}[) & \to & \mathbb{R} \\ & & v & \mapsto & \Phi(v) \end{array} = \begin{cases} \mathscr{J}(v) & v \in K \\ +\infty & \text{if not} \end{cases} \tag{1.23}$$

In order to prove that Φ admits a local minimum in the non-empty subset, we will proceed by the direct method.

First, if we let $u_{th} = \left(\frac{\chi}{2} - |x|\right)^{\frac{2}{3}}$ be the theoretical solution given by (1.1)*, then $v_{th} := u_{th}^{\frac{5}{4}} = \left(\frac{\chi}{2} - |x|\right)^{\frac{5}{6}}$ belongs to K.*

Furthermore, the subset $V = \{\Phi(v) / \ v \in K\}$ is nonempty and bounded from below. Indeed, we have

$v < v_0$, where $v_0 = \max_{x\in]-\frac{\chi}{2},\frac{\chi}{2}[} v(x)$. Hence

$$\int_{|x|<\frac{\chi}{2}} v^{-\frac{4}{5}} > \chi\ {v_0}^{-\frac{4}{5}}. \tag{1.24}$$

Using the Jensen's inequality for the first integral in (2.22)*, we obtain*

$$\begin{aligned}
\frac{1}{\chi}\int_{|x|<\frac{\chi}{2}} (v_x)^4\,dx &= \frac{2}{\chi}\int_0^{\frac{\chi}{2}} (v_x)^4\,dx \\
&\geq \left(\frac{2}{\chi}\right)^4 \left(\int_0^{\frac{\chi}{2}} (v_{0x})\,dx\right)^4 \\
&\geq 2^4\chi^{-4}\left(v\left(\frac{\chi}{2}\right) - v_0\right)^4 \\
&\geq 2^4\chi^{-4}{v_0}^4.
\end{aligned}$$

which implies

$$\int_{|x|<\frac{\chi}{2}} (v_x)^4 \geq 2^4\chi^{-3}{v_0}^4, \quad \forall\chi > 0. \tag{1.25}$$

i.e. we have

$$\Phi(v) \geq \left(\frac{4}{5}\right)^4 \varepsilon_1(\theta)2^4\chi^{-3}{v_0}^4 + \varepsilon_2(\theta)\chi\ {v_0}^{-\frac{4}{5}} + 2\Gamma\chi d\tan\left(\frac{\theta}{2}\right). \tag{1.26}$$

A simple computing of the minimum of the right term in equation (1.26) *leads to*

$$\Phi(v) \geq C\,\chi^{\frac{1}{3}}. \tag{1.27}$$

We can then take a minimizing sequence v_n i.e. such that $\Phi(v_n) \to \inf_{v\in K}\Phi(v)$.
Hence, for all $\varepsilon > 0$, there exists $\eta_0 > 0$, such that for all $\eta > \eta_0$:

$$\frac{L}{2} \leq \mathscr{J}(v_n) \leq \frac{3L}{2}, \quad L := \inf_{v\in K}\mathscr{J}(v). \tag{1.28}$$

Consequently:

$$\int_{-\frac{\chi}{2}}^{\frac{\chi}{2}} |\ v_{nx}\ |^4\,dx \leq 4\left(\frac{3L}{2} - \int_{-\frac{\chi}{2}}^{\frac{\chi}{2}} {v_n}^{\frac{-4}{5}}\right). \tag{1.29}$$

This means that v_n is bounded in $W_0^{1,4}(]-\frac{\chi}{2},\frac{\chi}{2}[)$. We then pick a subsequence, still denoted v_n that converges to v weakly in $W_0^{1,4}(]-\frac{\chi}{2},\frac{\chi}{2}[)$, strongly in $L^4(]-\frac{\chi}{2},\frac{\chi}{2}[)$ and $v_n(x) \longrightarrow v(x)$ a.e in $(]-\frac{\chi}{2},\frac{\chi}{2}[)$ up to subsequences.

Since $W_0^{1,p}$ is injected in the space of Holder continuous functions C^α, it follows that v_n converges uniformly to v in K, and we have

$$\underline{lim}\int_0^{\frac{\chi}{2}} \mid v_{nx} \mid^4 dx \geq \int_0^{\frac{\chi}{2}} \mid v_x \mid^4 dx. \tag{1.30}$$

Furthermore, we have

$$\begin{aligned}
\int_0^{\frac{\chi}{2}} \mid v_x \mid^4 + \int_0^{\frac{\chi}{2}-\varepsilon} v^{\frac{-4}{5}} &\leq \liminf_{n\to+\infty} \int_0^{\frac{\chi}{2}} \mid v_{nx} \mid^4 + lim \int_0^{\frac{\chi}{2}-\varepsilon} v_n{}^{\frac{-4}{5}} && (1.31)\\
&\leq \liminf_{n\to+\infty} \int_0^{\frac{\chi}{2}} \mid v_{nx} \mid^4 + lim \int_0^{\frac{\chi}{2}} v_n{}^{\frac{-4}{5}} && (1.32)\\
&\leq \liminf_{n\to+\infty} \int_0^{\frac{\chi}{2}} \mid v_{nx} \mid^4 + \liminf_{n\to+\infty} \int_0^{\frac{\chi}{2}} v_n{}^{\frac{-4}{5}} && (1.33)\\
&\leq \liminf_{n\to+\infty} \mathscr{J}(v_n) := \inf_{v\in K} \mathscr{J}(v). && (1.34)
\end{aligned}$$

Finally: $L \leq \mathscr{J}(v) \leq \liminf_{n\to+\infty} J(v_n) \leq L$, i.e $\mathscr{J}(v) = \inf_{v\in K} \mathscr{J}(v)$.

Furthermore, Let $\phi \in \mathscr{C}_c^\infty(]-1,1[)$, and $\nu > 0$ sufficiently small such that:

$$\forall t \in]-\nu,\nu[\quad v + t\phi \in K.$$

We have:

$$\begin{aligned}
\frac{\partial}{\partial t}\left(J(v+t\phi)\right)_{t=0} &= \int_{-1}^{1} \frac{4^5}{5^4}\varepsilon_1 v_x^3 \frac{\partial}{\partial t}(v_x + t\phi_x) - \frac{4}{5}\varepsilon_2 v^{-\frac{9}{5}} \frac{\partial}{\partial t}(v+t\phi) && (1.35)\\
&= \int_{-1}^{1} \frac{4^5}{5^4}\varepsilon_1 v_x^3 \phi_x - \int_{-1}^{1} \frac{4}{5}\varepsilon_2 v^{-\frac{9}{5}}\ \phi. && (1.36)
\end{aligned}$$

Since v is a minimum, we obtain that equation (1.22) *is satisfied in the sense of distributions.*

1.3 Classical Optimization Approaches and Algorithms

As mentioned in [198], a wrinkle is geometrically suppressed if $v(0) >= d^{5/4}$, hence the maximum length of a wrinkle will be determined under the condition $v(0) = d^{5/4}$. Note that $v(0)$ is in fact $v_{\chi,\theta}(0)$

denoted like that for simplification. We express the optimization problem as follows:

$$\begin{cases} \textit{Minimize} \quad \mathscr{F}(\chi,\theta) = \mid v(0) - d^{5/4} \mid^2 \\ \text{where } v \text{ is the unique solution to (1.22).} \end{cases} \tag{1.37}$$

The Lagrangian is then given by:

$$\mathscr{L}(v,\phi,\theta,\chi) = \mathscr{F}(\chi,\theta) + \varepsilon_1(\theta)\int_{|x|<\frac{\chi}{2}} v_x^3\phi_x\, dx - \frac{5^3}{4^4}\varepsilon_2(\theta)\int_{|x|<\frac{\chi}{2}} v^{\frac{-9}{5}}\phi\, dx. \tag{1.38}$$

Using the rapid derivation [44], we obtain:

(i)- $-\varepsilon_1(\theta)((v_x)^3)_x = \frac{5^3}{4^4}\varepsilon_2(\theta)\, v^{\frac{-9}{5}}$.

(ii)- $-\frac{4^4}{5^3}3\varepsilon_1(\theta)(v_x^2\phi_x)_x + \frac{9}{5}\varepsilon_2(\theta)v^{\frac{-14}{5}}\phi = -2(v(0)-d^{5/4})\,\delta_0$, where δ_0 is a dirac mass at the origin.

(iii)- $\mathscr{F}'(\theta) = -\dfrac{\partial}{\partial\theta}\varepsilon_1(\theta)\displaystyle\int_{|x|<\frac{\chi}{2}} v_x^3\phi_x + \frac{5^3}{4^4}\frac{\partial}{\partial\theta}\varepsilon_2(\theta)\int_{|x|<\frac{\chi}{2}} v^{\frac{-9}{5}}\phi$.

(iiii)- $\mathscr{F}'(\chi) = -\frac{1}{2}\frac{4^4}{5^3}\varepsilon_1(\theta)[(v_x(\frac{\chi}{2}))^3\phi_x(\frac{\chi}{2}) + (v_x(\frac{-\chi}{2}))^3\phi_x(\frac{-\chi}{2})]$.

The first equation can be solved using the regularized problem as one can see later on, but the second one is very hard to tackle if not impossible due to the degeneracy of its first term, which is our motivation behind using meta-heuristics. The main steps of this classical method using the finite elements are described in Algorithm 1 , where V_h is the P^1 finite element space, χ the distance between the two nanoparticles of diameters d, ε the tolerance, α, β and η are the steps of the gradient descent.

Indeed, unlike the classial methods, meta-heuristics have derivation-free mechanisms: the selected solution(s) to start the optimization process with are randomly chosen, which is key in meta-heuristics. Furthermore, it is not necessary to calculate the derivatives of the search spaces to find the optimum, which makes these methods very suitable for our problem although much slower than the classical methods. Due to the stochastic nature of meta-heuristics, these algorithms are excellent in avoiding local optima compared to classical optimization techniques. This makes them capable of looking for the optimum in the entire search space.

It is worth mentioning that the No Free Lunch (NFL) theorem [193], has logically proved that there is no such thing as a perfect meta-heuristic, which means it might seem that one meta-heuristic is best-suited

Algorithm 1 Steps of the classical method

while $|v^n - v^{n-1}| \geq \varepsilon$ **do**

• Solve for w^n the equation below $\forall \psi \in V_h$

$$\int_{|x|<\frac{\chi}{2}} w_x^n \psi_x \quad = \quad \int_{|x|<\frac{\chi}{2}} \varepsilon_1(\theta)((v_x^n)^3)\psi_x - \frac{5^3}{4^4}\varepsilon_2(\theta)(v^n)^{\frac{-9}{5}}\psi.$$

• Update $v^n \leftarrow v^n - \alpha\, w^n$

end while

• Solve the equation below $\forall h \in V_h$

$$\frac{4^4}{5^3}3\varepsilon_1(\theta)\int_{|x|<\frac{\chi}{2}}((v_x^n)^2)\phi_x^n h_x + \frac{9}{5}\varepsilon_2(\theta)\int_{|x|<\frac{\chi}{2}}(v^n)^{\frac{-14}{5}}\phi^n h = -2(v^n(0) - d^{5/4})h(0).$$

• Solve the equation below:

$$Y^n = -\frac{\partial}{\partial\theta}\varepsilon_1(\theta)\int_{|x|<\frac{\chi}{2}} v_x^3\phi_x + \frac{5^3}{4^4}\frac{\partial}{\partial\theta}\varepsilon_2(\theta)\int_{|x|<\frac{\chi}{2}} v^{\frac{-9}{5}}\phi.$$

• Update $\theta^n \leftarrow \theta^n - \eta Y^n$

• Solve the equation below:

$$Z^n = -\frac{1}{2}\frac{4^4}{5^3}\varepsilon_1(\theta)[((v_x^n)^3(\frac{\chi}{2}))\phi_x^n(\frac{\chi}{2}) + ((v_x^n)^3(\frac{-\chi}{2}))\phi_x^n(\frac{-\chi}{2})].$$

• Update $\chi^n \leftarrow \chi^n - \beta Z^n$

for one problem but may show very poor efficiency on another problem, which makes this field of study highly active, as there are always new proposed algorithms.

Some of the most well-known meta-heuristics, mainly inspired by optimization processes that occur in nature, and which are used in many works where the classical methods of Newton or fixed point type are not efficient as in [87], are: Particle Swarm Optimization (PSO), Genetic Algorithm (GA), Ant Colony Optimization (ACO), Evolution Strategy, Marriage in Honey Bees optimization (MBO), Monkey search, Bee collecting Pollen Algorithm, Bird Mating optimizer, and finally the relatively recent algorithm Grey Wolf Optimizer (GWO) based on the social hierarchy of grey wolves. This latter has shown very high performance compared to the other known meta-heuristics, we refer the reader to ([117], [118]) for detailed comparisons. In the next sections, the GWO algorithm is employed to minimize our cost function $\mathscr{F}$, and its effectiveness for our problem is evaluated by comparing the results we obtain with those obtained in literature.

1.4 An Enhanced GWO Algorithm for The Determination of the Critical Wrinkle Length of Graphene

1.4.1 Review of the GWO Search Algorithm

The GWO is a swarm-based meta-heuristic based on the social leadership and hunting behavior of grey wolves in nature (Canis Lupus), mathematically modeled by [117]. The population of this algorithm is divided into four populations: alpha (α), beta (β), delta (δ) and omega (ω) (see Figure 1.2).

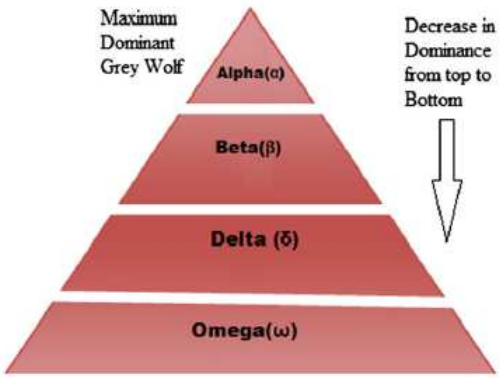

Figure 1.2: Hierarchy levels of grey wolves.

Alpha is the first category, its members are not chosen by their strength or violence but by their intelligence and decision making capacity. Beta is the second category, they help the alphas make decisions and they take their places in case one of them is absent or sick. The third category is Delta, its members are scouts, sentinels and hunters. Scouts are responsible for warning the pack in case of danger. Sentinels are responsible for the safety of the pack and hunters are the ones who help the alphas and betas during the hunt. The last category of the pack is omega. Omega wolves have to execute all the orders of the dominant wolves. The members of this class are usually the elders and the caretakers.

Alpha, beta and delta are stored as the three best solutions and the other wolves (omega) are forced to update their positions around them as follows:

$$\begin{cases} \overrightarrow{D} = \mid \overrightarrow{C}.\overrightarrow{X_p}(t) - \overrightarrow{X}(t) \mid \\ \overrightarrow{X}(t+1) = \overrightarrow{X_p}(t) - \overrightarrow{A}.\overrightarrow{D} \end{cases} \tag{1.39}$$

Where t indicates the current iteration, $\overrightarrow{A} = 2a.\overrightarrow{r_1} - a$, $\overrightarrow{C} = 2.\overrightarrow{r_2}$, $\overrightarrow{X_p}$ is the position vector of the prey,

$\overrightarrow{X}$ indicates the position vector of a grey wolf, a is linearly decreased from 2 to 0 for better exploration of candidate solutions which tend to diverge when $|\overrightarrow{A}|>1$ and to converge when $|\overrightarrow{A}|<1$ as shown in Figure (1.3) and $\overrightarrow{r_1}$, $\overrightarrow{r_2}$ are random vectors in $[0,1]$.

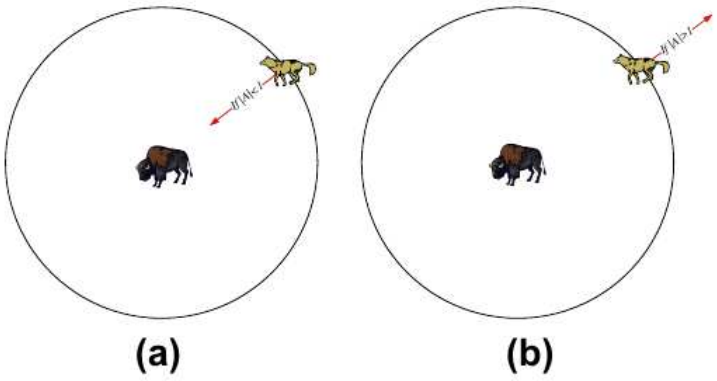

Figure 1.3: Attacking prey ($|\overrightarrow{A}|<1$) versus searching for prey($|\overrightarrow{A}|>1$).

Over the course of iterations, the first three fittest solutions we obtain so far are considered as α, β and δ respectively, which guide the optimization processus (the hunting) and are assumed to take the position of the optimum (the prey). The rest of the wolves are considered as ω and are required to encircle α, β and δ in order to find better results at each iteration, by following these three equations which calculate the approximate distance between the current solution and alpha, beta, and delta respectively:

$$\begin{cases} \overrightarrow{D}_\alpha = |\overrightarrow{C_1}.\overrightarrow{X_\alpha} - \overrightarrow{X}| \\ \overrightarrow{D}_\beta = |\overrightarrow{C_1}.\overrightarrow{X_\beta} - \overrightarrow{X}| \\ \overrightarrow{D}_\delta = |\overrightarrow{C_1}.\overrightarrow{X_\delta} - \overrightarrow{X}| \end{cases} \tag{1.40}$$

$\overrightarrow{C_1}$, $\overrightarrow{C_2}$ and $\overrightarrow{C_3}$ are random vectors. $\overrightarrow{X_\alpha}$, $\overrightarrow{X_\beta}$ and $\overrightarrow{X_\delta}$ are the positions of alpha, beta and delta respectively and $\overrightarrow{X}$ is the position of the current solution.

After calculating the three distances, the final position of the solution is given by:

$$\overrightarrow{X}(t+1) = \frac{\overrightarrow{X_1} + \overrightarrow{X_2} + \overrightarrow{X_3}}{3}, \tag{1.41}$$

where:

$$\begin{cases} \overrightarrow{X_1} = \overrightarrow{X_\alpha} - \overrightarrow{A_1}.\overrightarrow{D}_\alpha \\ \overrightarrow{X_2} = \overrightarrow{X_\beta} - \overrightarrow{A_2}.\overrightarrow{D}_\beta \\ \overrightarrow{X_3} = \overrightarrow{X_\delta} - \overrightarrow{A_3}.\overrightarrow{D}_\delta \end{cases} \tag{1.42}$$

$\overrightarrow{A_1}$, $\overrightarrow{A_2}$ and $\overrightarrow{A_3}$ are random vectors.

1.4.2 Application and Implementation

Our implementation generates a population of potential solutions (wolves), they take the form of the couple (χ, θ). The fittest solution is considered as the alpha, and the second and third best solutions are considered as beta and delta respectively. The initial population is created in a random way based on the upper and lower bounds chosen for the variables χ and θ. Then we initialize the position and the score of each search agent, and we return back the search agents that go beyond the lower and upper bounds of the search space. Next, we compute the solution v that corresponds to every wolf in the population, and we deduce the minimizer of the cost function (3.2).

The GWO implemented in the context of this problem follows the guidelines:

• **Fitness computation**: The objective function is what is called the fitness in the algorithm. It is computed to estimate the quality of the obtained solution. In our case, in order to compute it, for each (χ, θ), we need the value of $v(0)$, where v is the solution of (1.22). For this purpose, we transform (1.22) into:

$$\begin{cases} -(\mid v_x \mid^2 v_x)_x = -\rho'_\varepsilon(\mid v \mid) \qquad \mathscr{D}'(]-\frac{\chi}{2}, \frac{\chi}{2}[) \\ \qquad\qquad\qquad\qquad v(\pm\frac{\chi}{2}) = 0, \end{cases} \tag{1.43}$$

where :

$$\rho_\varepsilon(r) = \begin{cases} -\varepsilon^{-\frac{9}{5}} r + \frac{9}{4}\varepsilon^{-\frac{4}{5}} & 0 \le r < \varepsilon \\ \frac{5}{4} r^{-\frac{4}{5}} & r \ge \varepsilon \end{cases} \tag{1.44}$$

To determine the solution v, we use the finite elements as in Algorithm 1, and we solve the equation

below , for every direction ψ in the P^1 finite elements space:

$$\int_{|x|<\frac{\chi}{2}} w_x^n \psi_x \quad = \quad \int_{|x|<\frac{\chi}{2}} \varepsilon_1(\theta)((v_x^n)^3)\psi_x - \frac{5^3}{4^4}\varepsilon_2(\theta)(v^n)^{\frac{-9}{5}}\psi$$

and then we update the solution at each iteration :$v^{n+1} \leftarrow v^n - \alpha\, w^n$.

Finally, we determine $v(0)$ and calculate the cost function.

• **Selection**: We select the first three best wolves to guide the optimization (hunting) and save them as α, β and δ.

• **Update**: We update the positions of the search agents according to the positions of each category, and the parameters a, A and C. Finally, the algorithm is terminated when the end criterion is satisfied. The final generated result is the position of the alpha which is assumed to be the optimum (χ_c, θ_c), and the score of the alpha that is the value of the cost function at this optimum.

1.4.3 An enhanced GWO Search Algorithm and Results

Following the previous explanation of the implementation used in our program, the main steps of the GWO applied to the optimization problem (3.2) are given in Algorithm 2 which we implement for 40 search agents and 80 iterations.

Algorithm 2 The Grey Wolf Optimizer (GWO).

1: Initialize the input parameters for GWO, i.e the number of search agents, the dimension of the problem, maximum number of iterations, lower and upper bounds of the search spaces of the variables χ and θ, and the diameter d of the silica nanoparticle.
2: Initialize Alpha, Beta and Delta Position and Score.
3: Initialize the random positions of search agents.
4: Set iteration counter = 0.
5: While ($t < MaxIter$) or (stop criterion);
6: Return back the search agents that go beyond the lower and upper bounds of the search space.
7: Calculate the corresponding objective value for each wolf.
8: Select the first three best wolves and save them as α, β and δ.
9: Update the position of the rest of the population (the ω wolves) using (1.40) and (1.42).
10: Update the parameters a, A and C.
11: Go back to step (b) if the end criterion is not satisfied.
12: Return the position of α as the fittest optimum (χ_c, θ_c).

We investigate the critical angle θ_c in two different search spaces: the first one is the neighboring of 14^o and the second one is the neighboring of 35^o. Finally, for different diameters and each critical angle, we present the maximal wrinkle length χ_c obtained by the given expressions ((1.3), (1.18) and (1.19)) from the previous works on one hand, and by our algorithm on the other hand, in the tables below. Note

that the mean diameter of a silica nanoparticle is 7.4 ± 2.2 nm. The figures (1.4, 1.5, 1.6) are the 3d

Table 1.1 The critical wrinkle lengths for $d = 4.6nm$.

	χ_c (nm)	
Algorithm	$\theta_c = 15^o$	$\theta_c = 35.4432^o$
Yamamoto et al.	32.1844	54.9489
Zhu and Li	69.4784	69.4784
Guedda et al.	46.2731	79.0028
GWO	48.8693	83.4092

Table 1.2 The critical wrinkle lengths for $d = 5.2nm$.

	χ_c (nm)	
Algorithm	$\theta_c = 12^o$	$\theta_c = 35.9015^o$
Yamamoto et al.	34.1066	66.6375
Zhu and Li	85.5776	85.5776
Guedda et al.	49.0367	95.8080
GWO	52	101.40

Table 1.3 The critical wrinkle lengths for $d = 7.4nm$.

	χ_c (nm)	
Algorithm	$\theta_c = 15^o$	$\theta_c = 34.6869^o$
Yamamoto et al.	65.6684	110.4531
Zhu and Li	160.8704	160.8704
Guedda et al.	94.4147	158.8039
GWO	100	168.0948

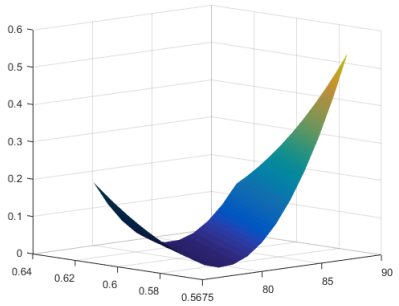

Figure 1.4: The 3d plot of the cost function vs χ and θ for $d = 4.6$ and θ in the neighborhood of 35^o .

plots of the cost function $\mathscr{F}$ in function of the critical angle θ_c and the critical length χ_c, associated to a diameter d. These plots agree well with the results presented in the tables since the function is convex at the exact optimums (θ_c, χ_c) obtained by the GWO. Indeed, using the Grey Wolf Optimizer allowed us to numerically obtain good results in comparison with the other analytical methods, however, the observed

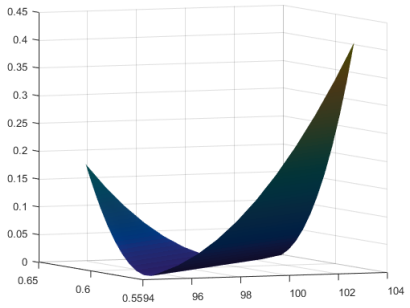

Figure 1.5: The 3d plot of the cost function vs χ and θ for $d = 5.2$ and θ in the neighborhood of 35^o.

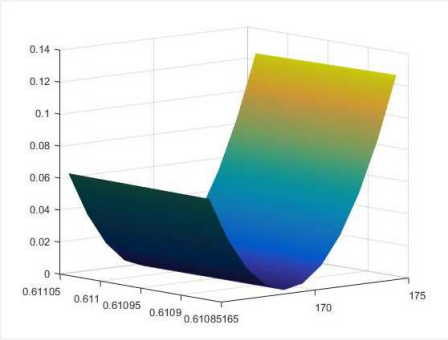

Figure 1.6: The 3d plot of the cost function vs χ and θ for $d = 7.4$ and θ in the neighborhood of 35^o .

maximum wrinkle length of 200*nm* is still underestimated.

1.5 Conclusion

Using the Grey Wolf Optimizer algorithm, we were able to determine the critical length below which wrinkling is induced, i.e if the distance between the two nanoparticles exceeds this critical length, the caternary-like profile of the wrinkle is suppressed. Using this algorithm, we were also able to determine the critical dihedral angle θ_c that minimizes our energy for different values of the nanoparticle's diameters. However, the observed maximum wrinkle length is still underestimated. This is actually kind of expected since our study does not include the possibilty of the two nanoparticles that might have different diameters, as mentioned by [198], and hence the wrinkle won't have to sag in the middle, nor that the random distribution of the nanoparticles might cause that the interaction between ridges could influence the maximum wrinkle length and introduce some complicated boundary conditions, [69]. Last but not least, another possible cause behind the discrepancy between the obtained and the observed results is the other physical mechanisms such as the thermal fluctuations and the impurites that might exist on the

substrate surface. This motivates the next chapter in which we treat the case when the nanoparticles have different diameters.

Chapter 2

Analytical results for the wrinkling of graphene on nanoparticles with different diameters.

2.1 Introduction

As mentioned before, one possible cause behind the discrepancy between the analytical and the observed results is that the two silica nanoparticles don't necessarily have the same size. Regarding the aforementioned point, our present purpose is to present a mathematical study of the wrinkling of graphene between two nanoparticles with different heights d and $d-\delta$, for $\delta > 0$ and $\frac{\delta}{d} \ll 1$, separated by a distance χ^{δ}. In particular, the aim is to determine the dependence of some graphene properties on the quantity δ. For example, the electronic property of the graphene in the middle. In [69], the authors showed that the pseudomagnetic field has, in the middle of a wrinkle, a broad minimum on the order of 10 T (for $\chi = 100nm$), while in [198] it is concluded that the middle of the wrinkled graphene may have a zero pseudomagnetic field. In fact, since the pseudomagnetic field varies linearly with the strain distribution along a wrinkle described by the deflection profile, the initial motivation of the present work concerns a mathematical analysis to investigate whether or not the first derivative of the profile vanishes at the middle.

The problem is to minimize the energy $\mathscr{J}$ defined by :

$$\begin{cases} \mathscr{J}(\zeta) = \varepsilon_1 \int_{\frac{\chi_-^\delta}{2}}^{\frac{\chi_+^\delta}{2}} \zeta\,(\zeta_x)^4 + \varepsilon_2 \int_{\frac{\chi_-^\delta}{2}}^{\frac{\chi_+^\delta}{2}} \zeta^{-1} + 2\Gamma\chi^\delta \left(d - \frac{\delta}{2}\right) \tan\left(\frac{\theta}{2}\right) \\ \\ \qquad \text{subject to } \zeta\left(\frac{\chi_-^\delta}{2}\right) = 0 \text{ and } \zeta\left(\frac{\chi_+^\delta}{2}\right) = \delta, \end{cases} \tag{2.1}$$

in which ε_1, ε_2, θ and Γ are the same as in the previous chapter, and χ_-^δ, χ_+^δ are to be determined. Note that $\chi_-^\delta \leq 0$ and $\chi_+^\delta \geq 0$.

To help minimize (2.1), we observe that the boundary conditions do not introduce any change depending on ζ. Therefore, the wrinkling profile has to satisfy the similar equilibrium equation with appropriate boundary conditions:

$$\begin{cases} 3(\zeta_x)^4 + 12\zeta(\zeta_x)^2\zeta_{xx} + \lambda^2\zeta^{-2} = 0, \\ \\ \text{subject to } \zeta\left(\frac{\chi_-^\delta}{2}\right) = 0 \text{ and } \zeta\left(\frac{\chi_+^\delta}{2}\right) = \delta, \end{cases} \tag{2.2}$$

where $\lambda = \sqrt{\frac{4k}{E_{2D}}}\left[\frac{1}{\sin(\frac{\theta}{2})} - 1\right]$.

Clearly, to determine the new critical length χ_c^δ one needs to be able to calculate the point $x^\delta := \frac{\chi_+^\delta}{2}$. The point $\frac{\chi_-^\delta}{2}$ coincides with $\frac{\chi}{2}$, which is calculated in [69], and is given by

$$\frac{\chi}{2} = d^{\frac{3}{2}} \left(\frac{3E_{2D}}{4k}\right)^{\frac{1}{4}} \left[\frac{1}{\sin(\frac{\theta}{2})} - 1\right]^{-\frac{1}{2}} \beta\left(\frac{3}{2}, \frac{3}{4}\right), \tag{2.3}$$

in which β is the complete beta function.

2.2 Spacial localization of the maximal deflection

In this section, we show how to calculate explicitly x^δ by providing the technical details of the analysis of the equilibrium equation (2.2) and derive an equation of deflection ζ.

As in [69], we find that the wrinkling profile can be fully determined by solving the following equation

$$\zeta^2(\zeta_x)^4 - D\zeta = \frac{\lambda^2}{3}, \text{ where } D = \zeta_0(\zeta_x(0))^4 - \frac{\lambda^2}{3}{\zeta_0}^{-1}. \tag{2.4}$$

The above equation is the Beltrami identity (1868) or Du Bois-Reymond equation (1879) associated to the energy $\mathscr{J}$.

We will now investigate equation (2.4) for different values of the parameters ζ_0 and $\zeta_x(0)$. Indeed, our aim is to determine the pairs $(\zeta_0, \zeta_x(0))$, $0 < \zeta_0 \leq d$, for which the associated solution satisfies the boundary conditions and has the largest distance between nanoparticles. We will then solve the simplified equilibrium equation by using a phase-plane analysis. From (2.4), we have

$$\zeta_x \zeta^{\frac{1}{4}} \left(\frac{\lambda^2}{3} \zeta^{-1} + D \right)^{\frac{-1}{4}} = \pm 1. \tag{2.5}$$

But since ζ is a function that strictly decreases on the interval $[0, x^\delta]$, we deduce

$$\int_0^x \zeta^{\frac{1}{4}} \left(\frac{\lambda^2}{3} \zeta^{-1} + D \right)^{\frac{-1}{4}} d\zeta = -x, \ \ \forall x \in [0, x^\delta], \tag{2.6}$$

so that

$$\int_{\zeta_0}^{\zeta(x)} s^{\frac{1}{4}} \left(\frac{\lambda^2}{3} s^{-1} + D \right)^{\frac{-1}{4}} ds = -x, \ \ \forall x \in [0, x^\delta]. \tag{2.7}$$

In fact, according to the continuum model, there exists a real number $x^\delta(\zeta_0) > 0$ such that the Beltrami equation (2.4) has a solution ζ; (see [74]), and x_δ is given by

$$x^\delta = \int_\delta^{\zeta_0} s^{\frac{1}{4}} \left(\frac{\lambda^2}{3} s^{-1} + D \right)^{\frac{-1}{4}} ds. \tag{2.8}$$

To obtain the maximal distance, D has to be $D = -\frac{\lambda^2}{3} \zeta_0^{-1}$, and then by using a change of variable, we have

$$x^\delta = \zeta_0^{\frac{3}{2}} \left(\frac{\lambda^2}{3} \right)^{\frac{-1}{4}} \int_{\frac{\zeta(x_\delta)}{\zeta_0}}^1 \frac{\sqrt{s}}{(1-s)^{\frac{1}{4}}} \, ds, \tag{2.9}$$

or equivalently

$$x^\delta = \zeta_0^{\frac{3}{2}} \left(\frac{\lambda^2}{3} \right)^{\frac{-1}{4}} \int_{\frac{\delta}{\zeta_0}}^1 \frac{\sqrt{s}}{(1-s)^{\frac{1}{4}}} \, ds. \tag{2.10}$$

Consequently, $\chi^\delta(\zeta_0)$ has the expression

$$\chi^\delta(\zeta_0) = 2 \, \zeta_0^{\frac{3}{2}} \left(\frac{\lambda^2}{3} \right)^{\frac{-1}{4}} \int_{\frac{\delta}{\zeta_0}}^1 \frac{\sqrt{s}}{(1-s)^{\frac{1}{4}}} \, ds, \tag{2.11}$$

which is finite and monotonically increases with ζ_0 as $\zeta_0^{\frac{3}{2}}$. Hence, since the goal is to make the distance between nanoparticles as large as possible, one deduces that the maximum wrinkle length is given by

$$\chi_c^{\delta} = 2\, d^{\frac{3}{2}} \left(\frac{\lambda^2}{3}\right)^{\frac{-1}{4}} \int_{\frac{\delta}{d}}^{1} \frac{\sqrt{s}}{(1-s)^{\frac{1}{4}}} ds. \tag{2.12}$$

For ease of comparison with the maximum wrinkle length obtained for nanoparticles having the same size, we have

$$\chi_c^{\delta} = 2\, d^{\frac{3}{2}} \left(\frac{\lambda^2}{3}\right)^{\frac{-1}{4}} \int_{0}^{1} \frac{\sqrt{s}}{(1-s)^{\frac{1}{4}}} ds - 2\, d^{\frac{3}{2}} \left(\frac{\lambda^2}{3}\right)^{\frac{-1}{4}} \int_{0}^{\frac{\delta}{d}} \frac{\sqrt{s}}{(1-s)^{\frac{1}{4}}} ds, \tag{2.13}$$

so that

$$\chi_c^{\delta} = \chi_c - 2\, d^{\frac{3}{2}} \left(\frac{\lambda^2}{3}\right)^{\frac{-1}{4}} \int_{0}^{\frac{\delta}{d}} \frac{\sqrt{s}}{(1-s)^{\frac{1}{4}}} ds. \tag{2.14}$$

We note here that for $\frac{\delta}{d} \ll 1$, χ_c^{δ} converges towards χ_c as expected.

Next, since the nanoparticles have different heights, the wrinkle sags asymmetrically toward the nanoparticle of smaller height. This was expected by [198], and we prove it in this section analytically. In fact, the middle part of the wrinkle will be translated toward the protrusion of height d by a distance to be determined shortly.

Indeed, the new center of the wrinkle is given by $x_0 = \frac{\chi_c^{\delta} - \chi_c}{4}$, it then follows that

$$x_0 = \frac{\chi_c}{4} - \frac{1}{2} d^{\frac{3}{2}} \left(\frac{\lambda^2}{3}\right)^{\frac{-1}{4}} \int_{0}^{\frac{\delta}{d}} \frac{\sqrt{s}}{(1-s)^{\frac{1}{4}}} ds - \frac{\chi_c}{4} \tag{2.15}$$

$$= -\frac{1}{2} d^{\frac{3}{2}} \left(\frac{\lambda^2}{3}\right)^{\frac{-1}{4}} \int_{0}^{\frac{\delta}{d}} \frac{\sqrt{s}}{(1-s)^{\frac{1}{4}}} ds. \tag{2.16}$$

Note that x_0 is negative, which means that the wrinkle sags asymmetrically towards the nanoparticle of smaller height as expected.

For $\frac{\delta}{d}$ sufficiently small, we have

$$\int_{0}^{\frac{\delta}{d}} \frac{\sqrt{s}}{(1-s)^{\frac{1}{4}}} ds \approx \sqrt{s}\, ds = \frac{2}{3} \left(\frac{\delta}{d}\right)^{\frac{3}{2}}. \tag{2.17}$$

Hence

$$x_0 = -\frac{1}{2} d^{\frac{3}{2}} \left(\frac{\lambda^2}{3}\right)^{\frac{-1}{4}} \frac{2}{3} \left(\frac{\delta}{d}\right)^{\frac{3}{2}} + o(\delta^{\frac{3}{2}}), \tag{2.18}$$

i.e.

$$x_0 = -\frac{1}{3}\left(\frac{\lambda^2}{3}\right)^{\frac{-1}{4}} \delta^{\frac{3}{2}} + o(\delta^{\frac{3}{2}}). \tag{2.19}$$

Finally, the middle part of the wrinkle will be translated towards the protrusion of height d by a distance

$$\varepsilon = \frac{1}{3}\left(\frac{\lambda^2}{3}\right)^{\frac{-1}{4}} \delta^{\frac{3}{2}} + o(\delta^{\frac{3}{2}}). \tag{2.20}$$

Remark 2.2.1

The translation ε of the center does not depend on the diameter d but depends only on the difference δ, and scales as $\delta^{\frac{3}{2}}$.

Finally, the critical length of the wrinkle for this case is given by:

$$\begin{aligned} \chi_c^{\delta} &= x^{\delta} - \frac{\chi_c}{2} \\ &= \frac{\chi_c}{2} - d^{\frac{3}{2}}\left(\frac{\lambda^2}{3}\right)^{\frac{-1}{4}} \int_0^{\frac{\delta}{d}} \frac{\sqrt{s}}{(1-s)^{\frac{1}{4}}} ds \\ &= \chi_c - \frac{2}{3}\left(\frac{\lambda^2}{3}\right)^{\frac{-1}{4}} \delta^{\frac{3}{2}} + o(\delta^{\frac{3}{2}}). \end{aligned}$$

Remark 2.2.2

Here, as in Remark 2.2.1, the difference between χ_c^{δ} and χ_c scales as $\delta^{\frac{3}{2}}$. This confirms the significant effect of the quantity δ on the maximum wrinkle length between the two silica nanoparticles. However, the present result cannot be used alone to explain the discrepancy between the analytical results and the experimental results.

2.3 Asymptotic deflection in the limit $k \to 0$

The aim of the present section is to analyse the instability properties that my result from the energy (2.1) in the case where the bending rigidity is neglected. This question is motivated by the result of Yamamoto et al.[198] and Guedda et al.[69]on the maximal wrinkle length. The authors showed that the maximal wrinkle length satisfies;

$$\chi_c \approx d\left(\frac{\mathrm{E_{2D}}}{\Gamma}\right)^{\frac{1}{4}}, \tag{2.21}$$

which is independent of the bending rigidity. In fact, here, we try to determine the effects of the bending rigidity on the maximal wrinkle length and on the regularity property of the deflection ζ. In this section, we will see that the limiting case $k \to 0$ (i.e. when the graphene membrane is very thin), favors the structure with singularity rather than smooth deflection. Neglecting the two energies at equilibrium , and assuming that the elastic energy is dominated by stretching, the total energy to minimize becomes:

$$\begin{cases} \mathscr{J}(\zeta) = \varepsilon_1 \int_{\frac{\chi_-^\delta}{2}}^{\frac{\chi_+^\delta}{2}} \zeta\,(\zeta_x)^4 + 2\Gamma\chi^\delta \left(d - \dfrac{\delta}{2}\right) \tan\left(\dfrac{\theta}{2}\right), \\ \qquad \text{subject to } \zeta\left(\dfrac{\chi_-^\delta}{2}\right) = 0 \text{ and } \zeta\left(\dfrac{\chi_+^\delta}{2}\right) = \delta. \end{cases} \tag{2.22}$$

The associated equilibrium equation is given by:

$$3(\zeta_x)^4 + 12\zeta(\zeta_x)^2\zeta_{xx} = 0. \tag{2.23}$$

Following the same steps we used to obtain (2.4), the associated Beltrami equation in this case reads

$$\zeta\,(\zeta_x)^4 = \zeta_0\,\gamma^4, \text{ where } \zeta_0 = \zeta(0) \text{ and } \gamma = \zeta_x(0). \tag{2.24}$$

Solving this equation yields us to the exact solution:

$$\zeta(x) = \left(\frac{5}{4}\right)^{\frac{4}{5}} \zeta_0^{\frac{1}{5}} |\gamma|^{\frac{4}{5}} \left[\frac{4}{5}\zeta_0|\gamma|^{-1} - |x|\right]^{\frac{4}{5}} \qquad \forall x/\ -\frac{4}{5}\zeta_0|\gamma|^{-1} \le x \le x^\delta. \tag{2.25}$$

On one hand, the boundary condition $\zeta\left(\dfrac{\chi_-^\delta}{2}\right) = 0$ implies

$$\frac{\chi_-^\delta}{2} = -\frac{4}{5}\zeta_0|\gamma|^{-1}, \tag{2.26}$$

so that

$$\frac{-\chi_c^\delta}{2} := \frac{4}{5}\, d\ {\gamma_c}^{-1}. \tag{2.27}$$

On the other hand, since $\zeta\left(\frac{\chi_+^\delta}{2}\right) = \delta$, then

$$\left(\frac{4}{5}d|\gamma_c|^{-1} - |x_\delta|\right)^{\frac{4}{5}} = \delta\left(\frac{4}{5}d^{-\frac{1}{4}}\gamma^{-1}\right)^{\frac{4}{5}}, \tag{2.28}$$

hence

$$x^\delta = \frac{4}{5}\, d\, |\gamma_c|^{-1} - \delta^{\frac{5}{4}}\left(\frac{4}{5}d^{-\frac{1}{4}}{\gamma_c}^{-1}\right), \tag{2.29}$$

which can be rewritten as follows

$$x^\delta = \left(\frac{4}{5}d^{\frac{-1}{4}}|\gamma_c|^{-1}\right)\left[d^{\frac{5}{4}} - \delta^{\frac{5}{4}}\right], \tag{2.30}$$

or

$$x^\delta = \left(\frac{4}{5}d|\gamma_c|^{-1}\right)\left[1 - \left(\frac{\delta}{d}\right)^{\frac{5}{4}}\right]. \tag{2.31}$$

Consequently, the critical wrinkle length is given by:

$$\chi_c^\delta = \frac{4}{5}\,|\gamma_c|^{-1}\, d\left(2 - \left(\frac{\delta}{d}\right)^{\frac{5}{4}}\right) \tag{2.32}$$

$$= \chi_c - \frac{4}{5}\,|\gamma_c|^{-1}\, d\left(\frac{\delta}{d}\right)^{\frac{5}{4}}, \tag{2.33}$$

and the solution on both sides of the center is given by:

$$\zeta_\pm^c(x) = \left(\frac{5}{4}\right)^{\frac{4}{5}} d^{\frac{1}{5}}|\gamma_c|^{\frac{4}{5}}\left[\frac{\chi_{\pm c}^{\delta}}{2} \pm x\right]^{\frac{4}{5}}. \tag{2.34}$$

Remark 2.3.1

Since $\chi_c^\delta > 0$, then

$$\frac{\delta}{d} < 2^{\frac{4}{5}},$$

or $\delta < 2^{\frac{4}{5}} d$.

Remark 2.3.2

We note here that for $\frac{\delta}{d} \ll 1$, χ_c^δ converges to χ_c . Furthermore, this solution is singular at the origin, which is expected as the flat graphene bends in preference to stretching.

Now, we aim to determine γ_c. In other words, we want to find the configuration that is energetically favorable. For this purpose, we rewrite the total energy given by (2.22) as follows:

$$\begin{aligned}
\mathscr{J}(\zeta) &= \varepsilon_1 \int_{x^0}^{x^\delta} \zeta\,(\zeta_x)^4 + 2\Gamma(x^\delta - x^0)\left(d - \frac{\delta}{2}\right)\tan\left(\frac{\theta}{2}\right) && (2.35)\\
&= \varepsilon_1\, D\,(x^\delta - x^0) + 2\Gamma\left(d - \frac{\delta}{2}\right)\tan\left(\frac{\theta}{2}\right)(x^\delta - x^0) && (2.36)\\
&= \varepsilon_1\, d\,(\gamma)^4\,(x^\delta - x^0) + 2\Gamma\left(d - \frac{\delta}{2}\right)\tan\left(\frac{\theta}{2}\right)(x^\delta - x^0) && (2.37)\\
&= (x^\delta - x^0)\left(\varepsilon_1\, d\,(\gamma)^4 + 2\Gamma\left(d - \frac{\delta}{2}\right)\tan\left(\frac{\theta}{2}\right)\right) && (2.38)\\
&= \left(\varepsilon_1\, d\,(\gamma)^4 + 2\Gamma\left(d - \frac{\delta}{2}\right)\tan\left(\frac{\theta}{2}\right)\right)\left[\frac{4}{5}\,|\gamma|^{-1}\, d\left(2 - \left(\frac{\delta}{d}\right)^{\frac{5}{4}}\right)\right] && (2.39)\\
&= d^2\left[\frac{8}{5} - \frac{4}{5}\left(\frac{\delta}{d}\right)^{\frac{5}{4}}\right]\left(\varepsilon_1\, d\,(\gamma)^3 + 2\Gamma\tan\left(\frac{\theta}{2}\right)|\gamma|^{-1} - \frac{\delta}{d}\Gamma\tan\left(\frac{\theta}{2}\right)|\gamma|^{-1}\right) && (2.40)\\
&= d^2\left[\frac{8}{5} - \frac{4}{5}\left(\frac{\delta}{d}\right)^{\frac{5}{4}}\right]\left(\varepsilon_1\, d\,(\gamma)^3 + \left(2 - \frac{\delta}{d}\right)\Gamma\tan\left(\frac{\theta}{2}\right)|\gamma|^{-1}\right) && (2.41)
\end{aligned}$$

Deriving this energy as a function of γ yields:

$$\gamma_c = \left(\frac{\left(2 - \frac{\delta}{d}\right)\left(\Gamma\tan\left(\frac{\theta}{2}\right)\right)}{3\varepsilon_1}\right)^{\frac{1}{4}}. \tag{2.42}$$

Hence, the favorable energy associated to this configuration is given by:

$$\mathscr{J}(\gamma_c) = 4\,3^{\frac{-3}{4}}\,8^{\frac{-1}{4}}\,d^2\left[\frac{8}{5} - \frac{4}{5}\left(\frac{\delta}{d}\right)^{\frac{5}{4}}\right](\mathrm{E_{2D}})^{\frac{1}{4}}(\pi - \theta)^{\frac{1}{4}}\left[\frac{1}{\sin(\frac{\theta}{2})} - 1\right]^{\frac{-1}{4}}\left(\left(2 - \frac{\delta}{\mathrm{d}}\right)\Gamma\tan\left(\frac{\theta}{2}\right)\right)^{\frac{3}{4}}, \tag{2.43}$$

and the critical length of the wrinkle of graphene becomes:

$$\chi_c^\delta = \frac{4}{5}\,3^{\frac{1}{4}}\left(2 - \frac{\delta}{d}\right)^{\frac{-1}{4}}\,8^{\frac{-1}{4}}\,\underbrace{d\left(\frac{\mathrm{E_{2D}}}{\Gamma}\right)^{\frac{1}{4}}}\left[\frac{1}{\sin(\frac{\theta}{2})} - 1\right]^{\frac{-1}{4}}(\pi - \theta)^{\frac{1}{4}}\left(\tan\left(\frac{\theta}{2}\right)\right)^{\frac{-1}{4}}\left(2 - \left(\frac{\delta}{d}\right)^{\frac{5}{4}}\right). \tag{2.44}$$

2.3.1 The asymptotic behavior of χ_c when $\theta \to 0$ and $\theta \to \pi$

When the opened angle θ goes to 0, the critical length can be approximated by:

$$\chi_c^{\delta} = \frac{4}{5}\, 3^{\frac{1}{4}} \left(2-\frac{\delta}{d}\right)^{\frac{-1}{4}} 8^{\frac{-1}{4}}\, \pi^{\frac{1}{4}}\, \underbrace{d\left(\frac{\mathrm{E_{2D}}}{\Gamma}\right)^{\frac{1}{4}}} \left(2-\left(\frac{\delta}{d}\right)^{\frac{5}{4}}\right). \tag{2.45}$$

When θ goes to π, i.e for $\Theta = \pi - \theta$ small, we obtain the same expression as above up to a constant:

$$\chi_c^{\delta} = \frac{1}{5}\, 3^{\frac{1}{4}} \left(2-\frac{\delta}{d}\right)^{\frac{-1}{4}} 8^{\frac{-1}{4}}\, \underbrace{d\left(\frac{\mathrm{E_{2D}}}{\Gamma}\right)^{\frac{1}{4}}} \left(2-\left(\frac{\delta}{d}\right)^{\frac{5}{4}}\right). \tag{2.46}$$

This explicitly shows that χ_c^{δ} scales as $\underline{\chi_c^{\delta} \approx d\left(\frac{\mathrm{E_{2D}}}{\Gamma}\right)^{\frac{1}{4}}}$,which agrees well with the previous results obtained for $k \neq 0$. The quotient $\left(\frac{\mathrm{E_{2D}}}{\Gamma}\right)^{\frac{1}{4}}$ can be seen as a reflection of the competition between the adhesion and the wrinkling of graphene on the substrate, i.e if $\left(\frac{\mathrm{E_{2D}}}{\Gamma}\right) \gg 1$, then we may understand that the graphene layer moves on the substrate without much resistance, in other words, the substrate doesn't resist much to the wrinkling of graphene.

2.4 The pseudomagnetic field

In this section, we will use the continuum theory used in the symmetrical case to evaluate the pseudomagnetic field at the center of the wrinkle for the nanoparticles of different diameters.

According to [43] and [74], Yamamoto et al. argued that the pseudomagnetic field can be simply given by:

$$B_{eff} \approx \frac{\Phi_0 \beta}{aW} (\zeta_x)^2, \tag{2.47}$$

where $\Phi_0 = 10^{-15} Wb$ is the flux quantum, $\beta \approx 2$ the change in the hopping amplitude between the neighboring atomic sites due to the lattice deformation, a (=0.142 nm) the lattice constant, and W the typical wrinkle width.

As we don't have an expression for ζ_x at the center of the wrinkle, we seek an approximation near the center, and since this latter x_0 given by (2.19) is in the neighboring of 0, we propose to determine an approximation of ζ of the form $\zeta(x) = d(1-ax^{\alpha})$.

The equilibrium equation (2.2) rewrites for x small,

$$d^2\left(1-ax^{\alpha}\right)^2.d^4\left(-\alpha a x^{\alpha-1}\right)^4+4d^3\left(1-ax^{\alpha}\right)^3.d^2\left(-\alpha a x^{\alpha-1}\right)^2.d\left(-\alpha a(\alpha-1)x^{\alpha-2}\right)+\frac{\lambda^2}{3}=0. \tag{2.48}$$

Then

$$d^6\left(1-ax^{\alpha}\right)^2\left(-\alpha a x^{\alpha-1}\right)^4-4d^6\left(1-ax^{\alpha}\right)^3\left(\alpha a x^{\alpha-1}\right)^2.d\left(\alpha a(\alpha-1)x^{\alpha-2}\right)+\frac{\lambda^2}{3}=0, \tag{2.49}$$

hence

$$x^{3\alpha-4}a^3\alpha^4\left(ax^{\alpha}\left(1-ax^{\alpha}\right)^2-4\alpha^{-1}(\alpha-1)\left(1-ax^{\alpha}\right)^3\right)=-\frac{\lambda^2}{3}d^{-6}, \tag{2.50}$$

so that

$$x^{3\alpha-4}a^3\alpha^4\left(1-ax^{\alpha}\right)^2\left(ax^{\alpha}-4\frac{(\alpha-1)}{\alpha}\left(1-ax^{\alpha}\right)\right)=-\frac{\lambda^2}{3}d^{-6}. \tag{2.51}$$

In the neighbouring of the center, we obtain the following approximation

$$x^{3\alpha-4}a^3\alpha^4\frac{4(\alpha-1)}{\alpha}\approx-\frac{\lambda^2}{3}d^{-6}. \tag{2.52}$$

Consequently, for $\alpha=\frac{4}{3}$, we have:

$$a=d^{-2}\left(\frac{\lambda^2}{3}\right)^{\frac{1}{3}}\left(\frac{3}{4}\right)^{\frac{4}{3}}. \tag{2.53}$$

Finally

$$\zeta\approx d-d^{-1}.\left(\frac{\lambda^2}{3}\right)^{\frac{1}{3}}\left(\frac{3}{4}\right)^{\frac{4}{3}}x^{\frac{4}{3}}. \tag{2.54}$$

Using the estimate , it follows, at $x=x_0$

$$B_{eff}\sim 4^{\frac{-2}{3}}\left(\frac{\lambda^2}{3}\right)^{\frac{1}{3}}\frac{\Phi_0\beta}{aW}\frac{\delta}{d^2}. \tag{2.55}$$

Using similar numerical values for Φ_0, β, a, W and d as above, we deduce for small θ

$$B_{eff}\sim 34.44\,\frac{\Delta}{\theta}\sim 11\frac{\Delta}{\Delta_\theta} \tag{2.56}$$

in which $\Delta=\frac{\delta}{d}$ and $\Delta_\theta=\frac{\theta}{\pi}$.

In particular, if $\Delta=\Delta_\theta$, the pseudomagnetic field is of order 11 T which agrees well with the findings of

Yamamoto et al. [198] for the case of nanoparticles having the same size.

2.5 Occurence of the Lavrentiev phenomenon

2.5.1 A brief introduction

Besides the wrinkling graphene, we briefly discuss the LGP phenomenon and Tonelli set. Firstly, we give a brief history of the famous gap phenomenon for one dimensional minimizer of integrals (or energies) having typically the form

$$\mathscr{E}(\zeta) = \int_a^b \mathscr{L}(x, \zeta, \partial_x \zeta) dx, \tag{2.57}$$

with the boundary conditions $\zeta(a) = A, \zeta(b) = B$, where a, b, A and B are given (finite) constants and the Lagrangian function $\mathscr{L} = \mathscr{L}(x, u, q)$ is assumed to satisfy the (standard) Tonelli conditions (1923) (see [176]).

The gap between the set of absolutely continuous trajectories, or what is now known also as the Sobolev space $W^{1,1}(a,b)$, and the set of Lipschitzian trajectories is demonstrated in 1926 by Lavrentiev [100] and it is referred to as the Lavrentiev gap phenomenon (LGP). At that time this gap between the infima was quite surprising since Lipschitz functions are dense in absolutely continuous functions.

In 1923, a general theory of existence and (first) partial regularity was established by Leonida Tonelli [176] by using the direct method. In particular, he proved that any minimizer ζ of $\mathscr{E}$, in the set of absolutely continuous functions, has a continuous derivative from $[a,b]$ to $\mathbb{R} \cup \{-\infty, \infty\} = \overline{\mathbb{R}}$ (provided one allows values in the extended real line), and there exists a closed set (Tonelli set) $\mathscr{T} \subset [a,b]$ of measure zero such that $\zeta \in C^\infty([a,b] \setminus \mathscr{T})$, $\mathscr{T}$ is characterized by

$$\mathscr{T} = \{x : |\partial_x \zeta| = \infty\}, \tag{2.58}$$

so that, if the Tonelli set is empty the minimizer ζ is smooth. However, at that time it was not known whether $\mathscr{T}$ is empty in general; or even if LGP does not occur. During a lecture in Moscow, Tonelli issued the challenge of finding a counterexample.

In 1934, Mania [113] provided a simpler and original example with $\mathscr{L} = (x^3 - \zeta)^2 (\partial_x \zeta)^6$ for the LGP. Examples where Tonelli set is nonempty were first described by Ball and Mizel in 1985 [13]. The authors presented some examples, which are closely related to the older example of Lavrentiev [100] and Mania [113], showing that smooth minimizers can exist as well as singular minimizers with or without

LGP (depending on the Lagrangian $\mathscr{L}$). They construct examples where $\mathscr{T}$ consists of an end-point of the interval, and another where $\mathscr{T}$ contains an interior point. In particular, Ball and Mizel showed that the Lagrangians $\mathscr{L} = (x^2 - \zeta^3)^2 |\partial_x \zeta|^s + \varepsilon(\partial_x \zeta)^2$ ($a > 0, s \geq 15$) satisfy the conditions of the Tonelli existence theorem and exhibit the LGP between $W^{1,1}$ and $W^{1,\infty}$ (the class of Lipschitzian functions) for some ε depending on s. They also showed that an arbitrary closed set of measure zero could occur as a singular set for a problem in which $\mathscr{E}$ depends only on ζ and q (the autonomous case). Ball and Mizel also gave another example in which $\mathscr{L}(\zeta_n) \to \infty$ for any sequence of admissible Lipschitz functions ζ_n which converge uniformly to the minimizer (the repulsion property). Clarke and Vinter [47] studied minimal smoothness assumptions under which points with bad behavior (or Tonelli set) cannot occur and LGP is then excluded. In 1988, Davie [52] showed that, given an arbitrary closed null set $\mathscr{T}$, there exists a C^∞ Lagrangian $\mathscr{L} = \mathscr{L}(x, \zeta, q)$, supper linear in q and with $\mathscr{L}_{qq} > 0$, such that any minimizer has singular set exactly $\mathscr{T}$. In particular, he constructed an admissible absolutely continuous function v (on (a,b)) and a Lagrangian $\mathscr{L}$ such that $\mathscr{L}(v) < \tau$, for some positive constant τ, and for any admissible absolutely continuous function ζ such that $\partial_x \zeta(c)$ exists and is finite for some $c \in \mathscr{T}$ the strict inequality $\mathscr{L}(\zeta) > \tau$ holds (i. e. LGP occurs). Therefore any minimizer has infinite derivative on $\mathscr{T}$.

In 1993, Ball and Nadirashvili [17] showed that the singularities of minimizers can also be studied in the (x, ζ) plane. In fact, the authors have investigated the case where the interval (a,b) and the boundary values A and B ($A = \zeta(a), B = \zeta(b)$) are varied (under natural hypotheses on Lagrangian $\mathscr{L}$, and proved that there is an *universal singular* set for Lagrangian $\mathscr{L}$ defined as the set $\mathscr{D}_{\mathscr{L}}$ of all points $(x_0, y_0) \in \mathbb{R}^2$ for which there are $a \leq x_0 \leq b$ and a minimizer ζ for $\mathscr{E}$ on $[a,b]$ such that $\zeta(x_0) = y_0$ and $|\partial_x \zeta(x_0)| = \infty$. Ball and Nadirashvili [17] proved that the universal singular set is of first category in $\mathbb{R}^2$ for Lagrangians of class C^3. Later in 1994, Sychev [171] lowers the smoothness assumption to Lagrangians of class C^1, and shows that $\mathscr{D}_{\mathscr{L}}$ is of zero two-dimensional Lebesgue measure.

Note that for polynomial Lagrangians the singular set is understood rather more precisely. In Ref. [48], Clarke and Vinter showed that if $\mathscr{L} = \mathscr{L}(x, \zeta, q)$ is such that $\mathscr{L}_{qq} > 0$ (condition required for classical partial regularity statements) and is a polynomial in q of the form

$$\mathscr{L} = \sum_{i=0}^{N} p_i(x, \zeta) q^i, \tag{2.59}$$

then

$$\mathscr{D}_{\mathscr{L}} \subset \{(x, \zeta) : p_N(x, \zeta) = 0\}, \tag{2.60}$$

implying that if p_N is a non-zero polynomial in x, ζ then $\mathscr{D}_{\mathscr{L}}$ is nowhere dense [17].

A number of examples for the occurrence/non occurrence of LGP and versions of Tonelli's partial regularity theorem under different assumptions (including higher dimensions and universal singular sets) can be found in the literature. An important remark is that the topological negligibility of the universal singular set does not imply, in general, the occurrence of LGP. Very recently, Gratwick [67] has examined the question of the exact relationship between the singular set and the occurrence of LGP. The author demonstrated that given given an arbitrary compact and Lebesgue null set $\mathscr{T}$, there exists a C^3 Lagrangian $\mathscr{L} = \mathscr{L}(x, \zeta, q)$, strictly convex in q and a function ζ absolutely continuous such that ζ is the unique minimizer of $\mathscr{E}$ with respect to its own boundary conditions, the singular set of ζ is precisely $\mathscr{T}$, and there exists admissible C^∞ functions ζ_k such that $\zeta_k \to \zeta$ uniformly and $\mathscr{E}(\zeta_k) \to \mathscr{E}(\zeta)$. Finally, we point out that Clarke and Vinter [48] show, in particular, that the LGP cannot occur (in one-dimensional case) when the Largangian is independent of x, i. e., $\mathscr{L} = \mathscr{L}(\zeta, q)$.

The possibility that a minimizer might be singular or LGP may constitute an obstacle for the interpretation of minimizers obtained numerically by means of the finite elements method. Ball and Knowles [26] have presented numerical technics that are capable of detecting the low-energy singular minimizers. The idea is to decouple the unknown function ζ from its gradient as in control theory. LGP could be related to a kind of fractures, dislocations, or phase boundaries in nonlinear elasticity theory [13], [14]. Analogous LGP can be found in stochastic control and in certain (deterministic) Bolza problems.

In the present work, we shall deal with the autonomous Lagrangian of the type (see below)

$$\mathscr{L}(\zeta, q) = \zeta q^4 + \zeta^{-1}, \tag{2.61}$$

that is derived to describe the wrinkling instability of graphene [198].

Here, the Lagrangian is somewhat distinctive among the (usual) Lagrangians studied in the cited references in the sense that (2.61) is not regular, i. e. $\partial_{qq}\mathscr{L}$ is not strictly positive for all ζ and q, it is singular at $\zeta = 0$, as in the classical Brachistochrome problem (1696), which involves an improper integral, and the interval $[a, b]$ is not fixed. Therefore, $\mathscr{L}$ may provide an example, or counter-example, of Tonelli partial regularity result of a physical situation in which the Lagrangian is singular and/or is not strict convex.

In fact, within the framework of nonlinear elasticity in connection with cavitation [65, 1958], [13], the present work was initially motivated by an attempt to present in its simplest form a complete mathematical-

physical example for which the energy may not attain its minimum within the class of smooth functions or/and has a minimizer having unbounded derivatives at certain points (as in [198]).

As noticed in [14], there is an important philosophical consequence of LGP. Since minimizers in different function spaces can be different, it follows that LGP leads to different (physical) predictions, except if the function space is part of the (mathematical physical) model and is introduced in the fundamental level [27], which is a difficult and complex task [178].

2.5.2 Tonelli set

As mentioned before, we will identify the Tonelli set associated to

$$\mathscr{I} = \inf\{\mathscr{E}(\zeta), \quad \zeta(\pm\chi/2) = 0\}, \tag{2.62}$$

where

$$\mathscr{E}(\zeta) = \int_{-\chi/2}^{+\chi/2} (\zeta(\partial_x\zeta)^4 + \frac{1}{\zeta})dx, \tag{2.63}$$

in which χ is fixed, and $\varepsilon_1 \equiv \varepsilon_2 \equiv 1$. As we have seen, any local minimizer satisfies

$$\zeta^2(\partial_x\zeta)^4 + \frac{1}{3}\frac{\zeta}{\zeta(0)} = \frac{1}{3}, \tag{2.64}$$

for all $0 \leq |x| < \chi/2$.

On the other hand, we have already noticed that ζ is not of class C^2 at $x = 0$, and as x tends to $\pm\chi/2$, we have

$$\zeta(x) \sim 2^{-2/3}3^{1/2}\left(\frac{\chi}{2} - |x|\right)^{2/3}. \tag{2.65}$$

Therefore, the Tonelli set is given by

$$\mathscr{T} = \{\pm\chi/2, 0\}. \tag{2.66}$$

We finally note that $\zeta \in C^2([-\chi/2, +\chi/2] \setminus \mathscr{T}) \cap W_0^{1,1}(-\chi/2, +\chi/2)$ for $1 \leq s < 3$. Therefore, minimizers of $\mathscr{E}$ in $W_0^{1,1}$ and in $W_0^{1,s}, s \geq 3$ may be different. This constitutes the goal of the next section.

2.5.3 Occurence of the Lavrentiev phenomenon

We show that for all $\zeta \in A(0,\frac{\chi}{2})$, and every $\varepsilon > 0$, there exists $\zeta_\varepsilon \in W^{1,\infty}$ such that ζ_ε converges strongly to ζ in $W^{1,1}(0,1)$ and $\mathscr{E}(\zeta_\varepsilon) = \infty$. Indeed, we introduce the following function:

$$\zeta_\varepsilon(x) = \begin{cases} \zeta & 0 \le x < x_\varepsilon \\ \frac{\zeta(x_\varepsilon)}{\frac{\chi}{2}-x_\varepsilon}\left(\frac{\chi}{2}-x\right) & x_\varepsilon < x \le \frac{\chi}{2} \end{cases} \tag{2.67}$$

On the first hand, we show that ζ_ε converges strongly to u in $W^{1,1}(0,1)$. Indeed, we have

$$\begin{aligned} \int_0^{\frac{\chi}{2}} |\zeta_\varepsilon - \zeta| &= \int_0^{x_\varepsilon} |\zeta_\varepsilon - \zeta|\, dx + \int_{x_\varepsilon}^{\frac{\chi}{2}} |\zeta_\varepsilon - \zeta|\, dx && (2.68)\\ &= \int_{x_\varepsilon}^{\frac{\chi}{2}} |\zeta_\varepsilon - \zeta|\, dx && (2.69)\\ &= \int_{x_\varepsilon}^{\frac{\chi}{2}} |\frac{\zeta(x_\varepsilon)}{\frac{\chi}{2}-x_\varepsilon}\left(\frac{\chi}{2}-x\right) - \zeta| \underset{\varepsilon\to 0^+}{\longrightarrow} 0. && (2.70) \end{aligned}$$

Furthermore, we have

$$\begin{aligned} \int_0^{\frac{\chi}{2}} |\zeta_\varepsilon' - \zeta'| &= \int_0^{x_\varepsilon} |\zeta_\varepsilon' - \zeta'|\, dx + \int_{x_\varepsilon}^{\frac{\chi}{2}} |\zeta_\varepsilon' - \zeta'|\, dx && (2.71)\\ &= \int_{x_\varepsilon}^{\frac{\chi}{2}} |\zeta_\varepsilon' - \zeta'|\, dx && (2.72)\\ &\le \int_{x_\varepsilon}^{\frac{\chi}{2}} \left(|u_{\varepsilon'}| + |\zeta'|\right)\, dx && (2.73)\\ &\le \int_{x_\varepsilon}^{\frac{\chi}{2}} \left(|-\frac{\zeta(x_\varepsilon)}{\frac{\chi}{2}-x_\varepsilon}| + |\zeta'|\right)\, dx && (2.74)\\ &\le \left(\frac{\chi}{2}-x_\varepsilon\right)\left(|-\frac{\zeta(x_\varepsilon)}{\frac{\chi}{2}-x_\varepsilon}|\right) + |\zeta(x_\varepsilon)|| \underset{\varepsilon\to 0^+}{\longrightarrow} 0. && (2.75) \end{aligned}$$

On the other hand, due to the symmetry $(x \to -x)$ in equation (2.2), we have:

$$\mathscr{E}(\zeta_\varepsilon) = 2\int_0^{\frac{\chi}{2}} \zeta_\varepsilon(\zeta_{\varepsilon_x})^4 dx + 2\int_0^{\frac{\chi}{2}} {\zeta_\varepsilon}^{-1} dx. \tag{2.76}$$

We will mainly be concerned by the second term of this energy $\mathscr{E}$ since the Lavrentiev phenomenon appears in this term. Indeed,

$$\begin{aligned}
\int_0^{\frac{\chi}{2}} {\zeta_\varepsilon}^{-1} dx &= \int_0^{x_\varepsilon} \zeta^{-1} dx + \int_{x_\varepsilon}^{\frac{\chi}{2}} \zeta^{-1} dx && (2.77)\\
&\geq \int_0^{x_\varepsilon} \zeta^{-1} dx + \lim_{\alpha \to \frac{\chi}{2}} \int_{x_\varepsilon}^{\alpha} \left(\frac{\zeta(x_\varepsilon)}{\frac{\chi}{2} - x_\varepsilon} \left(\frac{\chi}{2} - x \right) \right)^{-1} dx && (2.78)\\
&\geq \int_0^{x_\varepsilon} \zeta^{-1} dx + \lim_{\alpha \to \frac{\chi}{2}} \frac{\left(\frac{\chi}{2} - x_\varepsilon \right)}{\zeta(x_\varepsilon)} \int_{x_\varepsilon}^{\alpha} \left(\frac{\chi}{2} - x \right)^{-1} dx && (2.79)\\
&\geq \int_0^{x_\varepsilon} \zeta^{-1} dx - \frac{\left(\frac{\chi}{2} - x_\varepsilon \right)}{\zeta(x_\varepsilon)} \lim_{\alpha \to \frac{\chi}{2}} [-\ln(\frac{\chi}{2} - x)]_{x_\varepsilon}^{\alpha} && (2.80)\\
&= \infty. && (2.81)
\end{aligned}$$

This concludes the proof of the statement.

2.6 Conclusion

This chapter has the main objective to theoretically analyse the model that describes the wrinkling of graphene on a substrate decorated with silica nanoparticles having different heights. We have determined an explicit expression of the maximum wrinkle length below which the wrinkling is induced as a function of the diameter's difference given by δ. We deduced that the wrinkle sags asymmetrically toward the nanoparticle of smaller height. Furthermore, from this elastic energy, we have derived an expression of the pseudomagnetic field and concluded that it is of order $11T$ which agrees well with the finding of [198]. Finally, we showed the occurence of the Lavrentiev phenomenon in our energy.

Chapter 3

An obstacle problem for a graphene wrinkle model-type

3.1 Introduction

In this chapter we present a modified analytical approach to study a class of equations of the graphene model-type. In particular, we shall be interested in an algorithm for solving this class of problems which can be formulated as an obstacle problem. The present chapter is motivated by the desire to find an approximate numerical solution describing the equilibrium configuration of out of plane deformation of the graphene membrane (under consideration here).

As we have seen in Chapter 2, from the mathematical point of view, the energy of the deformed graphene may suffer from the GAP phenomenon. So, an important question is to develop an algorithm to solve the physical problem. The idea is to transform the wrinkling of graphene problem into an obstacle problem which enables to compute the energy and the graphene deflection simultaneously.

The first (classical) obstacle problem is introduced to describe the equilibrium configuration of an elastic membrane (a thin plate) offering no resistance to bending, but acting only in tension.

For the reader's convenience, we recall briefly the obstacle problem for the elastic membrane (see [151] for a detailed exposition).

We denote by ζ the (vertical) deflection of the membrane occupying a domain $\Omega \subset \mathbb{R}^2$, and by f the external forces. We assume that the membrane is constrained to lie above a given obstacle, ψ (unilateral

condition)

$$\zeta \geq \psi. \tag{3.1}$$

The obstacle function ψ satisfies the condition $\psi \in H^1(\Omega)$ and $\psi \leq 0$ on $\partial\Omega$. The obstacle problem for the membrane is to determine the deflection ζ such that

$$\zeta \in K : \mathscr{J}(\zeta) \leq \mathscr{J}(v), \forall v \in K, \tag{3.2}$$

where

$$K = \left\{ v \in H_0^1(\Omega) : v \geq \psi \text{ in } \Omega \right\} \tag{3.3}$$

and $\mathscr{J}$ is the total energy given by

$$\mathscr{J}(v) = \frac{1}{2}\int_\Omega |\nabla v|^2 dx - \int_\Omega f v dx. \tag{3.4}$$

For the case $f = 0$, the problem is called the boundary thin obstacle problem for the *Laplacian* or the *Signorini* problem in the case where the unilateral constraint is restricted to the boundary (or part of it) [151]. Assuming that the solution ζ is regular, it is found that ζ satisfies [151], [167]

$$\zeta \geq \psi, \quad -\Delta\zeta \geq 0 \quad \text{and} \quad (\zeta - \psi)\Delta\zeta = 0 \quad \text{in } \Omega. \tag{3.5}$$

A crucial property of the obstacle problem is that Ω is divided into two regions: $\Omega = \Omega_c \cup \Omega_c^c$, where Ω_c is the so-called coincidence set

$$\Omega_c = \{x \in \Omega : \zeta(x) = \psi(x)\} \tag{3.6}$$

and Ω_c^c is the complement of Ω_c;

$$\Omega_c^c = \{x \in \Omega : \zeta(x) > \psi(x)\}. \tag{3.7}$$

The boundary of the coincidence set Ω_c is called the *free boundary*, because Ω_c is not known *a priori*.

In fact, the solution ζ can be regarded as the solution of a Cauchy problem for Δ, with ζ and the

boundary $\partial\Omega_c$ are unknown;

$$\begin{cases} \Delta\zeta & = & 0 & \text{in} & \Omega_c^c \\ \zeta & = & \psi & \text{on} & \partial\Omega_c, \\ -\Delta\zeta & \geq & 0 & \text{in} & \Omega_c. \end{cases} \tag{3.8}$$

For $f \in L^2(\Omega)$ the analogous to (3.5) and (3.8) are, respectively, (see [167], [39] and the recent paper [184])

$$\zeta \geq \psi, \quad -\Delta\zeta \geq f \quad \text{and} \quad (\zeta - \psi)(\Delta\zeta + f) = 0 \quad \text{in } \Omega, \tag{3.9}$$

and

$$\begin{cases} -\Delta\zeta & = & f & \text{in} & \Omega_c^c \\ \zeta & = & \psi & \text{on} & \partial\Omega_c, \\ -\Delta\zeta & \geq & f & \text{in} & \Omega_c. \end{cases} \tag{3.10}$$

The solution ζ is also characterized by the following variational inequality (of the first kind)

$$\int_\Omega \nabla\zeta.\nabla(\varphi - \zeta)dx \geq \int_\Omega (\zeta - \varphi), \quad \forall\varphi \in K. \tag{3.11}$$

Regarding the regularity of ζ, it is indicated, for example in [167], that $\zeta \in H^2(\Omega) \cap H_0^1(\Omega)$ by using [30].

The above obstacle problems are considered as a typical example of elliptic variational inequalities (of the first kind). Many important problems in physics, engineering and finance are formulated by transforming the problem to an obstacle problem and then to an elliptic variational inequality which has an advantageous for analytical treatment and,especially, for numerical solutions [196], [184], even if the computation of approximate solutions and the approximate contact regions or the coincidence sets (Ω_c) can be a challenge.

As mentioned before, we propose in this chapter to use the obstacle problem strategy to revisite our wrinkling graphene problem. In this chapter, we assume that the distance between two nanoparticles is fixed ($\chi = 2$).

3.2 Formulation of the problem

In the preceding chapters, we have studied the wrinkling graphene properties by analyzing the graphene deflection ζ that minimizes the energy given by

$$\mathscr{J}(v) = \frac{1}{4}\int_{-1}^{1} |v_x|^4 dx + \frac{5}{4}\int_{-1}^{1} |v|^{-\frac{4}{5}} dx. \tag{3.12}$$

In this chapter, we present a different way to minimize the above energy. The idea consists in transforming the problem into an obstacle problem. To be more precise, the (initial) mathematical motivation is to extend the obstacle problem in $H_0^1(\Omega), \Omega \subset \mathbb{R}^N$, on the space $W_0^{1,p}(\Omega)$.

Thus, we investigate a minimizer of the (general) energy (in $\mathbb{R}$)

$$\mathscr{J}(v) = \frac{1}{p}\int_{-1}^{1} |\, v_x \,|^p + \frac{1}{\gamma - 1}\int_{-1}^{1} v^{1-\gamma}, \tag{3.13}$$

over the following convex admissible set

$$K = \left\{ v \in W_0^{1,p}(]-1,1[), v \geq \phi \right\}, \tag{3.14}$$

where $p > 1, 0 < \gamma - 1 < \frac{p}{p-1}$ and $\phi \in W_0^{1,p}(]-1,1[)$ to be specified later. Indeed, as we will see in Section 3.4, one of the candidates for the function ϕ is $v_1 = d\phi_1^{\frac{p}{\gamma+p-1}}$, in which ϕ_1 is the first eigenfunction associated to the p-laplacian given in Definition 3.18, and $\mathscr{J}(v_1)$ is finite under the condition $0 < \gamma - 1 < \frac{p}{p-1}$. Let us note that there are many articles that investigate obstacle problems (or p-obstacle problems) involving $p-$Laplacian operator but, to the best of our knowledge there is no publication of p-obstacle problem with nonlinear singular source term.

Recall that the case $p = 4$ and $\gamma = 9/5$ originates from wrinkling graphene problem in which the equilibrium deflection ζ satisfies $\zeta(0) = d$ and $\zeta \leq d$. Accordingly, the convexe set K will be defined by

$$K = \left\{ v \in W_0^{1,p}(]-1,1[), v \geq d\phi \text{ and } v(0) = d \right\} \tag{3.15}$$

so that, the problem can be formulated as to find parameter d such that the above (double) obstacle has a solution for a given $\phi > 0$ in $]-1,1[$ that satisfies $\phi(0) = 1$.

A particular form of the problem is to find a (minimizer) function $v^\star$ which solves the following problem

(see below)

$$\begin{cases} -(\mid v^*{}_x \mid^{p-2} v^*{}_x)_x = v^{*-\gamma} + \Lambda^* \ \delta_0 \qquad \mathscr{D}'(]-1,1[), \\ v(\pm 1) = 0 \text{ and } v(0) = d, \end{cases} \tag{3.16}$$

where Λ^* is a nonnegative constant and δ_0 is a Dirac mass at the origin.

3.3 Definitions and properties

Our aim in this work is to show the existence of a suitable weak solution to (3.16). The first step is to precise in which sense we want to solve our problem.

Definition 1

A weak solution to (3.16) *is a function v such that*

$$\begin{cases} v \in W_0^{1,p}(]-1,1[) \text{ and } v(0) = d, \\ v > 0 \text{ in }]-1,1[\text{ and } v^{-\gamma} \in L^1_{loc}(]-1,1[), \\ \displaystyle\int_{-1}^{1} \mid v_x \mid^{p-2} v_x \varphi_x = \int_{-1}^{1} v^{-\gamma}\varphi + \Lambda^* d, \ \forall \varphi \in C^1_c(]-1,1[). \end{cases} \tag{3.17}$$

Definition 2

For $a < b$, let $\Omega := (a,b)$. $\phi_1 \in W_0^{1,p}(\Omega)$ is the eigenfunction associated to the smallest eigenvalue $\lambda_1 > 0$ such that $||\phi_1||_{L^\infty} = 1$ satisfying:

$$\begin{cases} -\left(\mid \phi_{1x} \mid^{p-2} \phi_{1x}\right)_x = \lambda_1 \mid \phi_1 \mid^{p-2} \phi_1 \quad \text{in } \Omega, \\ \phi_1 > 0 \text{ in } \Omega, \\ \phi_1 = 0 \text{ on } \partial\Omega. \end{cases} \tag{3.18}$$

Moreover, $\lambda_1 = \left(\frac{\pi_p}{b-a}\right)^p$, where $\pi_p := \frac{2\pi(p-1)^{\frac{1}{p}}}{psin(\frac{\pi}{p})}$.

We also have the following useful lemma [101]:

Lemma 1

$$\int_{-1}^{1} {\phi_1}^r dx < \infty \tag{3.19}$$

if and only if $r > -1$.

3.4 Existence Result: sufficient condition for existence

In this section, we define ($\phi = \phi_1^{\frac{p}{\gamma+p-1}}$)

$$K = \left\{ v \in W_0^{1,p}(]-1,1[) \ / \ v \geq d\phi_1^{\frac{p}{\gamma+p-1}} \text{ and } v(0) = d \right\}. \tag{3.20}$$

Theorem 2

Let $1 < \gamma < \frac{2p-1}{p-1}$. There exists $d^* > 0$ such that for all $d \leq d^*$,

$$\inf_{v\in K} \mathscr{J}(v) = \min_{v\in K} \mathscr{J}(v) = \mathscr{J}(v^*). \tag{3.21}$$

Moreover, v^* satisfies:

$$\begin{cases} -(\mid v^*{}_x \mid^{p-2} v^*{}_x)_x = v^{*-\gamma} + \Lambda^* \ \delta_0 \qquad \mathscr{D}'(]-1,1[), \\ v^* \in K, \end{cases} \tag{3.22}$$

where $\Lambda^* = \frac{1}{d}\left[\int_{-1}^{1} \mid v^*{}_x \mid^p - {v^*}^{1-\gamma}\right]$ and δ_0 is a Dirac mass at the origin.

Proof.

Let $v_1 = d{\phi_1}^{\beta}$, where $0 < \beta < 1$ is a constant to be determined.

We have

$$\begin{aligned}
-\left(\mid v_{1x} \mid^{p-2} v_{1x}\right)_x &= -d^{p-1}\beta^{p-1}\left(\mid \phi_{1x} \mid^{p-2} \phi_{1x}\, {\phi_1}^{(p-1)(\beta-1)}\right)_x && (3.23)\\
&= d^{p-1}\beta^{p-1}[-\left(\mid \phi_{1x} \mid^{p-2} \phi_{1x}\right)_x {\phi_1}^{(p-1)(\beta-1)} && (3.24)\\
&+ (p-1)(1-\beta){\phi_1}^{(p-1)(\beta-1)-1} \mid \phi_{1x} \mid^p] && (3.25)\\
&= d^{p-1}\beta^{p-1}\left[\lambda_1\phi_1^{\beta(p-1)} + (p-1)(1-\beta){\phi_1}^{(p-1)(\beta-1)-1} \mid \phi_{1x} \mid^p\right] && (3.26)\\
&= {v_1}^{-\gamma} d^{\gamma+p-1}\beta^{p-1}\left[\lambda_1\phi_1^{\beta(\gamma+p-1)} + (p-1)(1-\beta){\phi_1}^{\beta(\gamma+p-1)-p} \mid \phi_{1x} \mid^p\right] && (3.27)
\end{aligned}$$

Hence, for $\beta = \frac{p}{\gamma+p-1}$, we get:

$$-\left(\mid v_{1x} \mid^{p-2} v_{1x}\right)_x = g(x,d)\ {v_1}^{-\gamma}, \tag{3.28}$$

in which

$$g(x,d) = d^{\gamma+p-1}\left[\beta^{p-1}(1-\beta)(p-1) \mid \phi_{1x} \mid^{p} + \lambda_1 \beta^{p-1} {\phi_1}^{p})\right]. \tag{3.29}$$

Note that the strong maximum and boundary point principles from Vasquez [179] guarantee $\phi_1 > 0$ *in* $]-1,1[$ *and* $\mid \phi_{1x} \mid \neq 0$ *on the boundary. Hence*

$$\Gamma_1 := max\left[\beta^{p-1}(1-\beta)(p-1) \mid \phi_{1x} \mid^{p} + \lambda_1 \beta^{p-1} {\phi_1}^{p})\right] > 0, \tag{3.30}$$

which means that $g(x,d) \leq 1$ *if and only if* $d \leq \left(\frac{1}{\Gamma_1}\right)^{\frac{1}{\gamma+p-1}} := d^*$.
We conclude that for $d \leq d^*$, *the function* v_1 *satisfies :*

$$\begin{cases} -(\mid v_{1x} \mid^{p-2} v_{1x})_x \leq {v_1}^{-\gamma} \qquad \mathscr{D}'(]-1,1[), \\ \qquad\qquad v_1 \in W_0^{1,p}(]-1,1[). \end{cases} \tag{3.31}$$

Recalling $\Lambda^* > 0$ *and* δ_0 *is a nonnegative measure,* v_1 *clearly verifies*

$$\begin{cases} -(\mid v_{1x} \mid^{p-2} v_{1x})_x \leq {v_1}^{-\gamma} + \Lambda^* \delta_0 \qquad \mathscr{D}'(]-1,1[), \\ \qquad\qquad v_1 \in W_0^{1,p}(]-1,1[). \end{cases} \tag{3.32}$$

Since v_1 *is a sub-solution of (3.16), if we insert it as a test function in the weak formulation of (3.16), we obtain*

$$\int_{-1}^{1} \mid v_{1x} \mid^{p} \leq \int_{-1}^{1} {v_1}^{1-\gamma} + \Lambda^* d. \tag{3.33}$$

Consequently

$$\begin{aligned} \mathscr{J}(v_1) &= \frac{1}{p}\int_{-1}^{1} \mid v_{1x} \mid^{p} + \frac{1}{\gamma-1}\int_{-1}^{1} {v_1}^{1-\gamma} && (3.34) \\ &\leq \left(\frac{1}{p} + \frac{1}{\gamma-1}\right)\int_{-1}^{1} {v_1}^{1-\gamma} + \Lambda^* d && (3.35) \\ &\leq \left(\frac{1}{p} + \frac{1}{\gamma-1}\right)\int_{-1}^{1} d^{1-\gamma} \phi_1^{\frac{p(1-\gamma)}{\gamma+p-1}} + \Lambda^* d. && (3.36) \end{aligned}$$

By Lemma 1, we conclude that since $\gamma < \frac{2p-1}{p-1}$, *then* $\phi_1^{\frac{p(1-\gamma)}{\gamma+p-1}} \in L^1(]-1,1[)$ *and* $\mathscr{J}(v_1) < \infty$. *In addition, for all* $v \in K$, $\mathscr{J}(v) \geq 0$. *This implies that the subset* K *is a non-empty closed convex of* $L^p(]-1,1[)$. *Therefore one can take a minimizing sequence* $(v_n)_n$ *in* K *i.e a sequence such that* $\Phi(v_n) \rightarrow$

$\inf_{v\in K}\Phi(v)$, *or* $\mathscr{J}(v_n)\to\inf_{v\in K}\mathscr{J}(v):=L$. *This implies that for all* $\varepsilon>0$, *there exists* $\eta_0>0$, *such that for all* $\eta>\eta_0$, *we have:*

$$\frac{L}{2}\leq\mathscr{J}(v_n)\leq\frac{3L}{2}, \tag{3.37}$$

consequently:

$$\int_{-1}^{1}\mid v_{nx}\mid^p dx\leq p\left(\frac{3L}{2}-\frac{1}{\gamma-1}\int_{-1}^{1}v_n^{1-\gamma}\right)dx. \tag{3.38}$$

Again, since $1<\gamma<\frac{2p-1}{p-1}$, *then* ${v_n}^{1-\gamma}\leq d_n^{1-\gamma}{\phi_1}^{\frac{p(1-\gamma)}{\gamma+p-1}}$ *which is in* $L^1(]-1,1[)$. *This gives the uniform boundedness of* v_n *in* $W_0^{1,p}(]-1,1[)$.

We pick a subsequence, still denoted v_n *that converges to* v^* *weakly in* $W_0^{1,p}(]-1,1[)$, *strongly in* $L^p(]-1,1[)$ *and* $v_n(x)\longrightarrow v^*(x)$ *a.e in* $]-1,1[$.

Since $W_0^{1,p}$ *is injected in the space of Holder continuous functions* C^α, *it follows that* v_n *converges uniformly to* v^* *in K, and* $v_n^{1-\gamma}$ *converges to* ${v^*}^{1-\gamma}$ *in* $L^1(]-1,1[)$. *Finally:* $L\leq\mathscr{J}(v)\leq\liminf_{n\to+\infty}J(v_n)\leq L$, *i.e* $\mathscr{J}(v)=\inf_{v\in K}\mathscr{J}(v)$.

Furthermore, the Euler-Lagrange equation associated to the minimization problem (3.13) is given by (3.22).

Indeed, let $\phi\in\mathscr{C}_c^\infty(]-1,1[)$. *It can easily be verified that there exists* $\delta>0$ *sufficiently small such that*

$$\forall t\in]-\delta,\delta[\quad\frac{v^*+t\phi}{1+t\phi(0)}\in K. \tag{3.39}$$

We have:

$$\begin{aligned}\frac{\partial}{\partial t}\left(\mathscr{J}\left(\frac{v^*+t\phi}{1+t\phi(0)}\right)\right)_{t=0} &= \int_{-1}^{1}\mid v_x^*\mid^{p-2}v_x^*\,\frac{\partial}{\partial t}\left(\frac{v_x^*+t\phi_x}{v^*(0)+t\phi(0)}\right)-{v^*}^{-\gamma}\,\frac{\partial}{\partial t}\left(\frac{v^*+t\phi}{v^*(0)+t\phi(0)}\right)\\ &= \int_{-1}^{1}\mid {v^*}_x\mid^{p-2}{v^*}_x\,\phi_x-\int_{-1}^{1}{v^*}^{-\gamma}\,\phi-\frac{1}{d}\left(\int_{-1}^{1}\mid {v^*}_x\mid^p-{v^*}^{1-\gamma}\right)\phi(0)\end{aligned}$$

Since v^* *is a minimum, we obtain:*

$$\int_{-1}^{1}\left(\mid {v^*}_x\mid^{p-2}{v^*}_x\,\phi_x-{v^*}^{-\gamma}\,\phi\right)=\frac{1}{d}\left(\int_{-1}^{1}\mid {v^*}_x\mid^p-{v^*}^{1-\gamma}\right)<\delta_0,\phi>, \tag{3.40}$$

which means that equation (3.22) is satisfied in the sense of distributions.

3.5 Numerical Algorithm and Results

3.5.1 Determination of the first eigenfunction of the p-Laplacian

In order to numerically determine the first eigenfunction ϕ_1 that verifies equation (3.18), we introduce the Lagragian:

$$\mathscr{L}(\phi,\lambda) = \frac{1}{p}\int_{-1}^{1} |\phi_x|^p + \lambda\left(\int_{-1}^{1} |\phi|^p - 1\right), \tag{3.41}$$

where $\lambda \in \mathbb{R}$ is referred to as the Lagrange multiplier.

According to [200], the Lagrange multiplier approach is based on solving the system of equations which constitute the necessary conditions of optimality. The first-order necessary condition of optimality can be expressed as a stationary point (ϕ^*,λ^*) of $\mathscr{L}(\phi,\lambda)$, That is a stationary point of the system

$$\begin{cases} \dfrac{d\phi}{dt}(t,x) = -\dfrac{\partial \mathscr{L}}{\partial \phi}(\phi,\lambda), \\ \dfrac{d\lambda}{dt}(t) = \dfrac{\partial \mathscr{L}}{\partial \lambda}(\phi,\lambda). \end{cases} \tag{3.42}$$

That is

$$\begin{cases} \left.\dfrac{d\phi}{dt}\right|_{(\phi^*,\lambda^*)} = 0, \\ \left.\dfrac{d\lambda}{dt}\right|_{(\phi^*,\lambda^*)} = 0. \end{cases} \tag{3.43}$$

In our case, we have

$$\begin{cases} \dfrac{\partial \phi}{\partial t}(t,x) = \left(|\ \phi_x\ |^{p-2}\ \phi_x\right)_x - \lambda p \phi^{p-1}, \\ \phi(t,-1) = \phi(t,1) = 0, \\ \dfrac{\partial \lambda}{\partial t}(t) = \displaystyle\int_1^1 |\phi|^p - 1. \end{cases} \tag{3.44}$$

with $\phi(0,x) = (1-x^2)$ and $\lambda(0) = \lambda_0$.

After the numerical simulation using finite elements method, we obtain

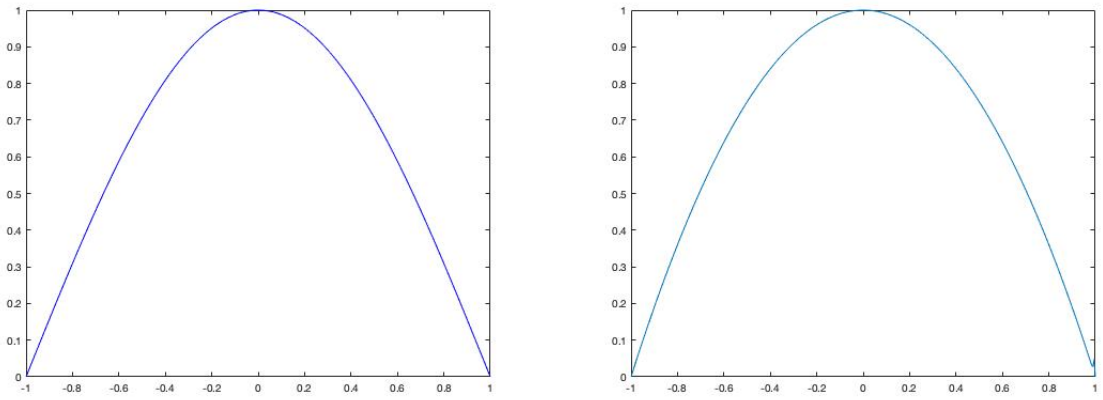

Figure 3.1: First eigenfunction of the Laplacian (left figure). First eigenfunction of the p-Laplacian for $p = 4$ (right figure).

3.5.2 Determination of the solution v^*

In order to numerically determine the solution of equation (3.40), we use the classical fourth-order Runge Kutta method [10].

Algorithm 3 Steps of the method

Require: $v^0 = d{\phi_1}^\beta$ initial guess of the solution and $tol = 10^{-6}$ is the tolerance.

while $\varepsilon_n = \mid \Lambda^{n+1} - \Lambda^n \mid < tol$ **do**

- Compute the equation below

$$\Lambda^n = \frac{1}{d}\left[\int_{-1}^{1} \mid {v^n}_x \mid^p - (v^n)^{1-\gamma}\right] \tag{3.45}$$

- Solve for v^n the equation below $\forall \phi \in \mathscr{C}_c^\infty(]-1,1[)$

$$\int_{|x|<1} (\mid {v^{n+1}}_x \mid^{p-2} {v^{n+1}}_x)_x \phi_x = \int_{|x|<1} (v^{n+1})^{1-\gamma}\phi + \Lambda^n \phi(0) \tag{3.46}$$

- Update

$$\Lambda^{n+1} = \frac{1}{d}\left[\int_{-1}^{1} \mid {v^{n+1}}_x \mid^p - (v^{n+1})^{1-\gamma}\right]. \tag{3.47}$$

end while

3.5.3 Numerical results

Implementing Algorithm 3, we obtain

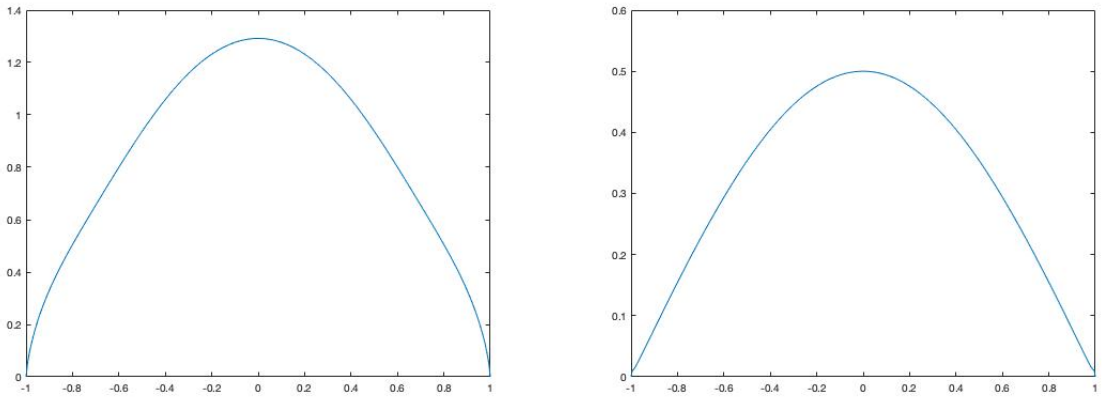

Figure 3.2: Numerical solution for v^*. Parameters are: $p = 2$, $\gamma = 2$, $d^* = 1.5$ and $d = 1.3$ (left figure), and $p = 4$, $\gamma = 9/5$, $d^* = 0.7562$ and $d = 0.5$ (right figure).

3.6 Conclusion

The numerical results coincide with the physical graphene wrinkle profile, as the derivative vanishes at the origin 0 and blows up at the boundaries, which is in good agreement with the physical properties of the profile. These properties appear very naturally when minimizing in the set K, which confirms the validity of the choice of the optimization space.

Chapter 4

Instabilities and scaling properties in certain one-dimensional singular interfacial equation

The first section of this chapter "Instabilities in certain one-dimensional singular interfacial equation" is published by Bognár,G., Guedda,M., Hriczó,K. and Taourirte Laila in Physica Scripta, 95(3), 035001. (2020).

4.1 Instabilities in certain one-dimensional singular interfacial equation

4.1.1 Introduction

Intense theoretical and experimental interest has been devoted to examine the dynamics of epitaxial growths in the presence of interfacial instabilities. The major challenge still remains the prediction and the control of these surfaces, which could serve as ideal templates for the growth of one- or twodimensional arrays with nanometer scale parameters such as superlattices, quantum wells, quantum wires, and quantum dots. These self-organized surfaces, which are structured laterally, are vital in the hybrid microelectronics, microwave, semiconductor, optical, medical, sensor, and related industries. A promising way is to make use of patterns evolving out of inherent instabilities in growth processes. A theorist's contribution to controlled unstable growth can then lie in understanding its basic mechanisms. One of the simplest methods of a self-assembly process is the growth of a crystalline film from a molecular or atomic beam, referred commonly to as molecular beam epitaxy (MBE). This enables scientists to build nanostructures as pyramidal objects or mounds. The remarkable richness of patterns forming during MBE is determined

solely by processes which occur locally at the surface.
Molecular beam epitaxy (MBE), which has many important technological and industrial applications, is often used to grow nanostructure on crystal surfaces. The evolution of the surface morphology during MBE growth results from a competition between the molecular flux and the relaxation of the surface profile through surface diffusion of adatoms. One crucial aspect of the growth process is its possible unstable character, due to deterministic mechanisms, which prevent the growing surface to stay parallel to the substrate [55]-[137]. In fact, the evolution of surface morphology during MBE growth results from an interplay between deposition of atoms onto the surface and the relaxation of the surface profile through surface diffusion. One of the most influential factors for instabilities in the evolution of the surface morphology of a growing film is the existence of energy barriers near steps. An adsorbed atom (adatom) approaching a step from above or below may have different probabilities. This phenomena was first observed experimentally by Ehrlich and Hudda [55] and analyzed by Schwoebel and Shipsey [159].

This phenomenon has turned out to be a source of a wide class of nonlinear dynamics, which varies from spatio-temporal chaos [21] to the formation of stable structures [157], from coarsening processes [133] to diverging amplitude structures [142]. One of the many challenges involved in applied mathematics and nonequilibrium physics is to predict the behavior of surface evolution, from the knowledge initial arbitrary profile, and the scaling relationships between surface features in various growth regimes.

In this chapter we consider a class of Ehrlich-Schwoebel (ES) barriers that induces pyramidal or mound-type structures on the growing surface ([180],[91]). In particular, we will study the one-dimensional dynamics of a MBE growth in which the mounds increase in both height and lateral size. In this context, an analytical approach has been developed by Golubović [66] in the spirit of the Bales and Zangwill theory [12]. To be more precise, Golubović studied the dynamics of a MBE growing interfaces in the absence of slope selection mechanism, when the mounds' slope indefinitely increases with time [164]. Assuming that the effects of adatom desorption [50] and diffusion anisotropy are neglected [137], the continuous interfacial height in one-dimensional case, is found to obey the following general phenomenological evolution equation (see Rost and Krug [154])

$$\partial_t h = -a\partial_x \left(\frac{\partial_x h}{1+|\partial_x h|^{1+\tau}} \right) - b\partial_x^4 h, \tag{4.1}$$

while it is standard form is

$$\partial_t h = -a\partial_x \left(\frac{\partial_x h}{\left(1+|\partial_x h|^2\right)^n} \right) - b\partial_x^4 h. \tag{4.2}$$

In the above equations a and b are physical positive constants and $n, \tau \geqslant 1$. The unknown smooth function h measures the film thickness above a substrate point x and at time t. The above equations have a conservation form $\partial_t h + \partial_x J = 0$ where the surface current J for equation (7.10) is given by

$$J(\partial_x h) = a\frac{\partial_x h}{\left(1+|\partial_x h|^2\right)^n} + b\partial_x^3 h. \tag{4.3}$$

The first term of the current J is the destabilizing surface current, the ES effect, which generalized the form discussed by Johnson et al [83] and Hunt et al [80] and is characterized by different asymptotic behaviors for $|\partial_x h| \to \infty$ in ([66],[143], [144]). The destabilizing term, which provides the nonlinear regime, is balanced by the classical stabilizing linear term à la Mullins [120]. Different coarsening process types are exhibited in [139]. The growth laws are investigated with phase diffusion approach that allows to determine the coarsening exponent for 2D growth. In [24], a classification of important unstable crystal growth dynamics in terms of universality classes are proposed and distinct properties and coarsening exponents are shown. The solutions to (7.10) with $n = 1$ are investigated both analytically and numerically. Global solutions were constructed to the parabolic evolution equation by Fujimura and Yagi [62]. Numerical techniques like finite difference, finite element and kinetic Monte Carlo method were used to provide approximate solutions to the equation describing crystal surface growth ([208], [23]]. The pyramidal structure characterized by the absence of preferred slope in one-dimension was examined by Guedda and Trojette [71] applying a similarity approach. We note that similarity technique is not applicable to the nonlinear term $\partial_x h/\left(1+|\partial_x h|^2\right)$ in (7.10). It is the purpose of this chapter to study the coarsening process that may result from equation (7.10) with $n > 0$ $n \neq 1$, called here n -model. In particular, an effort is made to report an analytical justification of solutions to n -model, which correspond to, or predict, the coarsening process. For the coarsening results concerning the case $n = 1$ we refer to the paper by Hunt et al [80]. In fact, we are mainly concerned with stationary solutions, which are successfully used to describe the major features of the process of coarsening in a wide class of surface growth phenomena ([142] [141]).

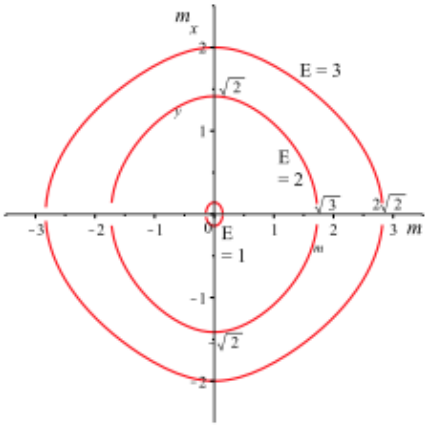

Figure 4.1: (Color online) Trajectory curves for $n = \frac{1}{2}$ and different values of E for case (i).

4.1.2 Stationary solutions

The goal of this section is to analyze the coarsening process by using the criteria of Politi and Misbah ([142], [141]). The authors showed that coarsening occurs if the wavelength is an increasing function of the amplitude or the maximum slope of periodic stationary solution.

Firstly, we note that if we assume $h = \varepsilon e^{\sigma t + \mathrm{i}\, q\, x}$, where ε is very small, we get $\sigma = \sigma(q) = aq^2 - bq^4$. Therefore, all wavelengths larger than $\lambda_0 = 2\pi\sqrt{\frac{b}{a}}$ are unstable.

4.1.3 Preliminary results

Stationary solution or time-independent solution $(h_t = 0)$ to $\partial_x J = 0$ with (4.3) and $a = b = 1$ satisfies

$$h_{xxx} = -\frac{h_x}{\left(1 + |h_x|^2\right)^n} + C. \tag{4.4}$$

Due to the symmetry $(x \to -x)$ in equation (7.10) we take $C = 0$. Applying substitution $h_x = m$ into (4.4), we arrive at

$$m_{xx} = -\frac{m}{(1+m^2)^n}. \tag{4.5}$$

Multiplying (4.5) with m_x and taking its integral we get the so called "energy" integral

$$\frac{1}{2}(m_x)^2 + \frac{1}{2(1-n)}\left(1+m^2\right)^{1-n} = E = \text{const.} \tag{4.6}$$

hence

$$m_x = \pm\sqrt{2}\sqrt{E - \frac{1}{2(1-n)}\left(1+m^2\right)^{1-n}} \tag{4.7}$$

On the phase plane we shall examine all possible cases for power n and E. It can be seen from (4.6) that for $n < 1, E$ has to be positive.

Case (i)

If $0 < n < 1$ and $E > 0$, it is deduced from (4.7) that m is periodic (see Figure 4.1) and E is given by

$$E = \frac{1}{2(1-n)}\left(1+M^2\right)^{1-n}, \tag{4.8}$$

where we denote the maximum slope of solution h by M, i.e. $M = \max(m)$.
Then for $m_x = 0$, connection $m = \pm\sqrt{[2(1-n)E]^{1-\frac{1}{1-n}} - 1}$ exists if

$$E \geqslant \frac{1}{2(1-n)}. \tag{4.9}$$

If $E = 1/2(1-n)$, then $m_x = 0$ implies that $m = 0$ (see Figure 4.2) which exhibits the phase plane $n = \frac{1}{2}$.

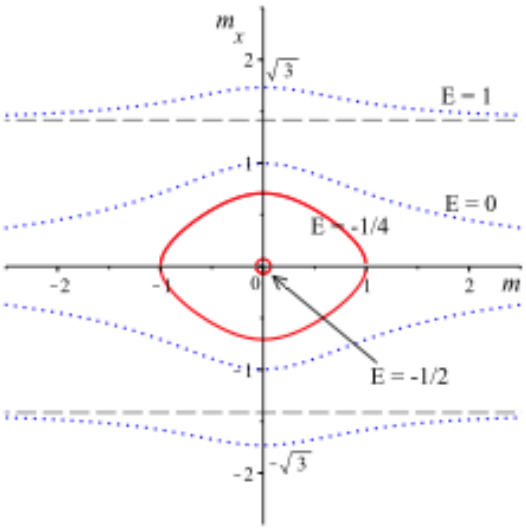

Figure 4.2: (Color online) Trajectory curves for $n = 2$ and different values of E for case (ii).

Case (ii)

If $n > 1$ and $E < 0$, then for $m_x = 0$ we must have

$$E \leq \frac{1}{2(1-n)}. \tag{4.10}$$

A simple analysis of equation (4.7) for (4.10) shows that the equation (4.4) has periodic solution. Particularly, if $E = 1/[2(1-n)], m_x = 0$ implies that $m = 0$ (see curves with solid lines on Figure 4.2 which exhibits the case $n = 2$). Case (iii) If $n > 1$ and $E > 0$, then m is not periodic as it is shown on Figure 4.2 with dotted curves. In particular, we see that $m \to \pm\sqrt{2E}x$ as $x \to \pm\infty$ (horizontal asymptotes). In summary, for $n > 0$ the n -model has a branch of stationary periodic solutions. In particular, Figure 4.2 shows that no periodic solution exists if $n > 1$ and $E > \frac{1}{2(1-n)}$ and periodic solution exists if $n > 1$ and $E \leqslant \frac{1}{2(1-n)}$.

4.1.4 Numerical solutions to time-independent equation

We again examine the time-independent equation

$$h_{xxxx} = -\left[\frac{h_x}{\left(1+(h_x)^2\right)^n}\right]_x \tag{4.11}$$

Solution $h = h(x)$ satisfies the third order nonlinear differential equation

$$h_{xxx} = -\frac{h_x}{\left(1+(h_x)^2\right)^n} \tag{4.12}$$

To exhibit the structure of the solutions in case (i), the corresponding initial conditions for $E = 2$ and $n = 1/2$ are chosen as

$$h(0) = 0, h'(0) = 0, h''(0) = \pm\sqrt{2}. \tag{4.13}$$

The numerical solution $h(x)$ to (4.12), (4.13) obtained by MAPLE 2015 can be seen on Figure 4.3 the red curve corresponds to $+$ sign and the blue curve to - sign.

The corresponding initial conditions in case (ii) for $E = -1/4$ and $n = 2$ are chosen as follows

$$h(0) = 0, h'(0) = 0, h''(0) = \pm\sqrt{3}. \tag{4.14}$$

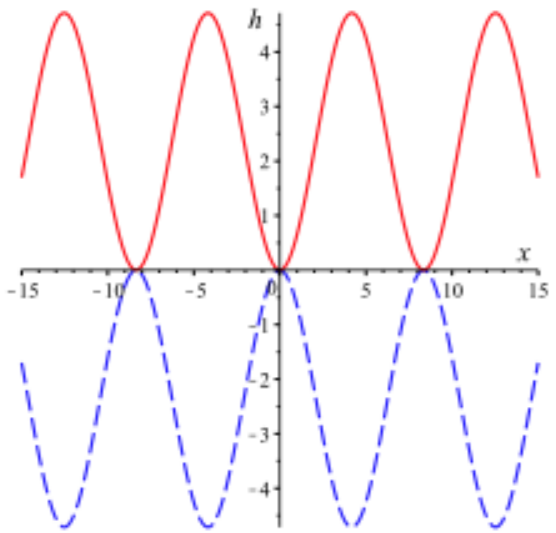

Figure 4.3: The curves of h and $-h$ as a function of x if $n = \frac{1}{2}$, $E = 2$ for case (i) denoted by solid and dashed lines, respectively.

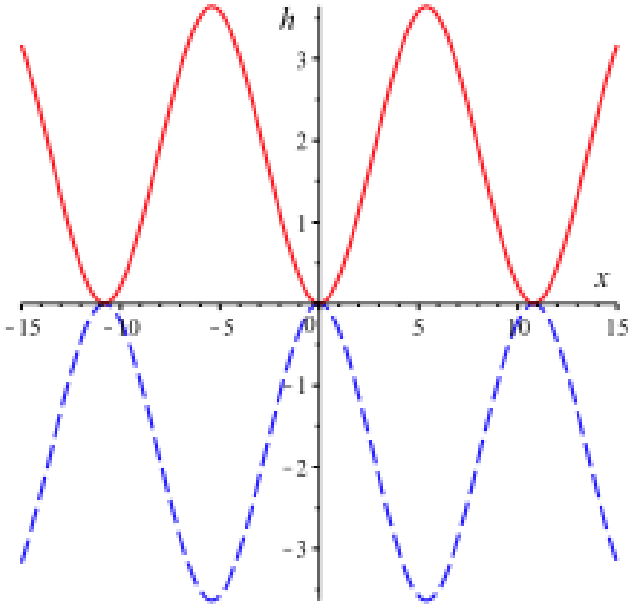

Figure 4.4: The curves of h and $-h$ as a function of x if $n = 2$, $E = -\frac{1}{4}$ for case (ii) denoted by solid and dashed lines, respectively.

The numerical solutions to (4.13) and (4.14) are illustrated on Figure 4.4 the solid curve corresponds to $+$ sign and the dashed curve to $-$ sign. In both cases the solution show periodic behavior.

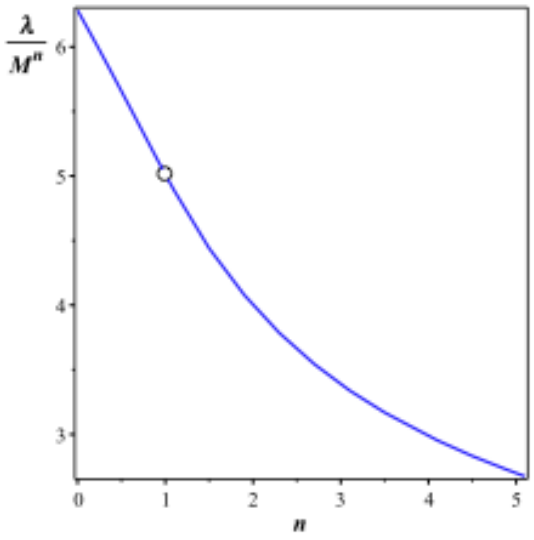

Figure 4.5: The figure of $\frac{\lambda(n)}{M^n}$ as a function of n.

4.1.5 Coarsening properties

Before considering more complicated time-dependent problems, it is usual to seek steady state solutions or/and similarity (self-affine) solutions which have relevance for the coarsening process (see below). The model, however, does not allow similarity solutions and so a global description of stationary solutions seems to be necessary. An analytical approach for the coarsening process in one-dimensional surface growth models, has been developed by Politi and Misbah ([142], [141]). It has been shown that periodic steady-state solutions, h_0 of period λ may play a major role in determining the type of nonlinear dynamics. For a certain class of nonlinear 1D equations, the authors argued that coarsening is possible if and only if the wavelength $\lambda(A)$ is an increasing function of the amplitude A of h_0. The presence of a maximum of $\lambda(A)$ signals that the coarsening is stopped (interrupted coarsening), while a decreasing $\lambda(A)$ indicates the absence of the coarsening. More importantly, in the limit of large λ, Misbah and Polity introduced an approach, called the phase diffusion method, for determining the coarsening exponent which characterizes the time dependence of the scale of the pattern. As mentioned in [123] the advantage of this method is that the coarsening exponent is determined without solving a timedependent equation. This is very suitable from the numerical point of view, since the phase diffusion method avoids the blow up of the integration scheme at large time steps. Nicoli et al. [123] proposed a recipe to implement numerically the determination of the coarsening exponent when coarsening is present by using the existence results.

We study the coarsening properties of the surface by using the method of Misbah and Politi ([142], [141]). We investigate as above the energy equation

$$E = \frac{1}{2}(m_x)^2 + \frac{1}{2(1-n)}\left(1+m^2\right)^{1-n} \tag{4.15}$$

$$= \frac{1}{2(1-n)}\left(1+M^2\right)^{1-n} \tag{4.16}$$

One gets for m_x that

$$m_x = \pm\sqrt{\frac{1}{1-n}\left[(1+M^2)^{1-n} - (1+m^2)^{1-n}\right]}. \tag{4.17}$$

We note that if $m = 0$ and $n < 1$, then

$$m_x = \pm\sqrt{\frac{1}{1-n}\left[(1+M^2)^{1-n} - 1\right]}, \tag{4.18}$$

which gives the maximum or minimum of m_x, respectively.

Moreover, since $E = 1/2(1-n)\left(1+M^2\right)^{n-1}$, then $E = 0$ if and only if $M = \infty$ and for large values of M

$$m_x = \pm\sqrt{\frac{1}{1-n}}m^{\frac{1-n}{2}}. \tag{4.19}$$

Therefore, from (4.19) we obtain the nonlinear differential equation for m in the form

$$m_x m^{\frac{n-1}{2}} = \pm\sqrt{\frac{1}{1-n}}. \tag{4.20}$$

Taking the integral of equation (4.20) for (x_0, x) we get

$$\frac{2}{n+1}\left[m(x)^{\frac{n+1}{2}} - m(x_0)^{\frac{n+1}{2}}\right] = \pm\sqrt{\frac{1}{1-n}}(x-x_0). \tag{4.21}$$

It shows that m is monotone and $m \approx |x|^{\frac{2}{n+1}}$.

The wavelength.

Our interest is the determination of the wavelength λ and the amplitude A of solution h. The wavelength $\lambda = \lambda(M)$ can be calculated depending on M. By using $\mathrm{dm}/\mathrm{m}_x = \mathrm{d}x$ we obtain the integral

$$\frac{\lambda}{4} = \int_0^M \frac{\mathrm{d}m}{m_x} = \int_0^M \frac{\mathrm{d}m}{\sqrt{\frac{1}{1-n}\left[(1+M^2)^{1-n} - (1+m^2)^{1-n}\right]}} \tag{4.22}$$

For $n > 1$ with substitution $m = Mv$ we can write that

$$\frac{\lambda}{4\sqrt{n-1}} = \int_0^1 \frac{M\mathrm{d}v}{\sqrt{(1+M^2v^2)^{1-n} - (1+M^2)^{1-n}}} \tag{4.23}$$

Now, $\lambda'(M)$ can be calculated from (4.23) applying the form $F(M) = \int_0^1 M\mathrm{d}v/\sqrt{G(M)}$ with $G(M) = \left(1+M^2v^2\right)^{1-n} - \left(1+M^2\right)^{1-n}$ since we have

$$F'(M) = \int_0^1 \frac{G - \frac{M}{2}G'}{G^{\frac{3}{2}}}\mathrm{d}v, \tag{4.24}$$

where

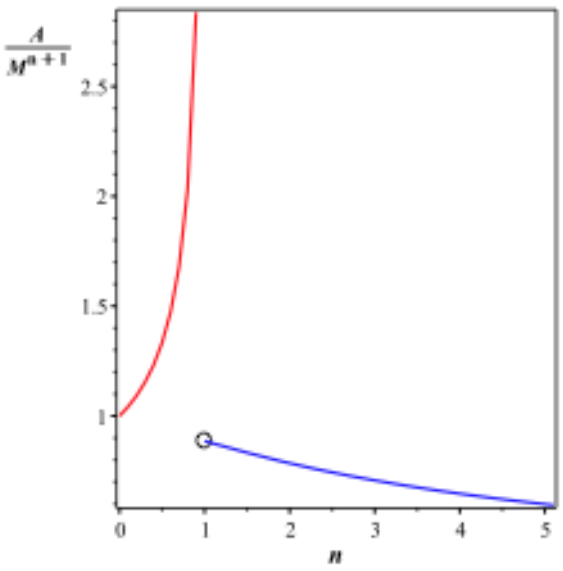

Figure 4.6: The figure of $\frac{A(n)}{M^{n+1}}$ as a function of n.

$$G - \frac{M}{2}G' = \frac{1+nM^2v^2}{(1+M^2v^2)^n} - \frac{1+nM^2}{(1+M^2)^n}. \tag{4.25}$$

The right side of (4.25) can be formulated as $g(Mv)-g(M)$ using function $g(x)=\left(1+nx^2\right)/\left(1+x^2\right)^n$, which is monotone decreasing since $g'(x)=\left[2n(1-n)x^3\right]/\left(1+x^2\right)^{n+1}<0$ for $n>1$ Hence $F'(M)>0$, which implies that $\lambda'(M)>0$. It shows that in the one-dimensional pattern forming system coarsening occurs. Two particular cases are of physical interest. Namely, M is small or large.

For small values of M, the wavelength $\lambda=\lambda(n)$ can be obtained from (4.23) for $n>1$ as follows

$$\begin{aligned}\frac{\lambda(n)}{4\sqrt{n-1}} &\approx \int_0^1 \frac{M}{\sqrt{(1+(1-n)M^2v^2)-(1+(1-n)M^2)}}\mathrm{d}v &(4.26)\\ &= \frac{1}{\sqrt{n-1}}\int_0^1 \frac{\mathrm{d}v}{\sqrt{1-v^2}} &(4.27)\\ &= \frac{1}{\sqrt{n-1}}\frac{\pi}{2}, &(4.28)\end{aligned}$$

and consequently $\lambda\approx 2\pi$. We note, that for $n<1$, similarly $\lambda\approx 2\pi$.

Remark that for $n=1$ the same relation yields [80].

For large values of M we again examine (4.23) with $n>1$ as

$$\begin{aligned}\frac{\lambda(n)}{4\sqrt{n-1}} &\approx \int_0^1 \frac{M\mathrm{d}v}{\sqrt{\left((M^2v^2)^{1-n}\right)-(M^2)^{1-n}}}\\ &= M^n\int_0^1 \frac{\mathrm{d}v}{\sqrt{v^{2(1-n)}-1}}\\ &= M^n\widetilde{\Gamma}(n),\end{aligned} \tag{4.29}$$

where

$$\widetilde{\Gamma}(n)=\frac{\sqrt{\pi}\Gamma\left(\frac{1}{2}+\frac{1}{2(n-1)}\right)}{2(n-1)\Gamma\left(1+\frac{1}{2(n-1)}\right)}. \tag{4.30}$$

For $n=1$, we refer to paper [80] that $\lambda(1)\approx 2\sqrt{2\pi}M$.

We note that from (4.29), for $n=2$, we get $\widetilde{\Gamma}(2)=1$ and the wavelength is $\lambda(2)\approx 4M^2$.

If $n=3$ then $\widetilde{\Gamma}(3)=\frac{1}{4}B\left(\frac{1}{2},\frac{3}{4}\right)$ and $\lambda(3)\approx\sqrt{3}B\left(\frac{1}{2},\frac{3}{4}\right)M^3$.

In general, for large values of M we find coarsening such as

$$\lambda(n)\approx 4\sqrt{n-1}\widetilde{\Gamma}(n)M^n \text{ for } n>1 \text{ and } n\neq 1$$

For $n < 1$, from equation (4.22), one gets that

$$\begin{aligned}\frac{\lambda(n)}{4\sqrt{1-n}} &\approx \int_0^1 \frac{M\mathrm{d}v}{\sqrt{\left((M^2v^2)^{1-n}\right)-(M^2)^{1-n}}} \\ &= M^n\int_0^1 \frac{\mathrm{d}v}{\sqrt{1-v^{2(1-n)}}} = M^n\widetilde{\Omega}(n),\end{aligned} \tag{4.31}$$

where

$$\widetilde{\Omega}(n) = \frac{\sqrt{\pi}\Gamma\left(\frac{1}{2(1-n)}\right)}{2(1-n)\Gamma\left(\frac{1}{2}+\frac{1}{2(1-n)}\right)}. \tag{4.32}$$

Note, that for example as $n = \frac{1}{2}$, then $\widetilde{\Omega}\left(\frac{1}{2}\right) = 2$ and $\lambda\left(\frac{1}{2}\right) \approx \frac{8}{\sqrt{2}}\sqrt{M}$. Figure 4.5 shows $\lambda(n)/M^n$ as a function of n.

This indicates that coarsening occurs for $n > 0$ and $n \neq 1$.

The amplitude

As in the previous part, the aim is to find the amplitude as a function of M :

$$\begin{aligned}A =& h_{\max} - h_{\min} \\ =& h(x_1) - h(x_0) \\ =& \int_{x_0}^{x_1} h_x \mathrm{d}x \\ =& \int_{x_0}^{x_1} m(x)\mathrm{d}x \\ =& \int_{x_0}^{x_1} m(x)\frac{1}{m_x}\mathrm{d}m \\ =& \int_0^M \frac{m}{\sqrt{\frac{1}{1-n}\left[(1+M^2)^{1-n}-(1+m^2)^{1-n}\right]}}\mathrm{d}m.\end{aligned} \tag{4.33}$$

Applying substitution $m = Mv$ to (4.33), one can get

$$A = \int_0^1 \frac{M^2 v\mathrm{d}v}{\sqrt{\frac{1}{1-n}\left[(1+M^2)^{1-n}-(1+M^2v^2)^{1-n}\right]}}. \tag{4.34}$$

If $n > 1$ then for the height profile $A = A(n)$

$$A(n) = \sqrt{n-1}M^2 \int_0^1 \frac{v\mathrm{d}v}{\sqrt{\left[(1+M^2v^2)^{1-n} - (1+M^2)^{1-n}\right]}} \tag{4.35}$$

If M is small

$$A \approx M \int_0^1 \frac{v\mathrm{d}v}{\sqrt{1-v^2}} = M \tag{4.36}$$

Note that for $n = 1$ the same relation yields [80]. We remark that for $n = 1$ we have $A(1) \approx \lambda(1)/16\sqrt{\pi}$ [80] . For $n < 1$ one gets again that $A \approx M$.

For large values of M, we can determine the amplitude for $n > 1$ as follows

$$\begin{aligned} A(n) &\approx \sqrt{n-1}\, M^2 \int_0^1 \frac{v\mathrm{d}v}{\sqrt{\left[(M^2v^2)^{1-n} - (M^2)^{1-n}\right]}} \\ &= \sqrt{n-1}\, M^{n+1} \int_0^1 \frac{v\,\mathrm{d}v}{\sqrt{\left(v^{2(1-n)}\right) - 1}} = M^{n+1}\widetilde{\gamma}(n), \end{aligned} \tag{4.37}$$

where

$$\widetilde{\gamma}(n) = \frac{1}{2}\sqrt{\frac{\pi}{n-1}}\frac{\Gamma\left(\frac{n+1}{2(n-1)}\right)}{\Gamma\left(\frac{1}{2}+\frac{n+1}{2(n-1)}\right)}. \tag{4.38}$$

For the special case $n = 1$, we also refer to [80], $A(1) \approx \sqrt{\pi}M^2/2$.

For $n = 2$ one gets that $\widetilde{\gamma}(2) = \pi/4$ and $A(2) \approx M^3\pi/4$.

For $n = 3$ as $\widetilde{\gamma}(3) = 1/\sqrt{2}$ the amplitude is $A(3) \approx M^4/\sqrt{2}$. Generally, $A(n) \approx M^{n+1}\widetilde{\gamma}(n)$ for $n > 1$ (see Figure 4.6).

Thus, the amplitude relations for large M values can be obtained as follows

$$\begin{aligned} &n = 1, A(1) \approx \tfrac{[\lambda(1)]^2}{16\sqrt{\pi}}, \\ &n = 2, A(2) \approx \tfrac{\pi}{32}[\lambda(2)]^{\frac{3}{2}}, \\ &n = 3, A(3) \approx \tfrac{1}{\sqrt{2}}\left[\tfrac{\lambda(3)}{\sqrt{3}B\left(\frac{1}{2},\frac{3}{4}\right)}\right]^{\frac{4}{3}}, \\ &n > 1, A(n) \approx \widetilde{\gamma}(n)\left[\tfrac{\lambda(n)}{4\sqrt{n-1}\widetilde{\Gamma}(n)}\right]^{\frac{n+1}{n}}. \end{aligned} \tag{4.39}$$

showing, as it is expected, that coarsening occurs.

If M is small, then $A \approx M$ and $\lambda(n) \approx 2\pi$.

If $n < 1$, then applying similar calculation one gets from (4.33) that

$$A(n) \approx \sqrt{1-n}\, M^2 \int_0^1 \frac{v\, \mathrm{d}v}{\sqrt{\left[(M^2)^{1-n} - (M^2 v^2)^{1-n}\right]}} \tag{4.40}$$

$$= \sqrt{1-n}\, M^{n+1} \int_0^1 \frac{v\, \mathrm{d}v}{\sqrt{\left(1 - v^{2(1-n)}\right)}} = M^{n+1} \widetilde{\omega}(n), \tag{4.41}$$

where

$$\widetilde{\omega}(n) = \frac{\sqrt{\pi}}{2(1-n)} \frac{\Gamma\left(\frac{1}{(1-n)}\right)}{\Gamma\left(\frac{1}{2} + \frac{1}{(1-n)}\right)}. \tag{4.42}$$

Note, that for $n = \frac{1}{2}$, we have $A\left(\frac{1}{2}\right) \approx \frac{4}{3}\sqrt{M^3}$ and $A\left(\frac{1}{2}\right) \approx \frac{\lambda^3\left(\frac{1}{2}\right)}{192}$.

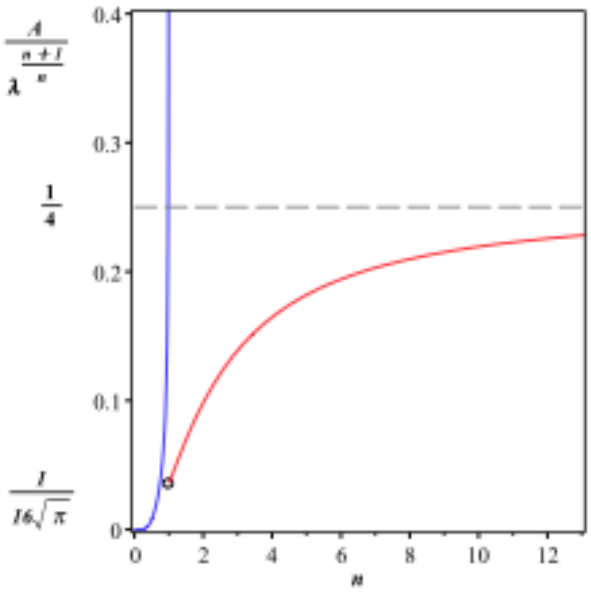

Figure 4.7: The dispersion relation (4.43).

The relation between the wavelength and the amplitude, called the dispersion relation according to [80], can be given as follows:

$$A(n) = \begin{cases} \frac{\sigma(n)}{(4\sqrt{1-n}\tilde{\Omega}(n))^{n+1}} \lambda(n)^{\frac{n+1}{n}} & \text{if } 0 < n < 1, \\ \frac{1}{16\sqrt{\pi}} \lambda^2 & \text{if } n = 1, [16] \\ \frac{\tilde{\gamma}(n)}{(4\sqrt{n-1}\tilde{\Gamma}(n))^{\frac{n+1}{n}}} \lambda(n)^{\frac{n+1}{n}} & \text{if } \quad n > 1. \end{cases} \tag{4.43}$$

Note, that for $n \to \infty$, one gets $\frac{A(n)}{\lambda(n)^{n+1}} \to \frac{1}{4}$ (see Figure 4.7). The relation (4.43) for any $n > 0$ shows that the amplitude is an increasing function of the wavelength meaning that coarsening occurs. We note that the function $\frac{A(n)}{\lambda(n)^{\frac{n-1}{n}}}$ and $\frac{A(n)}{M^{n+1}}$ as a function of n are discontinuous at 1 while $\frac{\lambda(n)}{M^n}$ has no singularity at any value of n.

4.1.6 Conclusion

In this chapter, the steady state solutions of the generalized phenomenological equation have been analytically analyzed. It is found that the equation has periodic and not periodic solutions as well. For large slope M of the particular solution we gave the connection between M and the amplitude or the wavelength. It was found that our results fit to the results given for $n = 1$ in the paper [80], but we remark that our calculations are not valid for $n = 1$. For the periodic solutions the dispersion relation have been shown, i.e. that the amplitude varies as $\lambda^{\frac{n+1}{n}}$ indicating that the model exhibits the coarsening phenomena according to Politi and Misbah. An important task for the future is to investigate the similarity solution of the generalized phenomenological model.

4.2 Scaling properties for one-dimensional singular interfacial equation

4.2.1 Introduction

As mentioned in the first section, assuming that the effects of beam fluctuation, adatom desorption and diffusion anisotropy are neglected, the continuous interfacial height is found to obey the following standard phenomenological evolution equation (conservation law), in the Cartesian coordinates (x, y),

$$\partial_t \mathscr{H} + \nabla J = F, \tag{4.44}$$

where F denotes the average deposition flux (or source term) and ∇ the standard differential operator in two space dimensions. The surface current J is written as a sum of two terms

$$J = al^2 \nabla \mathscr{H} + b\nabla(\Delta \mathscr{H}). \tag{4.45}$$

Here, a and b are physical positive constants and Δ is the Laplacian operator. The unknown function $\mathscr{H}$ measures the film thickness above a substrate point (x,y) and at time t. The local terrace width is $l = |\nabla\mathscr{H}|^{-1}$. It is not our purpose here to model the physical problem. Rather, we will explain the singular interfacial equation and focus on its properties. A special effort is made to present an analytical approach, based on the similarity reduction, which leads to a description of the coarsening dynamic. We refer to the works of [83], [181]-[28] and [91], for an useful physical background. The first term of J is the destabilizing surface current, $J_{dest} = a\frac{\nabla\mathscr{H}}{|\nabla\mathscr{H}|^2}$, which has the form suggested by Villain (the nonequilibrium current). The parameter a is the measure of the strength of the Ehrlich-Schwoebel-Villain (ESV) effect. The destabilizing term is balanced by the classical stabilizing linear term à la Mullins [120]; $J_{smooth} = b\nabla(\Delta\mathscr{H})$. This linear term describes relaxation through adatom diffusion driven by the surface free energy. The constant term F can be eliminated by using the comoving frame, i.e., $\mathscr{H} = Ft + h$. Thereby, the interfacial equation reads

$$\partial_t h = -a\nabla\frac{\nabla h}{|\nabla h|^2} - b\Delta^2 h. \tag{4.46}$$

Generally, the destabilizing surface current takes the form [91], [140], [145]

$$J_{dest} = g(|\nabla h|^2)\nabla h,$$

where the function $g(|\nabla h|^2)$ depends only on $|\nabla h|^2$. Under a Burton-Cabrera-Frank-type theory it is required that $g(r)$ approaches a constant for $r \to 0$, and it is proportional to r^{-1}, for $r \to \infty$ (large slope). In [66] Golubović considered firstly the case $g(r) = a/(1+r)$, discussed, with suitable scaling, by Johnson et al. [83].

In many cases function g has the following form ($\nu-$model) [154], [177],

$$g(r) = \frac{a}{(1+r)^\nu}, \quad \nu \geq 1, \tag{4.47}$$

or ($\mu = 2\nu - 1$)

$$g(r) = \frac{a}{1+r^{(1+\mu)/2}}, \quad \mu \geq 1, \tag{4.48}$$

characterized by different asymptotic behaviors for $r \to \infty$. Expressions (4.47) and (4.48) are interpolations between two regimes occurred at small slopes and large slopes [83], [154], [177].

The interfacial equation for the $\nu-$model (4.47) reads, for large slopes [66],

$$\partial_t h = -a\nabla\left(|\nabla h|^{-2\nu}\nabla h\right) - b\Delta^2 h, \tag{4.49}$$

in which, the nonlinear term is the well known $p-$Laplacian operator, with the exponent $p = 2(1-\nu)$, which is negative for $\nu > 1$. The one space dimension case of (4.49) reads

$$\partial_t h = -\partial_x\left(\frac{a\partial_x h}{(\partial_x h)^{2\nu}} + b\partial_{xxx}h\right), \tag{4.50}$$

which is a natural extension of

$$\partial_t h = -\partial_x\left(\frac{1}{\partial_x h} + \partial_{xxx}h\right). \tag{4.51}$$

Equation (4.50) appears also in the meandering instabilities [133] and in step bunching instabilities [138], for appropriate ν. To analyze the effect of step interactions due to elasticity on unstable step meandering during MBE, Paulin et al. [133] arrived, for large t (or for large slope), at (4.51), where the unknown h is the local displacement of the step with respect to its position. In the context of a classification scheme for step bunching instabilities Pimpinelli et al. [138] proposed a generic continuum equation of the form ($\nu = \frac{1-\rho}{2}$)

$$\partial_t h + \partial_x\left[K_1 m^\rho + K_2\partial_{xx}m^n\right] = 0, \tag{4.52}$$

where K_1, K_2, ρ and n are constants with $K_2 > 0, K_1\rho > 0$ and $m = \partial_x h$ is the local slope.

Equation of type (4.50) has triggered important developments of the theory. A particular proposal has been to study solutions that describe the roughness and the coarsening dynamics. In particular, explicit solutions, which are sought in a similarity form, often capture the essential physical properties and are often used in testing numerical schemes.

The aim of the present work is to reinforce the rule of similarity solutions of equation (4.50), where $\nu > 1/2$. In fact, the goal of the present work is to give a detailed analysis of the coarsening property based on the classical similarity argument. Although, our results concerning the roughness and coarsening exponents bear on many approaches, our aim here is not to introduce another intuitive or speculative physical scenario. Rather, an effort is made to exhibit important qualitative features of the scaling function f (see below). This analysis is the content of Sections 4 and 5. In Section 2 we state the question we

consider, while the question, which concerns the nature of the scaling function, is treated in Section 3.

4.2.2 The coarsening exponent or the scaling exponent ?

Physically, a typical configuration of a growing interface is characterized by a growing interface width $H(t)$ (typical mound height) and a growing coarsening length scale $\lambda(t)$ (typical mound lateral size). At late stages of growth pyramids or mounds, the lateral size is found experimentally to increase according to a power law in time, $\lambda(t) \sim t^{\alpha}$ with $\alpha = 1/z$, where the dynamic exponent $z \simeq 2.5-6$ depending on the material and possibly deposition condition used [154]. The interface width evolves as $H(t) \sim t^{\beta}$. A third characteristic is the typical slope, $S(t) = \max_x |\partial_x h|$, which is observed to either approach a constant or to increase with time as $S(t) \sim t^{\kappa}$. The exponents α and β are called the coarsening exponent and the roughness exponent, respectively, and are connected to exponent κ, via the relation $\beta - \alpha = \kappa$. The slope increases without bound with time (without slope selection) if $\beta > \alpha$.

Equation (4.49) has been studied by several authors. Since analytical solutions to (4.46) are difficult to extract, Golubović [66] examined the coarsening behavior by using a phase ordering type theory. The idea is to assume that the height function can be written in the form

$$\left\langle h(x_0+x,t), h(x_0,t) \right\rangle = H^2(t)\phi\left(\frac{x}{\lambda(t)}\right), \tag{4.53}$$

where ϕ is some structure characterizing the phase ordering process and the angular brackets represent a spacial average. Generally speaking, expression (4.53) is similar in many respects to the similarity form

$$h(x,t) = H(t) f(x/\lambda(t)). \tag{4.54}$$

Using equation (4.49) and supposing that (4.53) holds, it is proved that, for a large t,

$$H(t) \sim t^{\beta}, \quad \lambda(t) \sim t^{\alpha},$$

where the roughness exponent satisfies [66]

$$\beta = \begin{cases} \frac{1+\nu}{4\nu}, & \text{if } 0 < \nu < \frac{3}{2}, \\ \\ \frac{5}{12}, & \text{if } \nu > \frac{3}{2}, \end{cases} \tag{4.55}$$

and the coarsening exponent is found to be $\alpha = \frac{1}{4}$ or $z = 4$, irrespective of the interface dimension. In [154], Rost and Krug presented an analytical estimates for the scaling exponents α and β. The authors showed that $\alpha = 1/4$ and $\beta = \frac{1+\nu}{4\nu}$. Clearly this estimate clashes with (4.55) for $\nu > \frac{3}{2}$, which constitutes the first motivation of the present work.

The $\nu-$model (4.50) were also discussed by Politi and Torcini [143], [177], [144]. From the numerical results the authors concluded in [143], [144] that the coarsening exponent satisfies

$$\alpha = \begin{cases} \frac{1}{4}, & \text{if } 0 < \nu < 2, \\ \\ \frac{\nu}{5\nu-2}, & \text{if } \nu > 2. \end{cases} \tag{4.56}$$

Once again, as it is mentioned in [143], the above result contradicts the result obtained by Golubović [66] if $\nu > 2$. Details and supporting arguments are given in [177]. In paper [144] the authors reconsidered the same problem using an analytical approach developed by Politi and Misbah [141], [142]. Their theory relies the typical lateral size (or the wavelength of the mound structure) $\lambda(t)$ to the periodic stationary solutions (see below). The authors showed that the coarsening exponent is equal to $1/4$ irrespective of the parameter ν, and concluded that this exponent cannot be reached by direct integration of the growth equation. But, the roughness exponent is not investigated.

Using the scaling hypothesis

$$h(x,t) = t^{\beta} f\left(x/t^{\alpha}\right), \tag{4.57}$$

Paulin et al. [133] obtained, for (4.51), that the roughness exponent and coarsening exponent are $\beta = 1/2$ and $\alpha = 1/4$. In 2002 Pimpinelli et al. [138] investigated the scaling properties of the surface described by equation (4.52) (or (4.50) with $\rho = 1 - 2\nu$), where $K_1\rho > 0$. Using the invariance transformation (see below) the authors showed that the exponents β and α introduced in (4.57) have the expressions $\alpha = 1/4$ and $\beta = \frac{1+\nu}{4\nu}$ for $n = 1$. But the case $\nu > \frac{1}{2}$ (and $K_1 > 0$) is not discussed and will be the subject of the present investigation.

However, a limitation of the these previous studies, from the mathematical view point, is that the question of the existence of the shape function ϕ or f was ignored. Nonetheless, the shape function is relevant for the existence of the roughness and coarsening exponents, even if the partial differential equation, under consideration, is invariant under the Lie-group or the scaling transformation. Nevertheless, this approach is often a starting point for interesting mathematical problems and for rigorous results.

A second motivation is that the coarsening exponent and the scaling exponent are, sometimes, ambiguous. In order to clarify our presentation we use the conventional typical lateral size in the sense that the height function is a spatial periodic function with the period $\lambda(t)$ for any fixed t; $h(x+\lambda(t),t) = h(x,t)$.

We recall that the surface undergoes a coarsening process if the wavelength of the mound structure $\lambda(t)$ increases in time. In references [141], [142] a criterion for coarsening in the dynamics of one-dimension front is studied. The authors argued that a coarsening process occurs if and only if the period of the steady state solution is an increasing function of its amplitude (or its typical slope). In reference [144] the authors remarked that the knowledge of the stationary periodic solutions allows to determine the coarsening law $\lambda(t)$. In simple words, the exponent scaling α in (4.57) is a coarsening exponent if the shape function f is a periodic function. Hence, we may conclude that the coarsening process cannot be predicted by the simplest scaling hypothesis in all situations. However, the scaling exponents α and β can be obtained easily from the scaling transformation (provided that f exists).

In 1997 Kersner and Vicsek [86] analyzed the one-dimensional singular equation of Zhang [201]

$$\partial_t h = \partial_{xx} h + \ln|\partial_x h|, \tag{4.58}$$

which was introduced in a study on complex directed polymers. The authors obtained pseudo-similarity solutions having the form

$$h(x,t) = (t+t_0)\left[f(\eta) + \frac{1}{2}(\ln(t+t_0)-1))\right], \quad \eta = \frac{x}{\sqrt{t+t_0}}, \quad t_0 \geq e. \tag{4.59}$$

It is shown that $f(\eta)$ is monotonic increasing (resp. decreasing) for $\eta > 0$ (resp. $\eta < 0$). It follows immediately from this that any pseudo-similarity solution to (4.58) cannot admit a lateral periodicity. Similar conclusion was obtained in [70], where the authors studied the one-dimensional generalized KPZ equation [84], [94]

$$\partial_t h = \partial_{xx} h + \mu|\partial_x h|^q, \tag{4.60}$$

where μ and q are positive numbers. Assuming the scaling hypothesis (4.57) it is found that $\beta = \frac{q-2}{2(q-1)}$ and $\alpha = \frac{1}{2}$. Moreover, if $\beta > 0$ ($q < 1$ or $q > 2$) any shape function f such that $f(0) > 0$ and $f'(0) = 0$, is monotonic increasing for $\eta > 0$.

In the last example we shall consider our interfacial equation. As in [138] we look for a stationary

solution to (4.50) having the form

$$h(x,t) = h_s(x) = Ax^{\tau}, \tag{4.61}$$

where $x > 0$. Here it is required that A is a positive constant and $\nu > 1$. Inserting this scaling into equation (4.50) we obtain

$$A = \frac{\nu}{1+\nu}\left(\frac{a\nu^2}{b(\nu-1)}\right)^{\frac{1}{2\nu}}, \quad \tau = \frac{1+\nu}{\nu}. \tag{4.62}$$

Clearly, this stationary equation can be written as

$$h_s(x) = t^{\frac{1+\nu}{4\nu}} f_s(\eta), \quad \eta = xt^{-1/4}, \tag{4.63}$$

where the shape function $f_s(\eta) = A\eta^{(1+\nu)/\nu}$, which is monotonic increasing for $\eta > 0$.

As it is mentioned before, the aim of this work is to re-examine in detail the similarity reduction, for the one-dimensional case, where the exponent $\nu > \frac{1}{2}$. Thus the question of existence of the shape function arises, and together the question of whether a solution to the resulting equation has a physical meaning or is not distinguished from one being observed in practice. In the present study, we reinforce the vital role of the scaling function with respect the coarsening process. Roughly speaking we are going to explore the scaling assumption (4.54), in the next sections. We shall see that the shape function f has to satisfy a singular fourth-order ordinary differential equation which is interesting by its challenge for mathematical analytic and numerical methods. Under appropriate initial conditions we shall see that the singular fourth-order ordinary differential equation admits periodic solutions that capture the important features of the roughness and the coarsening dynamics.

4.2.3 Detailed scaling analysis

As it is said in the introduction the purpose of this work is to investigate periodic similarity solutions of the one-dimensional $\nu-$model (4.50);

$$\partial_t h = -\partial_x\left(\frac{a\partial_x h}{(\partial_x h)^{2\nu}} + b\partial_{xxx}h\right), \tag{4.64}$$

where a, b and ν are positive constants. In contrast to [138], here the positivity of the local slope $m = \partial_x h$ for all x is naturally ruled out.

In passing, we note that the local slope satisfies the following nonlinear equation

$$\partial_t m = -\partial_{xx}\left(am^p + b\partial_{xx}m\right), \quad p = 1-2\nu. \tag{4.65}$$

This equation is known, for $p > 1$, as the limit unstable Cahn-Hilliard equation [57]. Mathematically, it is a particular case of the following equation

$$\partial_t m = -A\partial_x(m^q\partial_x m) - B\partial_x(m^n\partial_{xxx}m), \tag{4.66}$$

which, for appropriate n and q, has been used to model one-dimensional dynamics of a thin film of viscous liquid, in the presence of van der Waals forces [128], [153]. One of the central questions concerning (4.66) is the finite time rupture, t_0, of the film i.e., m vanishes somewhere at t_0.

Recently, Evans et al. [57] studied the limit unstable d-dimensional Cahn-Hilliard equation

$$\partial_t m = -\Delta\left(\Delta m + |m|^{p-1}m\right), \tag{4.67}$$

where $p > 1$. The authors constructed blow-up and global similarity solutions in different ranges of the parameters p and d. It is shown, in the one dimensional case, that for any $p \neq 3$ any L^1- similarity profile for m has zero mass and hence changes sign. From this it is not unreasonable to predict that if $p < 0$ any bounded similarity profile f to (4.64) develops a singularity ($f' = 0$ or $\partial_x h = 0$).

Let us return to equation (4.64). Since the physical values of a and b turn out to be unimportant for the coarsening process we may assume that $a = b = 1$. A priori similarity solutions can be represented in the form

$$h(x,t) = t^{\frac{1+\nu}{4\nu}} f(\eta), \quad \eta = xt^{-\frac{1}{4}}. \tag{4.68}$$

We can also, as usual, impose the scaling hypothesis (4.57). This immediately leads to $\beta = \frac{1+\nu}{4\nu}$ and $\alpha = \frac{1}{4}$, and to the following singular ordinary differential equation (SODE) for the shape or the scaling function f

$$f^{(iv)} + (1-2\nu)\frac{f''}{f'^{2\nu}} - \frac{1}{4}\eta f' + \frac{1+\nu}{4\nu}f = 0, \tag{4.69}$$

where primes denote differentiation with respect to the similarity variable $\eta = xt^{-\frac{1}{4}}$.

Note that the scaling relation (4.68) and then the similarity equation (4.69) can be extracted from the

interfacial equation due to its natural scaling-invariant nature. As in [138], we use the following scaling

$$x = \mu y, \quad t = \chi \tau, \quad h(x,t) = \kappa u(y,\tau),$$

where μ, χ and κ are arbitrary constant parameters.

Since

$$\partial_t h = \frac{\kappa}{\chi}\partial_\tau u, \quad \partial_x h = \frac{\kappa}{\mu}\partial_y u, \quad \partial_x^2 h = \frac{\kappa}{\mu^2}\partial_y^2 u$$

we get from (4.50)

$$\frac{\kappa}{\chi}\partial_\tau u + \frac{\kappa^{1-2\nu}}{\mu^{2(1-\nu)}}\partial_y \left(\partial_y u\right)^{1-2\nu} + \frac{\kappa}{\mu^4}\partial_y^4 u = 0.$$

To keep the interfacial equation invariant, the following must be fulfilled

$$\frac{\kappa}{\chi} = \frac{\kappa^{1-2\nu}}{\mu^{2(1-\nu)}} = \frac{\kappa}{\mu^4}, \tag{4.70}$$

so that

$$\chi = \mu^4, \quad \kappa = \mu^{\frac{1+\nu}{\nu}}, \quad \text{and } h(x,t) = \mu^{\frac{1+\nu}{\nu}} u(x\mu^{-1}, t\mu^{-4}).$$

Consequently

$$h(x,t) = t^{\frac{1+\nu}{4\nu}} u(xt^{-1/4}, 1),$$

with $t = \mu^4$, which leads to (4.68), where $f(\eta) = u(\eta, 1)$, whenever u or f exists.

As anticipation, we can investigate directly the SODE. However, for a mathematical consideration, we are looking for a class of solutions having the following (general) pseudosimilarity form

$$h(x,t) = H(t)F(\eta, \zeta(t)), \quad \eta = x\Lambda(t), \tag{4.71}$$

where the functions $H, \Lambda(=1/\lambda), \zeta$ and F have to be determined. The variable ζ is referred as the pseudosimilarity variable. We shall be especially concerned with the question of wether or not the general scaling form (4.71) leads to (4.68) and when it does how the shape function f allows to describe periodic solutions.

Substituting (4.71) into (4.64), we obtain for F the equation

$$\partial_{\eta\eta\eta\eta} F + H^{-2\nu}\Lambda^{-2(1+\nu)}\partial_\eta \left(\partial_\eta F^{1-2\nu}\right) + H'H^{-1}\Lambda^{-4}F + \Lambda'\Lambda^{-5}\eta\,\partial_\eta F + \zeta'\Lambda^{-4}\partial_\zeta F = 0. \tag{4.72}$$

According to (4.68), we assume that $H(0) = 0$. Equation (4.72) must be a PDE for F, so that

$$H^{-2\nu}\Lambda^{-2(1+\nu)}, \quad H'H^{-1}\Lambda^{-4}, \quad \Lambda'\Lambda^{-5} \quad \text{and} \quad \zeta'\Lambda^{-4}$$

are constants. In this context equation (4.72) reads

$$\partial_{\eta\eta\eta\eta}F + p\partial_\eta\left(\partial_\eta F^{1-2\nu}\right) + qF + r\eta\partial_\eta F + s\partial_\zeta F = 0, \tag{4.73}$$

where

$$H^{-2\nu}\Lambda^{-2(1+\nu)} = p, \quad H'H^{-1}\Lambda^{-4} = q, \quad \Lambda'\Lambda^{-5} = r, \quad \text{and} \quad \zeta'\Lambda^{-4} = s. \tag{4.74}$$

It is easily shown that solutions to (4.74) can be expressed as, for some real parameters A, B, C and D,

$$H(t) = At^{\frac{1+\nu}{4\nu}}, \quad \Lambda(t) = Bt^{-\frac{1}{4}} \tag{4.75}$$

and

$$\zeta(t) = C\ln t + D, \tag{4.76}$$

for any $\nu > 0$, provided that F exists. Note that the constants A, B, C and D satisfy

$$A^{-2\nu}B^{-2(1+\nu)} = p, \quad \frac{1+\nu}{4\nu}B^{-4} = q, \quad -\frac{1}{4}B^{-4} = r, \quad CB^{-4} = s.$$

The above argument prompts us to examen a family of coordinates ζ. To this end, we consider a continuous function $\delta \not\equiv 0$ and look for ζ satisfying

$$\zeta'\Lambda^{-4} = \delta(\zeta). \tag{4.77}$$

Together with (4.75) we deduce $\frac{d\zeta}{\delta(\zeta)} = B^4\frac{dt}{t}$, so that the coordinate ζ is given implicitly by

$$\mathscr{F}(\zeta) = B^4\ln t, \tag{4.78}$$

where $\mathscr{F}$ is a primitive of $1/\delta$ whenever F exists.

With the above in hand, we may carry out a reduction of (4.73) with $\delta(\zeta)$ instead of s. This new PDE cannot be solved analytically in the general case. However, special solutions may be mapped out by

making use of the separation of variables method which assumes an additive solution of form

$$F(\eta,\zeta)=\mathscr{R}(\eta)+\mathscr{G}(\zeta).$$

Substituting of this assumed solution yields

$$\mathscr{R}^{(iv)}+p\left(\mathscr{R}'^{1-2\nu}\right)'+q\mathscr{R}+r\eta\mathscr{R}'=-q\mathscr{G}-\delta(\zeta)\frac{d\mathscr{G}}{d\zeta}=-\Gamma, \tag{4.79}$$

where Γ is a constant. A solution to the $\mathscr{G}-$equation is expressed, for an undetermined constant σ, as

$$\mathscr{G}(\zeta)=\sigma e^{-q\mathscr{F}(\zeta)}+\frac{\Gamma}{q},$$

or, equivalently,

$$\mathscr{G}=\sigma t^{-\frac{1+\nu}{4\nu}}+\Gamma B^4\frac{4\nu}{1+\nu}.$$

The determination of the function $\mathscr{R}$ is postponed for the next section.

The first surprising property is that the quantity $H(t)\mathscr{G}$ does not depend on δ. Then, in this event, (4.71) reads

$$h(x,t)=At^{\frac{1+\nu}{4\nu}}\left[\mathscr{R}(\eta)+\Gamma B^4\frac{4\nu}{1+\nu}\right]+A\sigma. \tag{4.80}$$

Since the constant $A\sigma$ can be eliminated by redefining $h=h-A\sigma$ we may assume $\sigma=0$. Note that the shifting function $f=\mathscr{R}+\Gamma B^4\frac{4\nu}{1+\nu}$ leads to (4.68), what one would expect, and needs to be a solution to the following singular ordinary differential equation

$$f^{(iv)}+p(1-2\nu)\frac{f''}{(f')^{2\nu}}+qf+r\eta f'=0. \tag{4.81}$$

Without loss of generality we may assume that $A=B=1$, which leads to (SODE);

$$f^{(iv)}+(1-2\nu)\frac{f''}{(f')^{2\nu}}+\frac{1+\nu}{4\nu}f-\frac{1}{4}\eta f'=0.$$

As a first conclusion, our approach, which has a remarkable degree of simplicity, leads to a wide range of pseudosimilarity variables and the associated pseudosimilarity solutions are in fact similarity solutions which have the same shape. The issue of this scaling argument will be clarified by showing that the scaling function is a periodic function.

4.2.4 Analytical properties of the scaling function

We now wish to consider the implication of the profile f to the coarsening phenomena. We shall present a mathematical analysis that verifies the existence of the profile and exhibit its geometrical properties. We add to SODE a natural assumption that f must be periodic, which will describe, according to (4.68), the coarsening dynamic to (4.50), completing in this way the results of [133], [66], [144] and [138].

The existence of a periodic solution will be established via a shooting argument. For this purpose we consider the following initial value problem

$$\begin{cases} f^{(iv)} + (1-2\nu)\frac{f''}{(f')^{2\nu}} - \frac{1}{4}\eta f' + \frac{1+\nu}{4\nu} f = 0, \quad \eta > 0, \\ \\ f(0) = \gamma_0, f'(0) = \gamma, f''(0) = \tau_0, f'''(0) = \tau, \end{cases} \tag{4.82}$$

where $\gamma_0 > 0, \gamma > 0, \tau_0 < 0$ and $\tau < 0$ are real (shooting) parameters. The real parameter γ plays the role the typical slope of the f. Note that since γ and $-\tau$ are positive the conditions on γ_0 and τ_0 may be relaxed to $\gamma_0 \geq 0$ and $\tau_0 \leq 0$. In addition, we may assume that $\gamma_0 = 0$ and $\tau_0 = -1$ without any essential physical change. Note that if f is periodic, we may identify exactly the coarsening length scale $\lambda(t)$ for (4.64); namely

$$\lambda(t) = \eta_p t^{1/4},$$

where η_p, depending on γ, τ and ν, is the period of f.

Most recently, the $1-$model has been studied by Guedda and Trojette [71]. It is shown that f is periodic and satisfies

$$f(\eta) \sim f(\eta_c) \pm \frac{1}{2}(\eta - \eta_c)^2 \sqrt{|\ln(\eta - \eta_c)^2|},$$

as $\eta \to \eta_c$, where η_c is an extrema point.

In the present work we shall see that the idea of [71] can be extended to any $\nu > \frac{1}{2}$.
The first property we use is that for any $\gamma \neq 0$ problem (4.82) can be locally transformed to a system of ordinary differential equations which, using the standard theory, admits a unique local solution f. Moreover, this solution satisfies

$$\begin{cases} f'''(\eta) f''(\eta) + \frac{1+\nu}{4\nu} f(\eta) f'(\eta) & -\frac{1}{8}\eta (f')^2(\eta) = \\ \\ & |\tau| + \int_0^\eta \left[(f''')^2 + (2\nu - 1)\frac{f''^2}{f'^{2\nu}} + \frac{1+2\nu}{8\nu} f'^2 \right] ds, \end{cases} \tag{4.83}$$

and

$$f'''(\eta)+{f'}^{1-2\nu}(\eta)=\tau+\gamma^{1-2\nu}+\frac{1}{4}\eta f(\eta)-\frac{1+2\nu}{4\nu}\int_0^\eta f(s)ds, \tag{4.84}$$

for all $\eta\in(0,\eta_c)$, where $(0,\eta_c)$ is the maximal interval of existence. Note that the real number η_c (the existence time) is characterized by

$$\lim_{\eta\uparrow\eta_c}|f(\eta)|+|f'(\eta)|+|f''(\eta)|+|f'''(\eta)|=\infty, \tag{4.85}$$

if η_c is finite. Identity (4.83) is obtained by multiplying the equation in (4.82) by f'' and integrating over $(0,\eta),\eta<\eta_c$, and identity (4.84) is obtained by a simple integration of the equation in (4.82), over $(0,\eta)$. Identity (4.84) indicates that f' cannot vanish on $(0,\eta_c)$. Hence f is monotonic strictly decreasing on $(0,\eta_c)$. Next, we shall see that $f''<0$ and $f'''\leq 0$ on $(0,\eta_c)$, which constitutes the second property. To confirm this, we assume, by contradiction, that there exists a real number $0<\eta_0<\eta_c$ such that $f'''\leq 0$ on $(0,\eta_0)$, $f'''(\eta_0)=0, f^{(iv)}(\eta_0)\geq 0, f'''>0$ on $(\eta_0,\eta_0+\varepsilon)$ and $f''<0$ on $(0,\eta_0+\varepsilon)$, for some $\varepsilon>0$ small enough. From identity (4.83) we find that

$$\frac{1}{4}\eta f'-\frac{1+\nu}{2\nu}f<0 \tag{4.86}$$

for all $\eta_0\leq\eta<\eta_0+\varepsilon$. From equation in (4.82) we deduce that the above inequality excludes $f^{(iv)}(\eta_0)\geq 0$. Therefore f''' is nonpositive and f'' is negative on $(0,\eta_c)$.

The third property that we need is that η_c is finite,

$$f'(\eta_c)=0 \tag{4.87}$$

and that $f'''(\eta)$ is unbounded as η approaches η_c. For the sake of contradiction we assume that f is global, i. e., $\eta_c=\infty$. Since f' is positive and monotonic decreasing $f'(\eta)\to f'_\infty$ as η approaches infinity, for some $0\leq f'_\infty<\gamma$. Moreover, since f'' is monotonic decreasing, we must have $f''(\eta)\to 0$ as $\eta\to 0$, and then $f''>0$, which is a contradiction. Therefore, f is not global. Let us now suppose that $f'(\eta_c)$ is positive. We deduce from (4.84) that f''' and (then) f'' are bounded on $(0,\eta_c)$, which violate (4.85). Finally, a closer inspection of (4.84) reveals that $f'''(\eta)\to-\infty$ as $\eta\to\eta_c$.

The last property we employ is that $f''{f'}^{1-2\nu}$ and $f^{(iv)}$ tend to $-\infty$ as $\eta\to\eta_c$ and that the behavior of

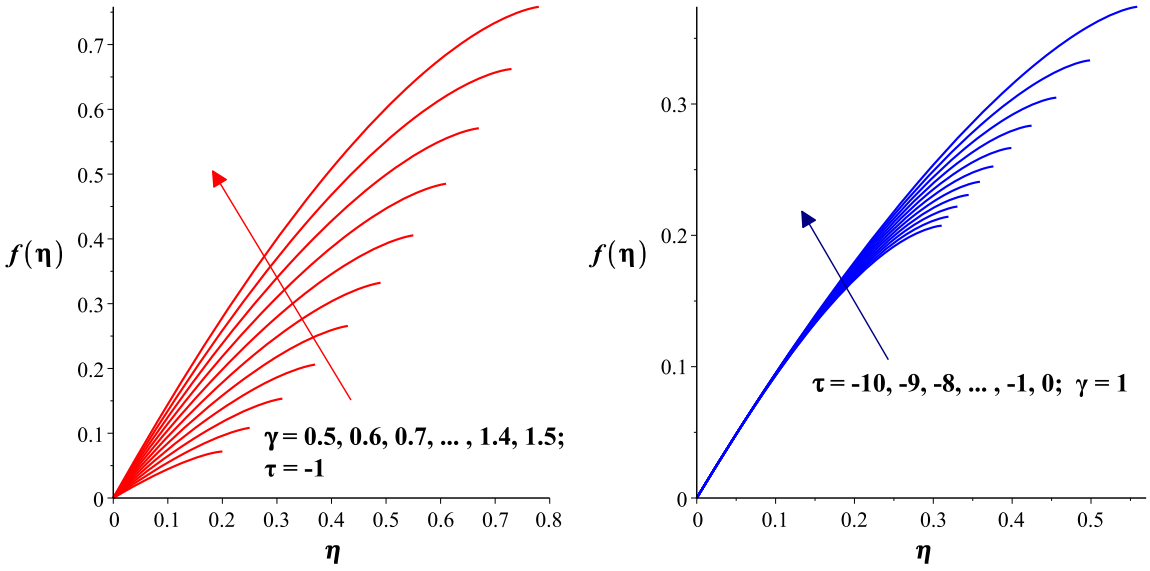

Figure 4.8: (Color online) Plots of f against similarity variable η, for $\nu = 2$ and for different parameters $\gamma = f'(0)$ (left figures) and $\tau = f''(0)$ (right figures). Numerical solutions indicate, in particular, that profile f is singular at the critical (finite) point η_c, such that $f'(\eta_c) = 0$.

$f(\eta)$ in a left neighbourhood of $\eta = \eta_c$ is controlled by the equation

$$f^{(iv)} + (1-2\nu)\frac{f''}{f'^{2\nu-1}} = 0,$$

or

$$f''' + f'^{1-2\nu} = 0. \tag{4.88}$$

For the purpose of investigating the influence of parameters γ and τ, computations were carried out, using ODE45. It emerges that at the blowing-up point (or at the boundary $\eta = \eta_c$) the first derivative of f vanishes, but the second derivative suffers an infinite jump for $\nu \geq 1$ (see Figure 4.8 for $\nu = 2$). An immediate consequence is that the interfacial equation (4.64) admits solutions h such that $\partial_x h(x(t),t) = 0$ and $|\partial_{xx} h(x(t),t)| = \infty$, where $x(t) = \eta_c t^{1/4}$, for $\nu > 1$.

We now summarize the pertinent observations from these analytical and numerical results. For any $\gamma > 0$ and any $\tau < 0$, problem (4.82) cannot be solved globally and cannot develop a periodic structure which, at first sight, clashes with that predicted in [66], [133] and with that observed by experiments. A natural desire would be to understand how the nonglobal solution behaves for $\eta > \eta_c$ (complete/incomplete singularity) and how it is intended to capture the coarsening law ? Those questions will be treated in the next section.

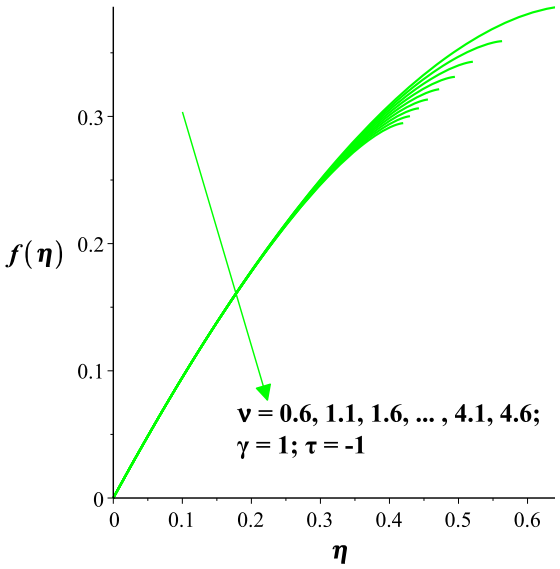

Figure 4.9: (Color online) Plots of f for different parameter ν, showing that the critical (finite) point η_c decreases as ν increases.

4.2.5 Steady-state solutions and coarsening process

According to the physical results given in [133], [66] and [138] the main mathematical deductions of the previous section have to be refined. Also the appearance of singularities in higher derivatives of f deserves attention. In preparation to the discussion of the coarsening properties, we recall that a partial answer to the above questions was given in Section 4, where it is proved that near the singular (or the interface) point the solution f can be regarded as a solution to the following ordinary differential equation

$$f''' + f'^{1-2\nu} = 0. \tag{4.89}$$

Let us note that (4.89) appears when studying stationary solutions to (4.64), which is the key of the coarsening process. To be more precise, it is reported in a large literature (see for example [140], [145], [136] and references therein) that the endless coarsening is related to the existence of periodic steady states at all wavelengths (larger than a certain critical wavelength).

Recently, Politi and Misbah [141], [142] studied a criterion for coarsening in the dynamics of one-dimension front. The authors argued that a coarsening process occurs if and only if the period of the steady state solution is an increasing function of its amplitude or its typical slope.

In the present section we reinforce the role of the periodic steady states to (4.64). Roughly speaking we are going to obtain a family of periodic solutions $h_S = h_S(x)$ that are parametrized by the typical slope

$S = \max_x |\partial_x h_S(x)|$. This allows us to analyze the coarsening process and to investigate whether the profile f admits an extension for $\eta > \eta_c$. If such continuation exists, we say that the singularity (or the blow-up) is incomplete.

The steady states solutions to (4.64) satisfy the equation

$$\frac{1}{(\partial_x h)^{2\nu-1}} + \partial_{xxx} h = c, \tag{4.90}$$

where c is an undetermined constant. Since equation (4.64) is invariant under the symmetry $x \to -x$, we may assume that $c = 0$. We therefore have to solve

$$h''' + {h'}^{1-2\nu} = 0, \tag{4.91}$$

where $h = h(x)$ and prime denotes differentiation with respect to the variable x. In term of the local slope $m = h'$, the above ODE reads

$$m'' + m^{1-2\nu} = 0. \tag{4.92}$$

With regard to (4.87), equation (4.92) will be solved with the initial condition

$$m(0) = 0. \tag{4.93}$$

It may be noted that equation (4.92) stems also from the $\nu'-$model, for appropriate ν' (dual index to ν) and for the particular case where the relaxation term is neglected in comparison with $\partial_x h/(\partial_x h)^{2\nu'}$. More precisely, if we consider the singular equation

$$\partial_t h = -\partial_x \left(\partial_x h/(\partial_x h)^{2\nu'} \right),$$

where $\nu' > 1/2$, or the singular equation for the local slope

$$\partial_t m = -\partial_x^2 \left(m^{1-2\nu'} \right),$$

and look for solutions of the form (variable separations)

$$m(x,t) = A^\star(t)\zeta^\star(x),$$

one finds that, for some constant σ

$$A^{\star}(t) = (A^{\star 2\nu'}(0) + 2\nu'\sigma t)^{1/2\nu'},$$

and ζ satisfies

$$(\zeta^{\star 1-2\nu'})'' + \sigma\zeta^{\star} = 0.$$

This leads, for $\sigma > 0$, to equation (4.92) with $\nu = \frac{\nu'}{2\nu'-1}$, which is connected to ν' via $\frac{1}{2\nu} + \frac{1}{2\nu'} = 1$.

We ought to mention that equation (4.92), which is referred as the singular Emden-Fowler equation, was studied in 1978 by Taliaferro [172]. The author showed that the problem ($q = 2\nu - 1$)

$$m'' + m^{-q} = 0, \quad 0 < x < 1, \tag{4.94}$$

$$m(0) = m(1) = 0, \tag{4.95}$$

where $q > 0$, has a unique positive solution.
Numerical positive solutions to problem (4.94), (4.95), for $q > 1$, can be found in the paper by Lima and Oliveira [108]. Based on [172], the authors concluded that any local positive solution satisfies

$$m(x) \sim \left(\frac{(1+q)^2}{2(q-1)}\right)^{1/(1+q)} x^{2/(1+q)} \quad \text{as } x \to 0^+. \tag{4.96}$$

In this section we are interested in the existence of periodic solutions to (4.92), (4.93), where $\nu > 1/2$. Note that estimate (4.96) breaks down if $q = 1$ or $\nu = 1$. As mentioned before this critical case is analysed in [71]. The authors obtained periodic solutions which behave like $m(x) \sim x\sqrt{-\ln x^2}$, as $x \to 0^+$. So, the next result deals with the existence of periodic solutions to (4.92), (4.93), where $1 \neq \nu > 1/2$. A global view of the nature of steady state solutions will be obtained via a construction of trajectories in the phase space (m, m').
Equation (4.92) has the first integral

$$(m')^2 + \frac{1}{1-\nu} m^{2(1-\nu)} = \frac{1}{1-\nu} S^{2(1-\nu)}, \tag{4.97}$$

where $\pm S$ is the turning point or the typical slope (i.e. $m' = 0$ when $|m| = S = \max_x |m|$). We look for

solutions having finite typical slope.

Consider first the case $\nu > 1$. From (4.97) we get

$$m' = \pm\sqrt{\frac{1}{\nu-1}\left[m^{2(1-\nu)} - S^{2(1-\nu)}\right]}. \tag{4.98}$$

Hence, m is given by $m(x) = \mathscr{F}^{-1}(\pm x)$, where

$$\mathscr{F}(y) = \sqrt{\nu-1}\int_0^y \frac{dz}{\sqrt{z^{2(1-\nu)} - S^{2(1-\nu)}}}. \tag{4.99}$$

This is an implicit equation for m if S is known. Moreover, a simple analysis of (4.98) reveals that m is periodic with the period,

$$\lambda_p(S) = S^\nu \lambda_p(1), \tag{4.100}$$

where

$$\lambda_p(1) = 2\frac{\sqrt{\pi}}{\sqrt{\nu-1}}\frac{\Gamma\left(\frac{1}{2}+\frac{1}{2(\nu-1)}\right)}{\Gamma\left(1+\frac{1}{2(\nu-1)}\right)}. \tag{4.101}$$

This proves that a perpetual coarsening takes place. Equation (4.100) also shows that the period of the steady state uniquely determines the typical slope and that a periodic steady state exists for any period $\lambda > 0$.

Equation (4.98) or function (4.99) will be also used to exhibit the behavior of $m(x)$ as x approaches 0. Because

$$\int_0^{m(x)/S} \frac{dz}{\sqrt{z^{2(1-\nu)}-1}} = \pm S^{-\nu}\sqrt{\frac{1}{\nu-1}}x,$$

it can be verified that

$$m(x) \sim \pm\left(\frac{\nu^2}{\nu-1}\right)^{1/2\nu} x^{1/\nu}, \tag{4.102}$$

as $x \to 0^+$, and then

$$h(x) \sim h(0) \pm \frac{\nu}{1+\nu}\left(\frac{\nu^2}{\nu-1}\right)^{1/2\nu} x^{(1+\nu)/\nu}, \tag{4.103}$$

as $x \to 0^+$. The above estimates can be deduced from (4.96) by setting $q = 2\nu - 1$.

Equation (4.98) can be solved exactly for $\nu = 2$. Using (4.99), we find

$$m(x) = \pm\sqrt{x(2-\frac{x}{S^2})},$$

for $0 \leq x \leq \lambda_p(S)/2 = 2S^2$.

Observe that the value $\lambda_p(S) = 4S^2$ can be obtained from Eq. (4.101) by taking $\nu = 2$.

Note also that if we look for solutions with a vertical tangent $S = \infty$, we obtain $m' = \pm\sqrt{\frac{1}{\nu-1}}|m|^{1-\nu}$. From which we may deduce, for $x \geq 0$, that

$$m(x) = \pm\left(\frac{\nu^2}{\nu-1}\right)^{1/2\nu} x^{1/\nu}, \tag{4.104}$$

and then, as it is expected (see (4.61) and (4.62)),

$$h(x) = h(0) \pm \frac{\nu}{1+\nu}\left(\frac{\nu^2}{\nu-1}\right)^{1/2\nu} x^{(1+\nu)/\nu}, \tag{4.105}$$

for $x \geq 0$.

For the case $\frac{1}{2} < \nu < 1$ the same treatment yields to

$$\int_0^{m(x)/S} \frac{dz}{\sqrt{1-z^{2(1-\nu)}}} = \pm S^{-\nu}\sqrt{\frac{1}{1-\nu}}x,$$

as soon as $|m(x)| \leq S$. From this we may deduce that m is $\lambda_p(S)-$periodic, where the period is given by

$$\lambda_p(S) = 2S^{\nu}\frac{\sqrt{\pi}}{\sqrt{1-\nu}}\frac{\Gamma\left(\frac{1}{2(1-\nu)}\right)}{\Gamma\left(\frac{1}{2}+\frac{1}{2(1-\nu)}\right)}. \tag{4.106}$$

Moreover m and h satisfy, for small x,

$$m(x) \sim \pm S^{1-\nu}\sqrt{\frac{1}{1-\nu}}x, \quad h(x) \sim h(0) \pm \frac{1}{2}S^{1-\nu}\sqrt{\frac{1}{1-\nu}}x^2. \tag{4.107}$$

Clearly, the above estimates can be extended to any values $0 < \nu < 1$. In particular if $\nu = 1/2$ we get the following exact solution

$$m(x) = \pm x\left(\sqrt{2S} - x/2\right),$$

for $0 \leq x \leq \sqrt{2S}$. However, the analysis of SODE, where $0 < \nu < \frac{1}{2}$, is more problematic.

As a final application, we return to SODE, where $1 \neq \nu > \frac{1}{2}$. Recall that close to $\eta = \eta_c$, this equation behaves like (4.91). Hence, we may deduce that the singularity is incomplete, and that f is a (global) periodic solution, with the period $n_p = \mathscr{O}(n_c)$. Our findings confirms that the typical mound lateral size, the typical mound height and the typical mound slope grow with time like $t^{1/4}, t^{(1+\nu)/4\nu}$ and $t^{1/4\nu}$ respec-

tively. Moreover, we have the following estimate

$$f(\eta) \sim f(\eta_c) \pm \frac{\nu}{1+\nu}\left(\frac{\nu^2}{\nu-1}\right)^{1/2\nu} |\eta_c - \eta|^{(1+\nu)/\nu},$$

for $\nu > 1$ and

$$f(\eta) \sim f(\eta_c) \pm \frac{1}{2} S^{1-\nu} \sqrt{\frac{1}{1-\nu}} (\eta_c - \eta)^2,$$

for $1/2 < \nu < 1$ near an extrema η_c.

4.2.6 Conclusion

We have presented a detailed analysis of similarity solutions to the one-dimensional singular interfacial equation. This equation was used, for large slope, to describe the mound-type structures on the growing surfaces, where the destabilizing current is of the form suggested by Villain. A central result of the similarity assumption is that the singular interfacial equation is reduced to a singular ordinary differential equation satisfied by the shape or the similarity profile f. Although the mathematical and numerical results proved the local existence of the profile which is singular at some point, our first approach cannot be directly used to understand the coarsening phenomenon. An additional analysis, based on periodic steady states, showed that the singularity is incomplete; that is the profile f is extended to a periodic solution which confirms the power law of the typical mound lateral size, the typical mound height and the typical mound slope. Moreover the interfacial equation admits solutions which satisfy $\partial_x h = 0$ at $(\eta_c t^{1/4}, t)$, for some real number $\eta_c > 0$, and have the following estimate

$$h(x,t) \sim \left(\frac{t}{t_0}\right)^{(1+\nu)/4\nu} h(x_0,t_0) \pm \frac{\nu}{1+\nu}\left(\frac{\nu^2}{\nu-1}\right)^{1/2\nu} |t^{1/4}\eta_c - x|^{\frac{1+\nu}{\nu}}, \tag{4.108}$$

for $\nu > 1$ and for $1/2 < \nu < 1$,

$$h(x,t) \sim \left(\frac{t}{t_0}\right)^{(1+\nu)/4\nu} h(x_0,t_0) \pm \frac{1}{2} t^{(1-\nu)/4\nu} S^{1-\nu} \sqrt{\frac{1}{1-\nu}} (t^{1/4}\eta_c - x)^2. \tag{4.109}$$

As a consequence of estimate (4.108) the second derivative of h suffers an infinite jump for $\nu > 1$.

Chapter 5

On singular quasilinear elliptic equations with data measures

This chapter "On singular quasilinear elliptic equations with data measures" by Taourirte Laila, Fatima Aqel and Alaa Nour Eddine, is accepted in the journal Advances in Nonlinear Analysis, (2020).

5.1 Introduction

In this work, we restrict our attention to the study of a class of quasilinear elliptic problem with a singular nonlinearity and data measure namely:

$$(P_\lambda)\begin{cases} -\Delta u = \dfrac{a(x)}{u^\gamma} + b(x)|\nabla u|^p + \lambda f \ \ in \ \ \Omega, \\ u > 0 \quad in \quad \Omega, \\ u = 0 \ \ on \ \ \partial\Omega. \end{cases} \tag{5.1}$$

Where Ω is an open bounded subset of $\mathbb{R}^N$ for $N \geq 2$, with smooth boundary $\partial\Omega$, $f \in M_B^+(\Omega)$ is a given finite nonnegative Radon measure, $\gamma > 0$, $\lambda > 0$, and under certain assumptions on the functions a and b. We stress that the problem is singular as one asks to the solution to be zero on the boundary.

The study of nonlinear elliptic problems with singular nonlinearities is motivated by its various applications in too many fields, for example, in fluid mechanics, newtonian fluids, in flow through porous media, in glaciology [46] and boundary layer phenomena for viscous fluids, chemical heterogeneous catalysts, as well as in the theory of heat conduction in electrically conducting materials and some equations that model the electrostatic MEMS devices or Micro-Electro Mechanical systems [78].
In order to trace the objectives of our work, we will start by recalling some previous researches where three types of problems were treated: quasilinear equations with regular data, semilinear problems with singular nonlinearities and coupling of the both problems in the regular case.
_ Case where f is regular:

- Case where $b \equiv 0$, the problem is simply written in the form

$$\begin{cases} -\Delta u = \dfrac{a(x)}{u^{\gamma}} + \lambda f(x) \quad in \quad \Omega, \\ u > 0 \quad in \quad \Omega, \\ u = 0 \quad on \quad \partial\Omega, \end{cases} \tag{5.2}$$

  for the homogeneous case (i.e. $\lambda = 0$), a large literature exists on the subject, we cite in particular the pioneer works of ([49], [101] and references therein) in which they show by using the method of sub- and supersolutions, that if $a(x)$ is a bounded smooth function, then (5.2) has a classical solution. The case where $a(x)$ is only a function in $L^1(\Omega)$ was treated in [37] where he proved some existence and regularity results for problem (5.2) depending on γ: if $\gamma \leq 1$, there exists a solution $u \in H_0^1(\Omega)$, otherwise if $\gamma > 1$, there exists a solution $u \in H_{loc}^1(\Omega)$ and $u^{\frac{\gamma+1}{2}} \in H_0^1(\Omega)$.
  The nonhomogeneous case (i.e. $\lambda > 0$) has also been considered in [64] where the authors proved the existence of bounded solutions to (5.2) if a and f are functions that belong to $L^q(\Omega)$ for $q > \frac{N}{2}$.

- Case where $a \equiv 0$, the problem is formulated in the following form

$$\begin{cases} -\Delta u = b(x)|\nabla u|^p + \lambda f(x) \quad in \quad \Omega, \\ u > 0 \quad in \quad \Omega, \\ u = 0 \quad on \quad \partial\Omega, \end{cases} \tag{5.3}$$

If $1 < p \leq 2$, $b \in L^{\infty}(\Omega)$ and f is regular enough, then (5.3) has been considered in the literature. For instance, it is shown in [7] that if (5.3) has a subsolution $\underline{u}$ and a supersolution $\overline{u}$ in $W^{2,q}$ $(q > N)$ with $\underline{u} \leq \overline{u}$ in Ω, then there exists a solution u to (5.3) such that $\underline{u} \leq u \leq \overline{u}$.

This problem has also been studied in [109] when $f \in W^{1,\infty}(\Omega)$. He showed that if (5.3) has a nonnegative supersolution defined in $W^{2,q}(\Omega)$ for $(q > N)$, then it has a solution no matter the value of p $(1 \leq p < \infty)$. A key step in this technique relies on the estimate of ∇u in $L^{\infty}(\Omega)$, that's why he used a method originally introduced by Bernstein and later developed in ([96],[97]),([161], [162]).

_ Case where f is only integrable or a Radon measure:

- Case where $b \equiv 0$, has been treated by [102], in which the two different cases $\gamma \leq 1$ and $\gamma > 1$ have been studied separately: for $\gamma \leq 1$, they obtain the existence of a weak solution $u \in W_0^{1,q}(\Omega)$ for $1 \leq q < \frac{N}{N-1}$ through an approximation argument, and for $\gamma > 1$, they prove the existence and uniqueness of the solution only in $W_{loc}^{1,q}(\Omega)$ for every $1 \leq q < \frac{N}{N-1}$, such that $T_k(u)^{\frac{\gamma+1}{2}} \in H_0^1(\Omega)$ for every fixed $k > 0$, (where $T_k(u)$ represents the truncated function of u) as we don't necessarily have $u^{\frac{\gamma+1}{2}} \in H_0^1(\Omega)$ since f and a are not regular enough.

- Case where $a \equiv 0$, the situation is quite different if f is a nonnegative integrable function or, more generally a given finite nonnegative measure on Ω. Since f is not regular enough in this case, the usual techniques that lead to the $W^{1,\infty}$-solutions can not be exploited. This difficulty was the main motivation behind the work [6]. They distinguished different cases where they found existence and nonexistence results for different p values in (5.3) using the isoperimetric inequality: if $p > 1$, the existence of a solution is obtained if λ is sufficiently small and the measure f does not charge the sets of $W^{1,p'}-$ capacity zero $\left(\frac{1}{p} + \frac{1}{p'} = 1\right)$, and if $p \leq 2$, assuming the existence of a supersolution $w \in W_0^{1,2}(\Omega)$, there exists a solution for problem (5.3).

For the case when $\lambda \equiv 0$, $b(x) \equiv I$ and $1 < p \leq 2$, the model problem is defined in [1] in the

following sense

$$\begin{cases} -\Delta u = \dfrac{a}{u^{\gamma}} + |\nabla u|^{p} \quad in\ \ \Omega, \\ u > 0 \qquad in\ \ \Omega, \\ u = 0 \qquad on\ \ \partial\Omega, \end{cases} \tag{5.4}$$

If $p = 2$, (5.4) admits a distributional solution for all $a \in L^1(\Omega)$.

If $1 < p < 2$, the treatment of (5.4) is different depending on the function a: if $a(x) \in L^{\infty}(\Omega)$, the existence is obtained for every $\gamma > 0$, however, for the general case $a(x) \in L^1(\Omega)$, there exists a constant $\gamma_0 \geq 0$ such that the solution exists under the condition $\gamma > \gamma_0$.

We note that in this work, we ask λ and the functions a and b to be not identically zero.

We conclude this section by recalling some recent work on parabolic version of our problem. The first work is that in [33] who deal with the problem:

$$\begin{cases} u_t - \Delta u = \dfrac{a}{u^{\gamma}} + \mu u^{r} & \text{in } \Omega \times (0,T) \\ u = 0 & \text{on } \partial\Omega \times (0,T) \\ u(0) = f & \text{in } \Omega \\ u > 0 & \text{in } \Omega \times (0,T) \end{cases} \tag{5.5}$$

where $\gamma > 0, \mu \geq 0, r > 0$ and $f \in M_B^{+}(\Omega)$. They show the existence of a solution for every value of T for suitable small data a and f if $r > 1$ and for every data if $0 < r < 1$. The second is the one studied in [127]:

$$\begin{cases} u_t - \Delta_p u = \dfrac{a}{u^{\gamma}} + f & \text{in } \Omega \times (0,T) \\ u = 0 & \text{on } \partial\Omega \times (0,T) \\ u(0) = u_0 & \text{in } \Omega \end{cases} \tag{5.6}$$

Where $p > 2 - \dfrac{1}{N+1}, \gamma > 0$. They establish that if $a, u_0 \in L^1(Q_T)^{+}$ and $f \in M_B^{+}(Q_T)$ then there exists a nonnegative distributional solution u.

The last is that in [9] who have studied the well-posedness of triply nonlinear degenerate elliptic-parabolic-hyperbolic problem:

$$b(u)_t - div(A(u, \nabla\phi(u)) + \psi(u) = f, \quad u|_{t=0} = u_0 \tag{5.7}$$

They obtain a general continuous dependence result on data u_0, f and nonlinearities b, ψ, ϕ, A. They obtain existence, uniqueness and continuous dependence on data u_0, f when $[b+\psi](\mathbb{R}) = \mathbb{R}$ and $\phi \circ [b+$

$\psi]^{-1}$ is continuous.

In the near future the authors will tackle the existence and the uniqueness of solutions for the quasilinear singular parabolic problem with initial data $f \in M_B^+(\Omega)$:

$$\begin{cases} u_t - \Delta u = \dfrac{a}{u^\gamma} + b|\nabla u|^p & \text{in } \Omega \times (0,T) \\ u = 0 & \text{on } \partial\Omega \times (0,T) \\ u(0) = \lambda f & \text{in } \Omega \\ u > 0 & \text{in } \Omega \times (0,T) \end{cases} \tag{5.8}$$

This chapter is organized as follows. We devote the next section to the necessary conditions on the data in order to get existence of weak solutions in (P_λ). The third section deals with the existence of solutions for the non-singular sublinear problem and the singular sublinear problem, for every nonnegative Radon measure depending on the value of γ. The main tool in this section is the isoperimetric inequality. In the last section, we show that the uniqueness of the solution holds for every $1 \leq p < \dfrac{N}{N+1}$ and $\gamma > 0$.

5.1.1 Definitions and properties

Our aim in this work is to prove the existence of a suitable weak solution to (P_λ). Here, as well as in the proof of other similar results, the first step is to precise in which sense we want to solve our problem. On one hand, a solution to (P_λ) has to be understood in the weak distributional meaning. On the other hand, we have to take into account the singular nonlinearity at zero. For this purpose, we adopt the following definition:

Definition 3

Let $u \in W^{1,1}_{loc}(\Omega)$. We say $u \leq 0$ on $\partial\Omega$ if $(u-\varepsilon)^+ \in W^{1,1}_0(\Omega)$ for every $\varepsilon > 0$. Furthermore, $u = 0$ on $\partial\Omega$ if u is nonnegative in Ω and $u \leq 0$ on $\partial\Omega$.

Definition 4

If $\gamma > 0$, then a weak solution to problem (P_λ) is a function

$$\begin{cases} u \in W^{1,1}_{loc}(\Omega) \text{ and } u = 0 \text{ on } \partial\Omega \text{ in the sense of Definition 3}, \\ \forall \omega \subset\subset \Omega, \exists c_\omega,\ u \geq c_\omega > 0 \text{ in } \omega, \\ \displaystyle\int_\Omega \nabla u \nabla \varphi = \int_\Omega \frac{a(x)}{u^\gamma}\varphi + \int_\Omega b(x)|\nabla u|^p \varphi + \lambda \int_\Omega < f, \varphi >, \forall \varphi \in C^1_c(\Omega). \end{cases} \tag{5.9}$$

5.2 Necessary conditions for existence

5.2.1 Size condition

Theorem 3

Let $p > 1$, $\gamma > 0$ and $\lambda > 0$. We suppose that $a \in L^1(\Omega)$ and there exists a ball B_0 in Ω such that $b(x) \geq C_0 > 0$ a.e $x \in B_0$ and $\int_{B_0} f > 0$. Then there exists $0 < \lambda^* < \infty$ such that (P_λ) does not have any solution for $\lambda > \lambda^*$.

Proof.

Assume u is the solution of (P_λ).

We have

$$-\Delta u = \frac{a(x)}{u^\gamma} + b(x)|\nabla u|^p + \lambda f \ \text{ in } D'(B_0). \tag{5.10}$$

Since $\frac{a(x)}{u^\gamma} \geq 0$, then we get

$$-\Delta u \geq b(x)|\nabla u|^p + \lambda f \ \text{ in } D'(B_0). \tag{5.11}$$

Let $\varphi \in C_0^\infty(B_0)$, $\varphi \geq 0$, we multiply (5.11) by φ and integrate to obtain

$$\begin{aligned}
\lambda \int_{B_0} \varphi f &\leq \int_{B_0} \nabla u \nabla \varphi - \int_{B_0} b(x)|\nabla u|^p \varphi \\
&\leq \int_{B_0} \nabla u \nabla \varphi - C_0 \int_{B_0} |\nabla u|^p \varphi \\
&\leq \int_{B_0} \varphi \left[\nabla u \frac{\nabla \varphi}{\varphi} - C_0 |\nabla u|^p \right] \\
&\leq C_p \int_{B_0} \varphi \left| \frac{\nabla \varphi}{\varphi} \right|^{p'},
\end{aligned}$$

in which $C_p = \dfrac{p-1}{p^{\frac{p}{p-1}} C_0^{\frac{1}{p-1}}}$.
This implies that

$$\forall \varphi \in C_0^\infty(B_0) \qquad \lambda \int_{B_0} \varphi f \leq C_p \int_{B_0} \frac{|\nabla \varphi|^{p'}}{\varphi^{p'-1}}. \tag{5.12}$$

Now, let us prove that this implies λ is finite (whence the existence of λ^*). By density, (5.12) remain valid for $\varphi \in W_0^{1,\infty}(B_0)$.

The existence of λ^* will be proved if we can construct φ such that

$$\varphi \in W_0^{1,\infty}(B_0), \varphi > 0 \text{ on } B_0, \qquad C_p \int_{B_0} \frac{|\nabla \varphi|^{p'}}{\varphi^{p'-1}} < \infty. \tag{5.13}$$

Here, we set $F(r) = \int_0^r \frac{ds}{C_0|s|^p + M}$, *where* $M > 0$ *is chosen large enough. Since* F *is continuously increasing, and*

$$\eta = \int_0^\infty \frac{ds}{C_0|s|^p + M} = F(+\infty) < \infty, \tag{5.14}$$

we may introduce the following function

$$g(r) = F^{-1}(r), \text{ where } g : [0,\eta) \to [0,\infty) \tag{5.15}$$

and

$$h(r) = \begin{cases} \dfrac{1}{C_0|g(r)|^p + M} & 0 \le r \le \eta \\ 0 & \eta < r < \infty \end{cases} \tag{5.16}$$

Writing $\varphi(x) = h(|x|)$, *we check that*

$$\begin{aligned} h'(r) &= \frac{-g'(r)C_0\ p\ |g(r)|^{p-1}}{(C_0|g(r)|^p + M)^2} = \frac{-\left(C_0\ |g(r)|^p + M\right)C_0\ p\ |g(r)|^{p-1}}{(C_0|g(r)|^p + M)^2} \\ &= \frac{-C_0\ p\ |g(r)|^{p-1}}{(C_0|g(r)|^p + M)} = -h(r)\left(C_0\ p\ |g(r)|^{p-1}\right), \end{aligned}$$

$$\begin{aligned} I = C_p \int_{B_0} \frac{|\nabla\varphi|^{p'}}{\varphi^{p'-1}} &= C_p\ \omega_N \int_0^\eta r^{N-1} h(r)\ |C_0\ p\ |g(r)|^{p-1}|^{p'} dr \\ &\le \tilde{C}_p \eta^{N-1} \int_0^\eta h(r)|g(r)|^p dr \end{aligned}$$

in which $\tilde{C}_p = C_p \omega_N C_0\ p$.

By using (5.16), *we have*

$$\begin{aligned} I &\le \tilde{C}_p \eta^{N-1} \int_0^\eta \frac{|g(r)|^p}{C_0|g(r)|^p + M} dr \\ &\le \frac{\tilde{C}_p}{C_0} \eta^{N-1} \int_0^\eta \frac{1}{1 + \frac{M}{C_0}} \\ &\le \frac{C\ \eta^N}{M} \end{aligned}$$

this proves (5.13) *and theorem 2.1.*

In order to prove existence of (P_λ) by approximation, we will need some preliminaries on the approxi-

mated sequences of solutions u_n that we can prove existence for any value of γ. To do that, we define the approximated equation associated to (P_λ).

5.3 Existence of solutions for the non-singular sublinear problem and for every nonnegative Radon measure

Let us consider the following approximated problem

$$(P_\varepsilon)\begin{cases} -\Delta u = \dfrac{a(x)}{(u+\varepsilon)^\gamma} + b(x)|\nabla u| + \lambda f & \text{in } \Omega, \\ u = 0 & \text{on } \partial\Omega. \end{cases} \tag{5.17}$$

where ε is nonnegative.

Theorem 4

Let $a \in L^1(\Omega)^+, b \in L^{N+\eta}(\Omega)$, then for all $\gamma > 0$, $\lambda > 0$ and for all $f \in M_B^+(\Omega)$, the problem (P_ε) has a nonnegative weak solution u in $W_0^{1,q}(\Omega)$ for $1 \le q < \dfrac{N}{N-1}$.

The main tool in the proof of this theorem is the isoperimetric inequality that we will use under the following form [114].

Lemma 2

Let $u \in W_0^{1,1}(\Omega)$. Then

$$\frac{-d}{dt}\int_{[u>t]} |\nabla u| \ge N\omega_N^{\frac{1}{N}}\mu(t)^{1-\frac{1}{N}}, \tag{5.18}$$

where ω_N is the measure of the unit ball and

$$\mu(t) = meas\{x \in \Omega : |u(x)| > t\}. \tag{5.19}$$

We now present the proof of Theorem 4;

Proof.

To approximate our problem (P_ε), we define the truncated function T_k given as follows

$$T_k(r) = \max(-k, \min(r,k)). \tag{5.20}$$

Now, we truncate the functions a, b and f by considering the three sequences a_n, b_n and f_n which are

defined by

$$\text{let } n \in \mathbb{N}, a_n(x) = \min(a(x), n),\ b_n(x) = \min(b(x), n), \tag{5.21}$$

and

$$f_n \in C_0^\infty(\Omega),\ \text{such that } f_n \geq 0,\ ||f_n||_{L^1(\Omega)} \leq ||f||_{M_B(\Omega)} \text{ and } f_n \to f \text{ in } M_B(\Omega). \tag{5.22}$$

Let us consider the following approximated problem

$$\begin{cases} u_n \in W_0^{1,\infty}(\Omega), \\ \dfrac{1}{n}u_n - \Delta u_n = \dfrac{a_n(x)}{(u_n+\varepsilon)^\gamma} + \dfrac{b_n(x)|\nabla u_n|}{1+\frac{1}{n}b_n(x)|\nabla u_n|} + \lambda f_n \quad \text{in } \Omega. \end{cases} \tag{5.23}$$

We consider the regularized problem (5.23)*. Then for all* $\varepsilon > 0$*, there exists* u_n *solution of* (5.23)*. Indeed, the constant* $\overline{M} = \max((2n||a_n||_\infty)^{\frac{1}{\gamma+1}} - \dfrac{1}{n} + 2\lambda n||f_n||_\infty)$ *is a supersolution of* (5.23) *and* $\underline{M} = 0$ *is a subsolution. Then by applying the classical theory (see [7]), we obtain the existence of* u_n *solution of* (5.23)*.*

At this level, we will prove the existence of a constant C independent of n such that

$$\int_\Omega |\nabla u_n|^q \leq C, \qquad 1 \leq q < \frac{N}{N-1}. \tag{5.24}$$

First of all, we introduce the following function

$$p_{t,h}(r) = \begin{cases} 0 & \text{if } r \leq t \\ \dfrac{r-t}{h} & \text{if } t \leq r \leq t+h \\ 1 & \text{if } r > t+h \end{cases} \tag{5.25}$$

We multiply (5.23) *by* $p_{t,h}(u_n)$ *and then we integrate on* Ω *to obtain*

$$\int_\Omega \left[\frac{1}{n}u_n - \Delta u_n\right] p_{t,h}(u_n) = \int_\Omega \left[\frac{a_n}{(u_n+\frac{1}{n})^\gamma} + \frac{b_n|\nabla u_n|}{1+\frac{1}{n}b_n|\nabla u_n|} + \lambda f_n\right] p_{t,h}(u_n). \tag{5.26}$$

Since

$$\frac{b_n|\nabla u_n|}{1+\frac{1}{n}b_n|\nabla u_n|} \leq b|\nabla u_n|, \tag{5.27}$$

then, we get

$$\begin{aligned}\frac{1}{h}\int_{[t\le u_n\le t+h]}|\nabla u_n|^2 &\le \int_{[t\le u_n\le t+h]}\frac{a_n}{(u_n+\varepsilon)^\gamma}\frac{u_n-t}{h}+\int_{[u_n\ge t+h]}\frac{a_n}{(u_n+\varepsilon)^\gamma}\\ &+ \int_{[u_n\ge t]} b|\nabla u_n|+\lambda||f_n||_{L^1(\Omega)}.\end{aligned}$$

Since $\frac{u_n-t}{h}\le 1$ *and* $||f_n||_{L^1(\Omega)}\le ||f||_{M_b(\Omega)}$, *we obtain*

$$\begin{aligned}\frac{1}{h}\int_{[t\le u_n\le t+h]}|\nabla u_n|^2 &\le \int_{[u_n\ge t]}\frac{a_n}{(u_n+\varepsilon)^\gamma}+||b||_{L^{N+\eta}(\Omega)}\left(\int_{[u_n\ge t]}|\nabla u_n|^q\right)^{\frac{1}{q}}\\ &+ \lambda||f||_{M_b(\Omega)},\end{aligned}$$

in which $q=(N+\eta)'=\frac{N}{N-1}-\varepsilon(\eta)$, $\varepsilon(\eta)>0$.

Thanks to the nonnegativity of u_n, *we get the following*

$$\frac{1}{h}\int_{[t\le u_n\le t+h]}|\nabla u_n|^2 \le \frac{C_1}{\varepsilon^\gamma}+C_q\left(\int_{[u_n\ge t]}|\nabla u_n|^q\right)^{\frac{1}{q}}+C_\lambda, \tag{5.28}$$

where $C_1=||a||_{L^1(\Omega)}$, $C_q=||b||_{L^{N+\eta}(\Omega)}$ *and* $C_\lambda=\lambda||f||_{M_b(\Omega)}$.

Now, we assume that $N\ge 2$ so that $q<2$ then we use the following two inequalities

$$\frac{1}{h}\int_{[t\le u_n\le t+h]}|\nabla u_n|^q\le\left(\frac{1}{h}\int_{[t\le u_n\le t+h]}|\nabla u_n|^2\right)^{\frac{q}{2}}\left(\frac{\mu(t)-\mu(t+h)}{h}\right)^{\frac{2-q}{2}}, \tag{5.29}$$

and

$$\frac{1}{h}\int_{[t\le u_n\le t+h]}|\nabla u_n|\le\left(\frac{1}{h}\int_{[t\le u_n\le t+h]}|\nabla u_n|^q\right)^{\frac{1}{q}}\left(\frac{\mu(t)-\mu(t+h)}{h}\right)^{\frac{q-1}{q}}. \tag{5.30}$$

Next, we take the q^{th} power of (5.30) and we multiply it by the square of (5.29) to find

$$\left(\frac{1}{h}\int_{[t\le u_n\le t+h]}|\nabla u_n|\right)^q\left(\frac{1}{h}\int_{[t\le u_n\le t+h]}|\nabla u_n|^q\right)\le\left(\frac{1}{h}\int_{[t\le u_n\le t+h]}|\nabla u_n|^2\right)^q\left(\frac{\mu(t)-\mu(t+h)}{h}\right). \tag{5.31}$$

Now, we plug the inequality (5.28) into the previous inequality, and we let h tend to zero, to obtain a differential inequality satisfied by $\sigma_n(t)=\int_{[u_n\ge t]}|\nabla u_n|^q$ and defined in the following sense

$$\left(-\frac{d}{dt}\int_{[u_n\ge t]}|\nabla u_n|\right)^q\left(-\sigma_n'(t)\right)\le\left(\frac{||a||_{L^1(\Omega)}}{\varepsilon^\gamma}+C_q\left(\sigma_n(t)\right)^{\frac{1}{q}}+C_\lambda\right)^q. \tag{5.32}$$

On the other hand, according to the isoperimetric inequality (5.18), we get

$$N^q \omega_n^{\frac{q}{N}} \mu_n(t)^{q(1-\frac{1}{N})}(-\sigma_n^{'}(t)) \leq \left(\frac{||a||_{L^1(\Omega)}}{\varepsilon^\gamma} + C_q (\sigma_n(t))^{\frac{1}{q}} + C_\lambda \right)^q \left(-\mu_n^{'}(t) \right), \tag{5.33}$$

using Young's inequality on the right hand side term, this also gives

$$-\sigma_n^{'}(t) \leq N^{-q} \omega_n^{\frac{-q}{N}} \left(\frac{D_1}{\varepsilon^{\gamma q}} + D_q \, \sigma_n(t) + D_\lambda \right) \mu_n(t)^{q(\frac{1}{N}-1)}(-\mu_n^{'}(t))), \tag{5.34}$$

in which $D_1 = \left(||a||_{L^1(\Omega)} \right)^q$, $D_q = {C_q}^q$ and $D_\lambda = {C_\lambda}^q$. This implies that

$$-\sigma_n^{'}(t) \leq \left(\frac{\hat{D_1}}{\varepsilon^{\gamma q}} + \hat{D_q}\sigma_n(t) + \hat{D_\lambda} \right) \mu_n(t)^{q(\frac{1}{N}-1)}(-\mu_n^{'}(t))), \tag{5.35}$$

where $\hat{D_1} = N^{-q}\omega_n^{\frac{-q}{N}} D_1$, $\hat{D_q} = N^{-q}\omega_n^{\frac{-q}{N}} D_q$ and $\hat{D_\lambda} = N^{-q}\omega_n^{\frac{-q}{N}} D_\lambda$.

This can be rewritten as

$$-\frac{d}{dt}\left(e^{-k\mu_n(t)^\alpha} \sigma_n(t) \right) \leq \frac{d}{dt}\left(e^{-k\mu_n(t)^\alpha} \right) \frac{1}{\hat{D_q}} \left(\frac{\hat{D_1}}{\varepsilon^{\gamma q}} + \hat{D_\lambda} \right), \tag{5.36}$$

in which $\alpha = 1 - q\,\frac{N-1}{N}$ and $k\alpha = \hat{D_q}$.

Then by integrating from $t = 0$ to $t = ||u_n||_\infty$, and knowing $\sigma_n(||u_n||_\infty) = 0$ and $\mu_n(||u_n||_\infty) = 0$, we get

$$e^{-k\mu_n(0)^\alpha} \sigma_n(0) \leq \frac{1}{\hat{D_q}} \left(\frac{\hat{D_1}}{\varepsilon^{\gamma q}} + \hat{D_\lambda} \right). \tag{5.37}$$

Since $\mu_n(0) \leq |\Omega|$, we get

$$\int_\Omega |\nabla u_n|^q \leq C, \tag{5.38}$$

where $C = e^{k|\Omega|^\alpha} \frac{1}{\hat{D_q}} \left(\frac{\hat{D_1}}{\varepsilon^{\gamma q}} + \hat{D_\lambda} \right)$.

Since

$$|| \frac{a_n}{(u_n + \varepsilon)^\gamma} ||_{L^1(\Omega)} \leq \frac{||a||_{L^1(\Omega)}}{\varepsilon^\gamma}, \tag{5.39}$$

we deduce from (5.23) and (5.38)

$$||\Delta u_n||_{L^1(\Omega)} \leq C \quad \textit{and} \quad ||u_n||_{W_0^{1,q}(\Omega)} \leq C. \tag{5.40}$$

This yields to the compactness of u_n in $W_0^{1,q}(\Omega)$ for $1 \leq q < \dfrac{N}{N-1}$. Then by passing to the limit, we conclude the main result.

5.3.1 Existence of solutions for the singular sublinear problem and for every nonnegative Radon measure

In this section, we consider the problem (P_λ) for $p = 1$, we have the following result

Theorem 5

Let $0 < \gamma < 1$, $a \in L^\infty(\Omega)^+$ and $b \in L^{N+\eta}(\Omega)$. Then for all $\lambda > 0$ and for all $f \in M_B^+(\Omega)$, the problem (P_λ) has a solution u in $W_0^{1,q}(\Omega)$ for every $1 \leq q < \dfrac{N}{N-1}$.

Proof.

For all $n > 0$, let $\varepsilon = \dfrac{1}{n}$, then from theorem (4), the approximated problem associated to (P_λ) admits a solution

$$\begin{cases} u_n \in W_0^{1,q}(\Omega) \text{ for all } 1 \leq q < \dfrac{N}{N-1}, \\ -\Delta u_n = \dfrac{a(x)}{(u_n + \dfrac{1}{n})^\gamma} + b(x)|\nabla u_n| + \lambda f \quad \text{in } \Omega. \end{cases} \tag{5.41}$$

Since we have

$$-\Delta u_n \geq \lambda f, \tag{5.42}$$

by using the uniform Hopf principle as formulated in [53], there exists a constant C only depending on Ω such that

$$Gf \geq C \left(\int_\Omega f \phi_1 \right) \phi_1, \tag{5.43}$$

where ϕ_1 denotes the first eigenfunction of $-\Delta$ with Dirichlet condition, and G denotes the inverse in $L^1(\Omega)$ of the operator $-\Delta$ under homogeneous Dirichlet conditions. Therefore we have

$$u_n \geq \lambda \; Gf \geq \lambda \; C(\Omega) \left(\int_\Omega f \phi_1 \right) \phi_1. \tag{5.44}$$

By taking $\varphi = p_{t,h}(u_n)$ as a test function in the weak formulation given above, where $p_{t,h}$ is given by (5.25)*, and using (5.44) and the fact that $u_n + \dfrac{1}{n} \geq u_n$, we obtain*

$$\int_\Omega \nabla u_n \nabla p_{t,h}(u_n) \leq \int_\Omega \frac{a(x) p_{t,h}(u_n)}{{\phi_1}^\gamma} + \int_\Omega b(x)|\nabla u_n| p_{t,h}(u_n) + \lambda \int_\Omega f p_{t,h}(u_n)$$

which implies that

$$\begin{aligned}\frac{1}{h}\int_{[t\le u_n\le t+h]}|\nabla u_n|^2 &\le \int_{[t\le u_n\le t+h]}\frac{a(x)}{{\phi_1}^\gamma}\frac{(u_n-t)}{h}\\ &+ \int_{[u_n\ge t+h]}\frac{a(x)}{{\phi_1}^\gamma}+\int_{[u_n\ge t]}b(x)|\nabla u_n|+\lambda||f||_{M_b(\Omega)}\end{aligned}$$

Since $0\le\dfrac{u_n-t}{h}\le 1$ *on the set* $[t\le u_n\le t+h]$, *we obtain*

$$\frac{1}{h}\int_{[t\le u_n\le t+h]}|\nabla u_n|^2 \le \int_\Omega\frac{a(x)}{{\phi_1}^\gamma}+\int_{[u_n\ge t]}b(x)|\nabla u_n|+\lambda||f||_{M_b(\Omega)}$$

Therefore

$$\begin{aligned}\frac{1}{h}\int_{[t\le u_n\le t+h]}|\nabla u_n|^2 &\le \int_\Omega\frac{a(x)}{{\phi_1}^\gamma}+||b||_{L^{N+\eta}(\Omega)}\left(\int_{[u_n\ge t]}|\nabla u_n|^q\right)^{\frac{1}{q}}\\ &+ \lambda||f||_{M_b(\Omega)}\end{aligned}$$

in which $q=(N+\eta)'=\frac{N}{N-1}-\varepsilon(\eta)$, $\varepsilon(\eta)>0$.

Then, we get

$$\frac{1}{h}\int_{[t\le u_n\le t+h]}|\nabla u_n|^2 \le C_1\int_\Omega\frac{1}{{\phi_1}^\gamma}+C_q\left(\int_{[u_n\ge t]}|\nabla u_n|^q\right)^{\frac{1}{q}}+C_\lambda,$$

where $C_1=||a||_{L^\infty(\Omega)}$, $C_q=||b||_{L^{N+\eta}(\Omega)}$ *and* $C_\lambda=\lambda||f||_{M_b(\Omega)}$.

Analogously to the proof of the previous theorem, we finally get

$$\int_\Omega|\nabla u_n|^q\le C. \tag{5.45}$$

Again as before, we have u_n *converges to* u *in* $W_0^{1,q}(\Omega)$ *for all* $1\le q<\dfrac{N}{N-1}$ *and a.e. in* Ω. *Then since* $b\in L^{N+\eta}(\Omega)$, $b|\nabla u_n|$ *converges to* $b|\nabla u|$ *in* $L^1(\Omega)$. *On the other hand, since* $\gamma<1$, *we have*

$$\left|\frac{a(x)}{{u_n}^\gamma}\right|\le\frac{||a||_{L^\infty(\Omega)}}{{\phi_1}^\gamma}\in L^1(\Omega). \tag{5.46}$$

Hence, by Lebesgue theorem, we deduce that $\dfrac{a}{{u_n}^\gamma}$ *converges to* $\dfrac{a}{u^\gamma}$ *in* $L^1(\Omega)$. *Finally,* u *is a solution to* (P_λ), *which concludes the proof.*

5.3.2 The strongly singular case: $\gamma > 1$

In this case, only local estimates on the approximated solution u_n can be obtained. Our aim here is mainly to give global estimates on $T_k^{\frac{\gamma+1}{2}}(u)$ in $H_0^1(\Omega)$ in order to provide at least a weak sense to u on the boundary of Ω.

Theorem 6

Let $\gamma > 1$ and $b \in L^{N+\eta}(\Omega)$. Then for all finite measure f and $\lambda \in \mathbb{R}$, the problem (P_λ) has a solution u in $W_{loc}^{1,q}(\Omega)$ for every $1 \leq q < \dfrac{N}{N-1}$ and $T_k(u)^{\frac{\gamma+1}{2}} \in H_0^1(\Omega)$.

Proof.

For all n, by theorem (4), the approximated problem associated to (P_λ) admits a solution

$$\begin{cases} -\Delta u_n = \dfrac{a_n(x)}{\left(u_n + \frac{1}{n}\right)^\gamma} + b_n(x)|\nabla u_n| + \lambda f, \quad \text{in } \Omega \\ u_n \in W_0^{1,q}(\Omega) \text{ for all } 1 \leq q < \dfrac{N}{N-1}. \end{cases} \tag{5.47}$$

First, we remark that

$$-\Delta u_n \geq \lambda f, \tag{5.48}$$

hence

$$u_n \geq \lambda\ Gf \geq \lambda\ C(\Omega)\phi_1. \tag{5.49}$$

Then for all $\omega \subset\subset \Omega$, there exists a constant $c_\omega > 0$ such that

$$u_n(x) \geq c_\omega \text{ in } \omega. \tag{5.50}$$

We first show that $T_k(u)^{\frac{\gamma+1}{2}} \in H_0^1(\Omega)$, for this we introduce the test function

$$\phi = T_k(u_n)^\gamma e^{\beta u_n}$$

Next, we multiply (5.47) *by ϕ and we integrate over Ω to obtain*

$$\begin{aligned} &\int_\Omega \gamma |\nabla u_n|^2 T_k'(u_n) T_k(u_n)^{\gamma-1} e^{\beta u_n} + \beta \int_\Omega |\nabla u_n|^2 T_k(u_n)^\gamma e^{\beta u_n} \\ &= \int_\Omega \frac{a_n}{(u_n + \frac{1}{n})^\gamma} T_k(u_n)^\gamma e^{\beta u_n} + \int_\Omega b_n |\nabla u_n| T_k(u_n)^\gamma e^{\beta u_n} + \int_\Omega \lambda f T_k(u_n)^\gamma e^{\beta u_n}. \end{aligned}$$

Recalling that $\frac{T_k(u_n)^\gamma}{(u_n+\frac{1}{n})^\gamma} \leq \frac{u_n^\gamma}{(u_n+\frac{1}{n})^\gamma} \leq 1$, *hence*

$$\begin{aligned}&\gamma\int_\Omega |\nabla T_k(u_n)^{\frac{\gamma+1}{2}}|^2 + \beta\int_\Omega |\nabla u_n|^2 T_k(u_n)^\gamma e^{\beta u_n}\\ &\leq e^{\beta k}||a||_{L^1} + \varepsilon\int_\Omega |\nabla u_n|^2 T_k(u_n)^\gamma e^{\beta u_n} + C(\varepsilon,k)\int_\Omega b^2 + C_k||f||_{M_B}.\end{aligned}$$

this implies

$$\begin{aligned}&\gamma\int_\Omega |\nabla T_k(u_n)^{\frac{\gamma+1}{2}}|^2 + (\beta-\varepsilon)\int_\Omega |\nabla u_n|^2 T_k(u_n)^\gamma e^{\beta u_n}\\ &\leq e^{\beta k}||a||_{L^1} + \varepsilon\int_\Omega |\nabla u_n|^2 T_k(u_n)^\gamma e^{\beta u_n} + C(\varepsilon,k)\int_\Omega b^2 + C_k||f||_{M_B}.\end{aligned}$$

Choosing β *such that* $\beta-\varepsilon>0$ *leads to*

$$\gamma\int_\Omega |\nabla T_k(u_n)^{\frac{\gamma+1}{2}}|^2 \leq e^{\beta k}||a||_{L^1} + C_k||f||_{M_B} + C(\varepsilon,k)\int_\Omega b^2. \tag{5.51}$$

Now we show the boundedness of u_n *in* $W^{1,q}_{loc}(\Omega)$ *into two steps.*

For fixed $k>0$, *we will make use of the two truncations functions* $T_k(s)$ *given by* (5.20) *and* $G_k(s)$ *defined as*

$$G_k(s) = (|s|-k)^+ sign(s).$$

Step 1: $G_1(u_n)$ *is bounded in* $W^{1,q}_0(\Omega)$ *for all* $1 \leq q < \frac{N}{N-1}$.

In other words, we have to prove that

$$\int_{[u_n\geq 1]} |\nabla u_n|^q \leq C(k). \tag{5.52}$$

Analogously to the case $\gamma \leq 1$, *we take* $\phi = p_{t,h}(u_n)$ *as a test function in (5.47), and we obtain*

$$\int_\Omega -\Delta u_n\ p_{t,h}(u_n) = \int_\Omega \left[\frac{a_n}{(u_n+\frac{1}{n})^\gamma} + b_n|\nabla u_n| + \lambda f_n\right] p_{t,h}(u_n). \tag{5.53}$$

Hence

$$\frac{1}{h}\int_{[t\leq u_n\leq t+h]}|\nabla u_n|^2 \quad\leq\quad \int_{[u_n\geq t]}\frac{a_n}{(u_n+\frac{1}{n})^{\gamma}}+\int_{[u_n\geq t]}b|\nabla u_n|+\lambda||f||_{M_b(\Omega)}$$

Therefore

$$\begin{aligned}\frac{1}{h}\int_{[t\leq u_n\leq t+h]}|\nabla u_n|^2 &\leq \int_{\Omega}\frac{a_n}{(t+\frac{1}{n})^{\gamma}}+||b||_{L^{N+\eta}(\Omega)}\left(\int_{[u_n\geq t]}|\nabla u_n|^q\right)^{\frac{1}{q}} &(5.54)\\ &+ \lambda||f||_{M_b(\Omega)} &(5.55)\end{aligned}$$

in which $q=(N+\eta)'=\frac{N}{N-1}-\varepsilon(\eta)$, $\varepsilon(\eta)>0$. *Then, we get*

$$\begin{aligned}\frac{1}{h}\int_{[t\leq u_n\leq t+h]}|\nabla u_n|^2 &\leq \frac{||a||_{L^1(\Omega)}}{t^{\gamma}}+||b||_{L^{N+\eta}(\Omega)}\left(\int_{[u_n\geq t]}|\nabla u_n|^q\right)^{\frac{1}{q}} &(5.56)\\ &+ \lambda||f||_{M_b(\Omega)} &(5.57)\end{aligned}$$

therefore we get the following inequality

$$\frac{1}{h}\int_{[t\leq u_n\leq t+h]}|\nabla u_n|^2 \quad\leq\quad \frac{C_1}{t^{\gamma}}+C_q\left(\int_{[u_n\geq t]}|\nabla u_n|^q\right)^{\frac{1}{q}}+C_{\lambda} \tag{5.58}$$

where the constants $C_1=||a||_{L^1(\Omega)}$, $C_q=||b||_{L^{N+\eta}(\Omega)}$ *and* $C_{\lambda}=\lambda||f||_{M_b(\Omega)}$.

Analogously to the case $\gamma\leq 1$, *we plug the inequality* (5.58) *into the previous inequality* (5.31). *By tending h to zero, we obtain a differential inequality satisfied by the function* σ_n *which is defined in the following sense* $\sigma_n(t)=\int_{[u_n\geq t]}|\nabla u_n|^q$,

$$(-\frac{d}{dt}\int_{[u_n\geq t]}|\nabla u_n|)^q(-\sigma_n^{'}(t))\leq\left(\frac{C_1}{t^{\gamma}}+C_q\sigma_n(t)^{\frac{1}{q}}+C_{\lambda}\right)^q(-\mu_n^{'}(t)) \tag{5.59}$$

On the other hand, according to the isoperimetric inequality (5.18), *we get*

$$N^q\omega_n^{\frac{q}{N}}\mu_n(t)^{q(1-\frac{1}{N})}(-\sigma_n^{'}(t))\leq\left(\frac{C_1}{t^{\gamma}}+C_q\left(\sigma_n(t)\right)^{\frac{1}{q}}+C_{\lambda}\right)^q\left(-\mu_n^{'}(t)\right), \tag{5.60}$$

using Young's inequality on the right hand side term, this also gives

$$-\sigma_n^{'}(t) \leq N^{-q}\omega_n^{\frac{-q}{N}}\left(\frac{D_1}{t^{\gamma q}} + D_q\ \sigma_n(t) + D_\lambda\right)\mu_n(t)^{q(\frac{1}{N}-1)}(-\mu_n^{'}(t))), \tag{5.61}$$

in which $D_1 = {C_1}^q$, $D_q = {C_q}^q$ *and* $D_\lambda = {C_\lambda}^q$. *This implies that*

$$-\sigma_n^{'}(t) \leq \left(\frac{\hat{D_1}}{t^{\gamma q}} + \hat{D_q}\sigma_n(t) + \hat{D_\lambda}\right)\mu_n(t)^{q(\frac{1}{N}-1)}(-\mu_n^{'}(t))), \tag{5.62}$$

where $\hat{D_1} = N^{-q}\omega_n^{\frac{-q}{N}} D_1$, $\hat{D_q} = N^{-q}\omega_n^{\frac{-q}{N}} D_q$ *and* $\hat{D_\lambda} = N^{-q}\omega_n^{\frac{-q}{N}} D_\lambda$.

This can be rewritten as

$$-\frac{d}{dt}\left(e^{-k\mu_n(t)^\alpha}\sigma_n(t)\right) \leq \frac{d}{dt}\left(e^{-k\mu_n(t)^\alpha}\right)\frac{1}{\hat{D_q}}\left(\frac{\hat{D_1}}{t^{\gamma q}} + \hat{D_\lambda}\right), \tag{5.63}$$

in which $\alpha = 1 - q\,\frac{N-1}{N}$ *and* $k\alpha = \hat{D_q}$.

Again, by integrating between 1 *and* $||u_n||_\infty$. *Since* $\sigma_n(||u_n||_\infty) = 0$ *and* $\mu_n(||u_n||_\infty) = 0$, *we get*

$$\int_{[u_n \geq 1]} |\nabla u_n|^q \leq \hat{C}_N[e^{k\mu_n(1)^\alpha} - 1]. \tag{5.64}$$

Step 2: $T_1(u_n)$ *is bounded in* $H^1_{loc}(\Omega)$.

We have to investigate the behaviour of (u_n) *for the small values* $(u_n \leq 1)$. *We then need to prove that* $\forall \omega \subset\subset \Omega$,

$$\int_\omega |\nabla T_1(u_n)|^2 \leq C^{'}. \tag{5.65}$$

First, we take $T_1^\gamma(u_n)$ *as a test function in (5.47), we get*

$$\gamma\int_\omega |\nabla T_1(u_n)|^2\ T_1^{\gamma-1}(u_n) = \int_\Omega \left[\frac{a_n}{(u_n + \frac{1}{n})^\gamma} + b_n|\nabla u_n| + \lambda f_n\right] T_1^\gamma(u_n) \leq C. \tag{5.66}$$

Then according to (5.49), *we have* $u_n \geq c_\omega$ *on* ω. *We observe that*

$$\gamma\, {c_\omega}^{\gamma-1}\int_\omega |\nabla T_1(u_n)|^2 \leq \gamma\int_\Omega |\nabla T_1(u_n)|^2\ T_1^{\gamma-1}(u_n) \leq C. \tag{5.67}$$

Now since $u_n = T_1(u_n) + G_1(u_n)$, *we deduce that* u_n *is bounded in* $W^{1,q}_{loc}(\Omega)$ *for every* $1 \leq q < \dfrac{N}{N-1}$.

By (5.47)*, we obtain*

$$||\Delta u_n||_{L^1_{loc}(\Omega)} \leq C(\omega),$$

which yields to the compactness of (u_n) *in* $W^{1,q}_{loc}(\Omega)$ *for* $1 \leq q < \dfrac{N}{N-1}$*, (see Lemma 4 in Appendix).*

Let $\omega \subset\subset \Omega$*,* $\varphi \in C^{\infty}_0(\Omega)$*, and supp* $\varphi = \omega$*.*

Since $u_n \geq c_\omega$ *in* ω*, then we have*

$$|\frac{a_n}{\left(u_n + \frac{1}{n}\right)^{\gamma}}\ \varphi| \leq \frac{||a||_{L^{\infty}(\Omega)}}{{c_\omega}^{\gamma}}\ |\varphi| \in L^1(\Omega). \tag{5.68}$$

Hence, by Lebesgue theorem, we deduce that $\dfrac{a_n}{\left(u_n + \frac{1}{n}\right)^{\gamma}}$ *converges to* $\dfrac{a}{u^{\gamma}}$ *in* $L^1_{loc}(\Omega)$*.*

Finally, we deduce that u is a solution to (P_λ)*, which concludes the proof of Theorem 6.*

5.4 Uniqueness of weak solutions

Theorem 7

Let $f \in M^+_B(\Omega)$*,* $a \in L^1(\Omega)^+$*,* $b \in L^{N+\eta}(\Omega)$*,* $1 \leq p < \dfrac{N}{N-1}$ *and* $\gamma > 0$*. Then for all* $\lambda > 0$ *and for all* $f \in M^+_B(\Omega)$*, the solution of* (P_λ) *is unique if it exists.*

The uniqueness result that we obtain is a consequence of the following lemma:

Lemma 3

Let $A \in L^{N+\eta}(\Omega)^N$*,* $\theta \in W^{1,q}_{loc}(\Omega)$*,* $1 \leq q < \dfrac{N}{N-1}$*,* $\theta \geq 0$ *in* Ω *and* $\theta = 0$ *on* $\partial\Omega$ *in the sense of Definition 3 , and such that*

$$-\Delta\theta \leq A.\nabla\theta \quad \text{ in } \mathscr{D}'(\Omega). \tag{5.69}$$

Then $\theta = 0$ *in* Ω*.*

Proof.

We have $(\theta - \varepsilon)^+ \in W^{1,q}_0(\Omega)$ *for all* $\varepsilon > 0$*, and by mean of Kato's inequality up to the boundary (see [146]), we obtain*

$$\begin{aligned} -\Delta(\theta-\varepsilon)^+ &\leq -\Delta(\theta-\varepsilon)\ \chi_{[\theta-\varepsilon>0]} \\ &\leq -\Delta\theta\ \chi_{[\theta-\varepsilon>0]} \\ &\leq A.\nabla\theta\ \chi_{[\theta-\varepsilon>0]} \end{aligned}$$

Hence

$$\begin{cases} (\theta-\varepsilon)^+ \in W_0^{1,1}(\Omega), \\ -\Delta(\theta-\varepsilon)^+ \leq A.\nabla(\theta-\varepsilon)^+ \quad \text{in } \mathscr{D}'(\Omega). \end{cases} \tag{5.70}$$

Now using Lemma 4.6 of [6], we obtain

$$\theta-\varepsilon \leq 0, \text{ i.e. } \theta \leq \varepsilon, \ \forall \varepsilon > 0, \tag{5.71}$$

and since $\theta \geq 0$ in Ω, then $\theta = 0$ in Ω.

Proof.

Let u be a supersolution of (P_λ) and $\hat{u}$ a subsolution, and let $w = u - \hat{u}$.

We take the difference between the equations associated to u and $\hat{u}$ respectively, we obtain

$$-\Delta w = \frac{a(x)}{u^\gamma} - \frac{a(x)}{\hat{u}^\gamma} + |\nabla u|^p - |\nabla \hat{u}|^p. \tag{5.72}$$

By the convexity, there exists $A \in L^{N+\eta}(\Omega, \mathbb{R}^n)$ for $\eta > 0$ such that

$$|\nabla u|^p - |\nabla \hat{u}|^p \geq A.\nabla(u-\hat{u}). \tag{5.73}$$

hence

$$-\Delta w \leq \frac{a(x)}{u^\gamma} - \frac{a(x)}{\hat{u}^\gamma} + A.\nabla(u-\hat{u}). \tag{5.74}$$

Then by Kato's inequality, we obtain

$$-\Delta w^+ \leq \chi_{[u-\hat{u}>0]} \left[\frac{a(x)}{u^\gamma} - \frac{a(x)}{\hat{u}^\gamma} + A.\nabla(u-\hat{u}) \right]. \tag{5.75}$$

which implies that

$$-\Delta w^+ \leq A.\nabla w^+. \tag{5.76}$$

Therefore, thanks to Lemma 3, we get $w = 0$, which completes the proof.

5.5 Appendix : Compactness in $W^{1,q}_{loc}(\Omega)$

Lemma 4

Let $u_n \in W^{1,q}_{loc}(\Omega)$, $1 \leq q < \dfrac{N}{N-1}$ such that

$$||u_n||_{W^{1,q}_{loc}} \leq C \quad \textit{and} \quad ||\Delta u_n||_{L^1_{loc}(\Omega)} \leq C. \tag{5.77}$$

Then we can extract a subsequence of (u_n) still denoted u_n such that

$$\begin{aligned} u_n &\rightarrow u \textit{ in } W^{1,q}_{loc}(\Omega), \\ u_n &\rightarrow u \textit{ almost everywhere in } \Omega. \end{aligned}$$

Proof.

See Lemma A.2 of [18] for a detailed proof.

Chapter 6

Mathematical Analysis of a quasilinear elliptic equation with singular non-linearity

6.1 Introduction

In this chapter, we focus our interest on the existence of a weak solution for a class of quasilinear elliptic problems in the form

$$(Q)\begin{cases} -\Delta u + |\nabla u|^2 = u^{-\gamma} & in\ \ \Omega, \\ u = 0 & on\ \partial\Omega, \end{cases}$$

where Ω is an open bounded subset of $\mathbb{R}^N$ for $N \geq 1$, with smooth boundary $\partial\Omega$, and $\gamma > 0$.

The problem without gradient term is well known in the literature as "the singular Lane-Emden-Fowler equation". To detail the discussion on this problem, we take for instance the following elliptic problem

$$\begin{cases} -\Delta u = f(x)s^{-\gamma} & \text{in } \Omega, \\ u = 0 & \text{on } \partial\Omega. \end{cases} \tag{6.1}$$

Lazer and Mckenna in [101] considered the problem (6.1), with f a continuous function and $\gamma > 0$. For $\gamma < 3$, the authors showed the existence of a solution in $H_0^1(\Omega)$ and they proved that the solution does not belong to $C^1(\overline{\Omega})$ if $\gamma > 1$.

In [98], Lair and Shaker generalized the result of Lazer and Mckenna [101] to the case where f is a non-negative function belonging in $L^2(\Omega)$ and γ is a nonnegative constant. In this case, the authors obtained the existence and uniqueness of a weak solution in $H_0^1(\Omega)$ when $0 < \gamma < 1$.

Boccardo and Orsina [37] dealt with the problem (6.1) where f is a nonnegative integrable function and γ is a positive constant. They established the existence of a weak solution to (6.1) and they discussed the regularity of the obtained solution by using the summability of f and the values of γ.

In our case, the situation is completely different, since the main goal of this work is to analyze the interaction between the gradient term and the singular nonlinearity to obtain existence results. To the best of our knowledge, there are only few partial results in this direction.

In order to detail this discussion, we mention here the work of Porretta [147] in which the author considered the following type of nonlinear elliptic equation

$$\begin{cases} -\Delta u + g(x,u,\nabla u) = f(x,u) & \text{in } \Omega, \\ u = 0 & \text{on } \partial\Omega, \end{cases} \tag{6.2}$$

where $g(x,s,\zeta)$ is a Carathéodory function, has a quadratic growth with respect to ζ and satisfies a sign condition on s, that is

$$g(x,s,\zeta)\, s \geq 0, \tag{6.3}$$

for every s in $\mathbb{R}$.

For $f \in L^1(\Omega) + H^{-1}(\Omega)$, the authors proved the existence of a weak solution u of (6.5) which belongs to the Sobolev space $W_0^{1,q}(\Omega)$ for every $q < \dfrac{N}{N-1}$, by adapting a technique that relies on Fatou lemma combined with the sign assumption on g.

If $f \in L^1(\Omega)$, Boccardo and Gallouët [34] proved the existence of a solution for (6.4) in $W_0^{1,p}(\Omega)$.

If $f \in W^{-1,p'}(\Omega)$, the reader is referred to ([22], [35], [30]) and references therein, for existence results.

On the other hand, let us consider the more general problem

$$\begin{cases} -\Delta_p u + |\nabla u|^{\mu} = f(x,u) & in\ \Omega, \\ u > 0 & in\ \Omega, \\ u = 0 & on\ \partial\Omega, \end{cases} \tag{6.4}$$

where $\Delta_p u$ is the p-Laplacian or the p-Laplace operator written as $\Delta_p v := \left(|v_x|^{p-2} v_x\right)_x$, $p > 1$, $0 < \mu \leq p$ and f is a nonnegative function.

Miri [116] showed by using the method of sub- and supersolutions, that if f is Hölder continuous and verifies other specific assumptions, then (6.4) has at least one entropy solution $u \in W_0^{1,p}(\Omega)$.

We conclude this section by recalling the work of Blanchard and Poretta[25] in which they deal with the

parabolic version of this problem:

$$\begin{cases} \dfrac{\partial u}{\partial t} - \Delta u + g(u)|\nabla u|^2 = f & \text{in } \Omega \times (0,T), \\ u = 0 & \text{on } \partial\Omega \times (0,T), \end{cases} \tag{6.5}$$

where $f \in L^1(\Omega)$ and g satisfies the sign condition (6.3). In this paper, the authors extend the notion of renormalized solutions for this problem. Under a natural condition on the convergence of the initial data, they prove the compactness of the truncation of solutions in the energy space. Then they show that the integrability of g at infinity is a necessary and sufficient condition for the stability of the problem with respect to general measure data, as well as for the existence of renormalized solutions.

Our focus in this work is to study the existence of a nonnegative weak solution to (Q) with general assumptions. We start by the approximated problem for which we establish the existence of a weak solution. Last but not least, we show some estimates and we finally pass to the limit in the approximated problem.

6.2 Preliminary Results and Definitions

For the readers convenience, we start by giving the notions and the main tools used throughout this chapter. We first precise in which sense we understand the solution of problem (Q):

Definition 5

We say that u is a solution of (Q) *if:*

$$\begin{cases} u \in H^1_{loc}(\Omega) \cap L^\infty_{loc}(\Omega), \\ \forall \omega \subset\subset \Omega,\ \exists c_\omega > 0 \text{ such that } u(x) \geq c_\omega > 0, \\ \forall \phi \in C^\infty_c(\Omega),\ \int_\Omega \nabla u \nabla \phi + |\nabla u|^2 \phi = \int_\Omega u^{-\gamma} \phi. \end{cases} \tag{6.6}$$

On the other hand, since the main tool used in this study is based on the approximation method, we consider an approximating scheme to approach problem (Q) in two steps.

6.2.1 An equivalent problem

Step 1: Let: $v = 1 - e^{-u}$, or equivalently $u = -\,ln(1-v)$. Problem (Q) then rewrites

$$(Q') \begin{cases} -\Delta v + \beta(v) = 0 \ \ in\ \Omega, \\ v = 0 \quad \text{on } \partial\Omega, \end{cases}$$

in which $\beta(v) = -(1-v)[-\log(1-v)]^{-\gamma}$.

The function $\beta :]0,1] \to]-\infty, 0]$ is strictly increasing with $\beta(0^+) = -\infty$ and $\beta(1) = 0$. We then extend the definition of β by letting $\beta(r) = 0$ for all $r > 1$.

The operator defined this way is maximal monotone in $\mathbb{R}$ with $D(\beta) =]0, +\infty[$ and β is continuous on $]0, +\infty[$.

Step 2: Let β_λ be the Yosida approximation of β defined by

$$\beta_\lambda = \left[I - (I + \lambda\beta)^{-1}\right]/\lambda. \tag{6.7}$$

The problem (Q') can be approximated by the following problem

$$(Q_\lambda) \begin{cases} -\Delta v_\lambda + \beta_\lambda(v_\lambda) = 0 \quad in\ \ \Omega, \\ v_\lambda = 0 \quad on\ \partial\Omega. \end{cases}$$

Remark 6.2.1

Since $\beta \leq 0$, then $\beta_\lambda \leq 0$. Furthermore, for all $r > 1$, $\beta_\lambda r = 0$, as by the classical inequality, we have

$$|\beta_\lambda r| \leq |\beta(r)|, \qquad \forall r \in]0, +\infty[, \tag{6.8}$$

The starting point is to ensure the existence of a solution v_λ for (Q_λ) and extract its properties. To this aim, we have the following Lemma:

Lemma 5

- *There exists $C_0 = C_0(\Omega)$, for all λ small, $v_\lambda \geq C_0 \phi_1 \left(\int_\Omega \phi_1 (-\beta_\lambda v_\lambda)\right)$,*
  where ϕ_1 is the first eigenfunction of $-\triangle$ with Dirichlet condition.
- *There exists $C_1 = C_1(\Omega)$, for all λ small, $\int_\Omega \phi_1 (-\beta_\lambda v_\lambda) \geq C_1$,.*

Proof.

The existence of a regular solution to (Q_λ) is obtained by applying the classical theory of [31] since

$r \to \beta_\lambda(r)$ is maximal monotone and $D(\beta_\lambda) = \mathbb{R}$.

Furthermore, on the first hand, by Kato's inequality, we have

$$-\Delta(v_\lambda - 1)^+ \leq \text{sign}^+(v_\lambda - 1)(-\Delta v_\lambda) = \text{sign}^+(v_\lambda - 1)[-\beta_\lambda(v_\lambda)] = 0. \tag{6.9}$$

Hence, since $(v_\lambda - 1)^+ = 0$ on $\partial\Omega$, then $v_\lambda \leq 1$ in Ω.

On the other hand, since $-\Delta v_\lambda = -\beta_\lambda v_\lambda \geq 0$, then $v_\lambda > 0$. Lemma 1 of [53] ensures that there exists a constant C_0 only depending on Ω such that

$$v_\lambda \geq C_0\, \phi_1 \left(\int_\Omega \phi_1 (-\beta_\lambda v_\lambda) \right), \tag{6.10}$$

where ϕ_1 denotes the first normalized $\left(\int_\Omega \phi_1 = 1 \right)$ eigenfunction of $-\Delta$ with Dirichlet condition.

Now, suppose that $\int_\Omega v_\lambda$ converges to 0 as λ goes to 0 up to a subsequence still denoted v_λ. Hence v_λ converges to 0 a.e. in Ω.

By Egorov's theorem [54], there exists a measurable subset K of Ω such that its measure $\mu(K) < \varepsilon$ and v_λ converges uniformly to 0.

This implies that there exists $\eta \in]0,1[$ such that $v_\lambda(x) \leq \eta$, for all x in K for λ sufficiently small. By the monotony of β_λ, we have $\beta_\lambda v_\lambda \leq \beta_\lambda \eta$ sur K, and then we obtain

$$\int_\Omega \phi_1 (-\beta_\lambda v_\lambda) \geq (-\beta_\lambda \eta) \int_K \phi_1. \tag{6.11}$$

But since $\lambda \to 0, \beta_\lambda \eta$ converges to $\beta(\eta) \in (-\infty, 0)$.

Finally we have

$$\int_\Omega \phi_1 (-\beta_\lambda v_\lambda) \geq C_1 > 0, \tag{6.12}$$

where C_1 is independant of λ.

This concludes the proof of the two statements of the lemma.

6.3 Main Results

In this section, we present two theorems which sum up the main results of this chapter. We start by the first existence result concerning the approximate problem (Q').

Theorem 6.3.1

Let $p \geq 1$. Problem (Q') admits a solution $v \in W^{2,p}_{loc}(\Omega)$ such that $0 < v \leq 1$. Moreover, $v^{(\gamma+1)/2} \in H^1_0(\Omega)$.

Proof.

Using Lemma 5, we have

$$v_\lambda \geq C_0\, C_1 \phi_1. \tag{6.13}$$

On the other hand, from (6.13)*, we deduce that for all $a \in]0,1]$, there exists a constant $C_a > 0$ independent of λ such that*

$$v_\lambda \geq C_a \text{ on } \Omega_a := \{x \in \Omega; d(x, \partial\Omega > a)\}, \tag{6.14}$$

where the constant C_a can be taken as $C_a := C_0 C_1 \min\{\phi_1(x); x \in \Omega_a\}$.

Hence

$$|\beta_\lambda v_\lambda| \leq |\beta_\lambda C_a| \leq |\beta(C_a)| < +\infty. \tag{6.15}$$

Consequently Δv_λ is uniformly bounded on Ω_a for all $a \in]0,1]$.

Since $0 \leq v_\lambda \leq 1$, then v_λ and ∇v_λ converge uniformly on Ω_a up to a subsequence. We denote the limit by $v \in W^{1,\infty}_{loc}(\Omega) \cap W^{2,p}_{loc}(\Omega), \forall p < +\infty$.

Furthermore, since $\beta_\lambda v_\lambda = \beta\left((I+\lambda\beta)^{-1} v_\lambda\right)$, then $\beta_\lambda v_\lambda$ also converges to $\beta(v)$ uniformly on Ω_a.

At this stage, we need to understand what happens on the boundary of Ω.

To this aim, we introduce the following function

$$j(r) = \int_0^r \frac{\beta'(s)^{1/2}}{-\beta(s)} ds = \int_0^r \frac{[-\log(1-s)]^\gamma}{1-s} \left\{ \frac{1}{[-\log(1-s)]^\gamma} + \frac{\gamma}{[-\log(1-s)]^{\gamma+1}} \right\}^{1/2} \forall r \in [0,1], \tag{6.16}$$

The function j is a strictly increasing continuous function on $[0,1[$.

Indeed, we note that in the neighbourhood of $r = 0$, we have $j'(r) \sim r^{(\gamma-1)/2}$, and in the neighbourhood of $r = 1$, we have $j'(r) \sim [-\log(1-r)]^{\gamma/2}/(1-r)$.

Now, we multiply (Q_λ) by $\beta(v_\lambda)^{-1}$, and we obtain

$$-\frac{\Delta v_\lambda}{\beta(v_\lambda)} + \frac{\beta_\lambda(v_\lambda)}{\beta(v_\lambda)} = 0. \tag{6.17}$$

But since β_λ is the Yosida approximation of β, we have

$$|\beta_\lambda(r)| \leq |\beta(r)|, \quad \forall r \in D(\beta) =]0, \infty[.$$

Hence

$$\left\| \frac{\beta_\lambda(v_\lambda)}{\beta(v_\lambda)} \right\|_{L^\infty(\Omega))} \leq 1, \text{ and then } \int_\Omega \frac{\beta_\lambda v_\lambda}{\beta(v_\lambda)} \leq |\Omega|. \tag{6.18}$$

Now integrating (6.17) *and knowing* $\beta(0^+)^{-1} = 0$, *we have*

$$|\Omega| \geq \int_\Omega \frac{\beta_\lambda v_\lambda}{\beta(v_\lambda)} = -\int_\Omega \nabla \frac{1}{\beta(v_\lambda)} \nabla v_\lambda = \int_\Omega \frac{\beta'(v_\lambda)}{\beta(v_\lambda)^2} |\nabla v_\lambda|^2 = \int_\Omega |\nabla j(v_\lambda)|^2. \tag{6.19}$$

We then deduce that $j(v_\lambda)$ *is bounded in* $H_0^1(\Omega)$ *and then relatively compact in* $L^2(\Omega)$. *So that, since* j *is continuous,* $j(v_\lambda)$ *converges to* $j(v)$ *up to a subsequence.*

By the weak convergence of $j(v_\lambda)$, *in* $H_0^1(\Omega)$, *we deduce that* $j(v) \in H_0^1(\Omega)$.

Now since $j'(r) \sim r^{(\gamma-1)/2}$ *as* $r \to 0$, *we deduce that*

$$2\nabla v^{(\gamma+1)/2} = (\gamma+1) v^{(\gamma-1)/2} \nabla v \in L^2(\Omega), \tag{6.20}$$

i.e.

$$v^{(\gamma+1)/2} \in H_0^1(\Omega), \tag{6.21}$$

which concludes the proof of the theorem.

The second theorem states the existence concerning the singular problem (Q).

Theorem 6.3.2

Let $p \geq 1$. *The problem* (Q) *admits a solution* $u \in W^{2,p}_{loc}(\Omega)$. *Moreover,* $u^{\gamma+1} \in W_0^{1,q}(\Omega)$, *for all* $1 \leq q \leq \frac{N}{N-1}$ *and* $e^{-\frac{\gamma+1}{2}u} \in H_0^1(\Omega)$.

Proof.

The equation (Q') *can be rewritten as follows:*

$$-\frac{\Delta v}{\beta(v)} + 1 = 0. \tag{6.22}$$

We note that

$$\begin{aligned} \beta(r)^{-1} &= -\frac{[-\log(1-v)]^\gamma}{1-r}, \quad \forall r \in]0,1[&& (6.23)\\ &= -(\gamma+1)^{-1} \frac{d}{dr}[-\log(1-v)]^{\gamma+1} && (6.24)\\ &= -\frac{d}{dr}\, g(r), && (6.25) \end{aligned}$$

in which

$$g(v) = \frac{[-\log(1-v)]^{\gamma+1}}{\gamma+1} := \frac{u^{\gamma+1}}{\gamma+1}. \tag{6.26}$$

Furthermore, we have

$$div\left(\frac{\nabla v}{\beta(v)}\right) = \frac{\Delta v}{\beta(v)} + \frac{\beta'(v)|\nabla v|^2}{\beta(v)^2}, \tag{6.27}$$

hence (6.22) *becomes*

$$-div\left(\frac{\nabla v}{\beta(v)}\right) - \frac{\beta'(v)|\nabla v|^2}{\beta(v)^2} + 1 = 0. \tag{6.28}$$

Now since

$$\beta(v)^{-1} = -\frac{\nabla g(v)}{\nabla v}, \tag{6.29}$$

equivalently

$$-\nabla g(v) = \frac{\nabla v}{\beta(v)}. \tag{6.30}$$

This implies

$$div(\nabla g(v)) = -div\left(\frac{\nabla v}{\beta(v)}\right), \tag{6.31}$$

so that

$$\Delta g(v) = -div\left(\frac{\nabla v}{\beta(v)}\right). \tag{6.32}$$

Finally, we have

$$\Delta g(v) - |\nabla j(v)|^2 + 1 = 0. \tag{6.33}$$

Since $j(v) \in H_0^1(\Omega)$, *then* $\Delta g(v) \in L^1(\Omega)$ *and hence* $\nabla g(v) \in L^p(\Omega)$. *This means that* $g(v) \in W_0^{1,p}(\Omega)$ *for all* $p \in [1, \frac{N}{N-1}[$, *and* $g(v) \in L^q(\Omega)$ *for all* $q \in [1, \frac{N}{(N-2)^+}[$ *and* $q = +\infty$ *if* $N = 1$.

We then deduce that for $N = 1$, $g(v) \in L^\infty(\Omega)$, *i.e.* $u \in L^\infty(\Omega)$ *and hence* $v < 1$ *in* $\bar{\Omega}$.

We then conclude that u has the same regularity as v in Ω, *i.e.* $u \in W_{loc}^{2,p}(\Omega)$ *for all* $p < \infty$.

The case when $N = 2$ *is more difficult to tackle.*

Let V the compact subset given as the complementary of the subset $[v = 1]$.

The function u is infinite in $[v = 1]$, *hence* $u^{-\gamma}$ *tends to* 0 *in the neighbourhood of* $[v = 1]$.

This implies that there exists $\eta > 0$ *such that* $-\Delta u \leq \eta$ *in the neighbourhood of* $[v = 1]$.

We conclude that u is bounded which is absurd and then $[v = 1] = \emptyset$.

Again, u has the same regularity as v in Ω, *i.e.* $u \in W_{loc}^{2,p}(\Omega)$, *for all* $p < \infty$.

This concludes the proof of the theorem.

Chapter 7

On the Existence of Global Weak Solutions to a Generalized Keller Segel Model with Growth and Nonlinear Signal Production

This chapter "On the existence of global weak solutions to a generalized Keller Segel model with arbitrary growth and nonlinear signal production" is published by Lefraich.H., Taourirte Laila, Khalfi.H. and Alaa.N. E. in Annals of the University of Craiova- Mathematics and Computer Science series, Volume 46(1), (2019), Pages 99-108, 1223-69345.

7.1 Introduction

We talk about chemotaxis phenomenon when the movement of organisms (cells, bacteria) is affected or even directed by the presence of a chemical substance. This movement is characterized by both repulsion and attraction phenomena, and in the latter case, the chemical is called a chemoattractant. For example, cells may be attracted to nutrients or repelled in the presence of a substance which is toxic to them. A more interesting example is that of the amoebae Dyctyostelium discoideum which, in cases of lack of nutrients, start to secrete adenosine monophosphate cyclic (cAMP) that attracts other amoebae. Chemotaxis is revealed to be a powerful means of communication between amoebae that induces a collective movement. It has been observed aggregation phenomena where amoebae, initially monocellular, ultimately form a society, i.e. a multicellular organism. It can then move to get food or form like a stem at the end of which

spores are created. These ones are then projected away in the hope of a more lenient environment, the cells forming the stem are sacrificing themselves for the survival of the society. To learn more about life social amoeba Dyctyostelium discoideum, we refer the reader to the article [76].

Keller and Segel [85] derived the first mathematical model describing the aggregation process of amoebae by chemotaxis and nowadays it is called Keller Segel model. Then several modifications of the original model have been done by various authors, with the aim of improving its consistency with the biological reality. The celebrated model has attracted applied mathematicians and has lead to many challenging problems; one can see [175, 191, 173, 185, 184, 207, 41]. The Keller Segel model, consists in two parabolic (some times one parabolic and one elliptic) partial differential equations for the cell density and chemo-attractant density.

$$\begin{cases} \frac{\partial u}{\partial t} - \Delta u - \chi div(u\nabla v) = f(u) & \text{in } Q_T =]0,T[\times\Omega \\ \tau\frac{\partial v}{\partial t} - \Delta v + v = g(u) & \text{in } Q_T \\ \frac{\partial u}{\partial \upsilon} = \frac{\partial v}{\partial \upsilon} = 0 & \text{in } \sum_T =]0,T[\times\partial\Omega \\ u(0,x) = u_0(x); v(0,x) = v_0(x) & \text{in } \Omega \end{cases} \tag{7.1}$$

with $\tau\varepsilon\{0,1\}$, where $\Omega\subset\mathbb{R}^n$ ($n\geq 2$) is a bounded domain with smooth boundary $\partial\Omega$ and $\frac{\partial}{\partial v}$ denote the derivative with respect to the outward normal vector v of $\partial\Omega$. $u(x,t)$ denotes the cell density and $v(x,t)$ denotes the concentration of the chemoattractant. $\chi(>0)$ is referred to as the chemotactic sensitivity coefficient measuring the strength of chemotaxis. The kinetic term f describes cell proliferation and death and $g(u)$ accounts for the chemical secretion by cells. A diffusion hypothesis is made for both the cells and the chemical product. The flow of cells due to the chemoattractant is assumed proportional to the gradient of the concentration of chemoattractant. The system presents two time scales, which justify the possibility of taking $\tau = 0$.

As already mentioned the mathematical modelling of cell movement goes back to Patlak (1953), E. Keller and L. Segel (70s). This simplified system was first introduced for the case f(u) = 0 and g(u) = u (minimal model) and thereafter was studied by other authors in various contexts. It has been well-known that when $f(u) = 0$ and $g(u) = u$, the minimal model possesses blow-up solutions in finite/infinite time in two or higher dimensions (see [79, 189, 188]). This limits the value of the model to explain the aggregation phenomena observed in experiment. The question for the system (7.1) is whether or not the appearance of growth source $f(u)$ can enforce the boundedness of solutions so that blow-up is inhibited.

Toward this end, many efforts have been made first for the linear chemical production and the logistic

source:

$$f(u) = ru - \mu u^2 \text{ and } g(u) = u \tag{7.2}$$

First, Osaki et al [129] showed that in the case n=2, the model (7.1) with $\tau = 1$ and (7.2) has a classical uniform in time bounded solution for any $r \in \mathbb{R}$, $\mu > 0$. Concerning higher dimensions ($n \geq 3$, Winkler [190] proved, under the logistic source:

$$f(u) = au - bu^2,\ f(0) \geq 0,\ a \geq 0,\ b > 0,\ u \geq 0, \tag{7.3}$$

there exists a large positive number b_0 such that if $b > b_0$, then the chemotaxis-growth system (7.1) with $\tau = 1$ and $g(u) = u$ has a classical uniform in time bounded solutions.

The existence of global weak solutions to (7.1) is newly known for $\mu > 0$ in convex domains (see [99]). Some progress for (7.1) ($\tau = 0$) has been made by Tello and Winkler (2007) wherein they showed that for $f(u) \leq a - bu^2$, $f(0) \geq 0$, $a \geq 0$, $b > 0$, $u \geq 0$ and $g(u) = u$ and $b > b_0 = (n-2)\chi/n$ the system admits globally bounded classical solutions.

This paper is devoted to the existence of weak solutions to the following chemotaxis system with nonlinear production of signal and growth source:

$$\begin{cases} \frac{\partial u}{\partial t} - \Delta u - \chi div(u\nabla v) = f(u) & \text{in } Q_T =]0,T[\times \Omega \\ -\Delta v + v = g(u) & \text{in } Q_T \\ \frac{\partial u}{\partial \upsilon} = \frac{\partial v}{\partial \upsilon} = 0 & \text{in } \sum_T =]0,T[\times \partial\Omega \\ u(0,x) = u_0(x) & \text{in } \Omega \end{cases} \tag{7.4}$$

7.2 Mathematical analysis of the problem:

7.2.1 Position problem:

We suggest to consider the chemotaxis-growth model (7.4) with $0 < \gamma < 1$, more general conditions on $f(u)$ and the following less regular nonnegative initial data:

- $f : \mathbb{R} \longrightarrow \mathbb{R}$, $f \in C^1(\mathbb{R})$ with $f(0) = 0$ and

$$f(u) \leqslant 0, \text{ for all } u \geqslant 0, \tag{7.5}$$

•

$$u_0 \in L^2(\Omega), \quad u_0 \geq 0 \tag{7.6}$$

Before stating the main result of this paper, we have to clarify in which sense we want to solve problem (7.4).

Definition 6

(u,v) is a weak solution of (7.4) if and only if

$$\begin{cases} u \in C([0,T],L^2(\Omega)) \cap L^2(0,T,H^1(\Omega)), v \in L^\infty\left(0,T,H^1(\Omega)\right), f(u) \in L^1(Q_T) \\ \bullet \text{ for every } \varphi \in C^1(Q_T) \text{ such that } \varphi(T,.) = 0 \\ \int_{Q_T}(-u\frac{\partial \varphi}{\partial t} + \nabla u \nabla \varphi + \chi u \nabla v \nabla \varphi) = \int_\Omega u_0(x)\varphi(0,x) + \int_{Q_T} f(u)\varphi \\ \bullet \text{ for all } \psi \in H^1(\Omega) \text{ and a.e } 0 < t < T \\ \int_\Omega \nabla v \nabla \psi + \int_\Omega v\psi = \int_\Omega u^\gamma \psi \end{cases} \tag{7.7}$$

7.2.2 Main result:

The main result of this paper is the following theorem.

Theorem 8

We suppose that the hypothesis (7.5) and (7.6) are satisfied, then the problem (7.4) admits a weak solution (u,v) satisfying $u \geq 0$ and $v \geq 0$, in Q_T.

7.2.3 Proof of the main result:

In order to develop the mathematical analysis of our model, we define an approximating scheme with a more regular initial condition in $C(\overline{\Omega})$, then we show the existence solutions for this approached problem. Finally by making some estimates we prove that the solution of the approximated problem converge to the solution of our problem.

Approximating scheme:

We associate to the function f the function f_m such that

$$f_m(r) = \frac{-r^2}{m} + \frac{f(r)}{1 + \frac{|f(r)|}{m}}$$

Now, let's consider the following approximated system

$$\begin{cases} \frac{\partial}{\partial t}u_m - \Delta u_m - \chi div(u_m \nabla v_m) = f_m(u_m) & \text{in } Q_T \\ -\Delta v_m + v_m = u_m^{\gamma} & \text{in } Q_T \\ \frac{\partial u_m}{\partial \upsilon} = \frac{\partial v_m}{\partial \upsilon} = 0 & \text{in } \sum_T \\ u_m(0,x) = u_m^0(x) & \text{in } \Omega \end{cases} \tag{7.8}$$

where $u_m^0 \in C(\overline{\Omega})$, furthermore $u_m^0 \to u_0$ strongly in $L^2(\Omega)$.

The existence of (u_m, v_m) solution to the chemotaxis-growth system (7.8) is ensured by the work of Wang and Xiang [186] (one can see Theorem 3.1 which is still valid for the model with $-\chi div(u_m \nabla v_m)$); because $0 < \gamma < 1$ and the growth function f_m is defined such that there are $a_m \geqslant 0$ and $b_m > 0$ such that

$$f_m(r) \leqslant a_m - b_m r^2, \text{ for all } r \geqslant 0.$$

As $f_m(0) = 0$, the maximum principle ensure that both u_m and v_m are nonnegative, as shown in [194]. By integrating the equation on u_m in (7.8) and using (7.5), we have

$$\frac{d}{dt}\int_\Omega u_m = \int_\Omega f_m(u_m) \leqslant 0,$$

which yields that the L^1-norm of u_m is uniformly bounded.

A priori estimates:

Till the end of this paper we design by C every generic and positive constant. This constant can change its value in different situations, can depend on γ, $|u_0|_{L^2}(\Omega)$, and $|\Omega|$ but remains independent of m. In this part we give estimates concerning u_m, v_m in appropriate spaces. We start by proving in the following lemma, that $\sup\limits_{0\leq t\leq T}(\|u_m(t)\|_{L^2(\Omega)} + \|v_m(t)\|_{L^2(\Omega)} + \|\nabla v_m(t)\|_{L^2(\Omega)})$ is bounded independently of m.

Lemma 6

There exist a constant $C = C(\|u_0\|_{L^2(\Omega)}, \gamma, |\Omega|)$ *such that*

(i) $\sup\limits_{0\leq t\leq T}\|u_m(t)\|_{L^2(\Omega)} \leq \int_\Omega (u_0)^2$,

(ii) $\int_0^T \int_\Omega |\nabla u_m|^2 \leq \frac{1}{2}\int_\Omega (u_0)^2$,

(iii) $\sup\limits_{0\leq t\leq T}\|v_m(t)\|_{L^2(\Omega)} \leq C$,

(iv) $\sup_{0\le t\le T} \|\nabla v_m(t)\|_{L^2(\Omega)} \le C.$

Proof.

(i) and (ii): Multiplying the u_m-equation in (7.8) by u_m and integrating over Ω by parts

$$\frac{1}{2}\frac{d}{dt}\int_0^t\int_\Omega u_m^2 + \int_0^t\int_\Omega |\nabla u_m|^2 + \chi\int_0^t\int_\Omega u_m\nabla(u_m)\nabla v_m = \int_0^t\int_\Omega f_m(u_m)u_m \le 0$$

we end up with

$$\frac{1}{2}\frac{d}{dt}\int_0^t\int_\Omega u_m^2 + \int_0^t\int_\Omega |\nabla u_m|^2 + \chi\int_0^t\int_\Omega u_m\nabla(u_m)\nabla v_m \le 0$$

which implies

$$\frac{1}{2}\frac{d}{dt}\int_0^t\int_\Omega u_m^2 + \int_0^t\int_\Omega |\nabla u_m|^2 \le \chi\int_0^t\int_\Omega u_m^2\Delta v_m$$

we have $0 = \Delta v_m - v_m + u_m^\gamma$, *so it follows*

$$\frac{1}{2}\frac{d}{dt}\int_0^t\int_\Omega u_m^2 + \int_0^t\int_\Omega |\nabla u_m|^2 \le \chi\Big(\int_0^t\int_\Omega u_m^2 v_m - \int_0^t\int_\Omega u_m^{2+\gamma}\Big)$$

upon a use of Young inequality, we get

$$u_m^2 v_m \le \frac{2}{2+\gamma}\left(u_m^2\right)^{\frac{2+\gamma}{2}} + \frac{\gamma}{2+\gamma}v_m^{\frac{2+\gamma}{\gamma}}$$

then,

$$\int_0^t\int_\Omega u_m^2 v_m \le \int_0^t\int_\Omega \frac{2}{2+\gamma}u_m^{2+\gamma} + \int_0^t\int_\Omega \frac{\gamma}{2+\gamma}v_m^{\frac{2+\gamma}{\gamma}}$$

then it follows that

$$\frac{1}{2}\frac{d}{dt}\int_0^t\int_\Omega u_m^2 + \int_0^t\int_\Omega |\nabla u_m|^2 \le \chi\Big(\int_0^t\int_\Omega \frac{2}{2+\gamma}u_m^{2+\gamma} + \int_0^t\int_\Omega \frac{\gamma}{2+\gamma}v_m^{\frac{2+\gamma}{\gamma}} - \int_0^t\int_\Omega u_m^{2+\gamma}\Big)$$

$$\begin{aligned}\tfrac{1}{2}\tfrac{d}{dt}\textstyle\int_0^t\int_\Omega u_m^2 + \int_0^t\int_\Omega |\nabla u_m|^2 &\le \chi\Big(\int_0^t\int_\Omega \tfrac{2}{2+\gamma}u_m^{2+\gamma} + \int_0^t\int_\Omega \tfrac{\gamma}{2+\gamma}v_m^{\frac{2+\gamma}{\gamma}} - \int_0^t\int_\Omega u_m^{2+\gamma}\Big)\\ &\le \chi\big(\tfrac{2}{2+\gamma}-1\big)\textstyle\int_0^t\int_\Omega u_m^{2+\gamma} + \chi\tfrac{\gamma}{2+\gamma}\int_0^t\int_\Omega v_m^{\frac{2+\gamma}{\gamma}}\end{aligned}$$

which immediately gives

$$\frac{1}{2}\frac{d}{dt}\int_0^t\int_\Omega u_m^2+\int_0^t\int_\Omega|\nabla u_m|^2\leq\frac{-\gamma\chi}{2+\gamma}\int_0^t\int_\Omega u_m^{2+\gamma}+\frac{\gamma\chi}{2+\gamma}\int_0^t\int_\Omega v_m^{\frac{2+\gamma}{\gamma}} \tag{7.9}$$

Multiplying the v_m-equation in (7.8) by $v_m^{\frac{2}{\gamma}}$ and integrating over Ω by parts

$$\int_0^t\int_\Omega v_m^{\frac{2}{\gamma}+1}+\frac{2}{\gamma}\int_0^t\int_\Omega v_m^{\frac{2}{\gamma}-1}|\nabla v_m|^2=\int_0^t\int_\Omega u_m^\gamma v_m^{\frac{2}{\gamma}}$$

using Young inequality yields

$$u_m^\gamma v_m^{\frac{2}{\gamma}}\leq\frac{2}{2+\gamma}v_m^{\frac{2+\gamma}{\gamma}}+\frac{\gamma}{2+\gamma}u_m^{\gamma+2}$$

then

$$\int_0^t\int_\Omega v_m^{\frac{\gamma+2}{\gamma}}+\frac{8\gamma}{(\gamma+2)^2}\int_0^t\int_\Omega\left|\nabla v_m^{\frac{\gamma+2}{2\gamma}}\right|^2\leq\frac{2}{2+\gamma}\int_0^t\int_\Omega v_m^{\frac{2+\gamma}{\gamma}}+\frac{\gamma}{2+\gamma}\int_0^t\int_\Omega u_m^{\gamma+2}$$

which implies

$$\frac{\gamma}{2+\gamma}\int_0^t\int_\Omega v_m^{\frac{\gamma+2}{\gamma}}+\frac{8\gamma}{(\gamma+2)^2}\int_0^t\int_\Omega\left|\nabla v_m^{\frac{\gamma+2}{2\gamma}}\right|^2\leq\frac{\gamma}{2+\gamma}\int_0^t\int_\Omega u_m^{\gamma+2} \tag{7.10}$$

combining (8.1) and (7.10) gives

$$\frac{1}{2}\frac{d}{dt}\int_0^t\int_\Omega u_m^2+\int_0^t\int_\Omega|\nabla u_m|^2\leq\frac{-\gamma\chi}{2+\gamma}\int_0^t\int_\Omega u_m^{2+\gamma}-\frac{8\gamma\chi}{(\gamma+2)^2}\int_0^t\int_\Omega\left|\nabla v_m^{\frac{\gamma+2}{2\gamma}}\right|^2+\frac{\gamma\chi}{2+\gamma}\int_0^t\int_\Omega u_m^{2+\gamma} \tag{7.11}$$

which implies

$$\frac{1}{2}\frac{d}{dt}\int_0^t\int_\Omega u_m^2+\int_0^t\int_\Omega|\nabla u_m|^2+\frac{8\gamma\chi}{(\gamma+2)^2}\int_0^t\int_\Omega\left|\nabla v_m^{\frac{\gamma+2}{2\gamma}}\right|^2\leq 0$$

Finally we conclude that

$$\begin{cases}\sup\limits_{0\leq t\leq T}\int_\Omega u_m^2(t)\leq\int_\Omega(u_0)^2\\ \int_0^T\int_\Omega|\nabla u_m|^2\leq\frac{1}{2}\int_\Omega(u_0)^2\end{cases}$$

(iii) and (iv):

Multiplying the v_m-equation in (7.8) by v_m and integrating over Ω by parts

$$-\int_\Omega \Delta v_m v_m + \int_\Omega v_m^2 = \int_\Omega u_m^\gamma v_m$$

which implies

$$\int_\Omega |\nabla v_m|^2 + \int_\Omega v_m^2 = \int_\Omega u_m^\gamma v_m$$

a simple use of Young's inequality, directly yields that

$$\int_\Omega u_m^\gamma v_m \leq \frac{\gamma}{2}\int_\Omega u_m^2 + \frac{2-\gamma}{2}\int_\Omega v_m^{\frac{2}{2-\gamma}}$$

we deduce

$$\int_\Omega |\nabla v_m|^2 + \int_\Omega v_m^2 \leq \frac{\gamma}{2}\int_\Omega u_m^2 + \frac{2-\gamma}{2}\int_\Omega v_m^{\frac{2}{2-\gamma}}.$$

using young inequality gives

$$\int_\Omega v_m^{\frac{2}{2-\gamma}} \leq \varepsilon \int_\Omega v_m^2 + \varepsilon^{\frac{1}{1-\gamma}} |\Omega|$$

which implies

$$\int_\Omega |\nabla v_m|^2 + \int_\Omega v_m^2 \leq \frac{\gamma}{2}\int_\Omega u_m^2 + \frac{\varepsilon(2-\gamma)}{2}\int_\Omega v_m^2 + \frac{\varepsilon^{(\frac{1}{1-\gamma})}(2-\gamma)}{2}|\Omega|$$

By choosing $\varepsilon < \frac{2}{2-\gamma}$*, we get*

$$\int_\Omega |\nabla v_m|^2 + \int_\Omega v_m^2 \leq C(\|u_0\|_{L^2(\Omega)}, \gamma, |\Omega|).$$

Finally

$$\begin{cases} \sup\limits_{0\leq t\leq T} \|v_m(t)\|_{L^2(\Omega)} \leq C \\ \sup\limits_{0\leq t\leq T} \|\nabla v_m(t)\|_{L^2(\Omega)} \leq C \end{cases}$$

Concerning the term $f_m(u_m)$, we have the following result.

Lemma 7

(i) There exist a constant $C = C(\|u_0\|_{L^1(\Omega)})$ independent on m, such that

$$\|f_m(u_m)\|_{L^1(Q_T)} \leq C$$

(ii) There exist a constant $C = C(\|u_0\|_{L^2(\Omega)}, \gamma, |\Omega|)$ independent on m, such that

$$\sup_{0\leq t\leq T} \|u_m(t) \bigtriangledown v_m(t)\|_{L^1(\Omega)} \leq C$$

Proof.

(i) Let's consider the equation satisfied by u_m, we have

$$\frac{\partial u_m}{\partial t} - \Delta u_m - \chi div(u_m \nabla v_m) = f_m(u_m)$$

Then we integrate on Q_T

$$\int_0^T \int_\Omega |f_m(u_m)| = -\int_{Q_T} \frac{\partial u_m}{\partial t} = \int_\Omega u_m^0(x) - \int_\Omega u_m(T,x) \leq \int_\Omega u_m^0(x)$$

because we know that

$$u_m(T,x) \geq 0$$

we conclude that

$$\|f_m(u_m)\|_{L^1(Q_T)} \leq C = C(\|u_0\|_{L^1(\Omega)})$$

(ii) Using young inequality yields

$$\int_\Omega |u_m \bigtriangledown v_m| \leq \frac{1}{2}\int_\Omega u_m^2 + \frac{1}{2}\int_\Omega |\nabla v_m|^2 \leq C(\|u_0\|_{L^2(\Omega)}, \gamma, |\Omega|)$$

The following lemma gives estimate on $u_m f_m(u_m)$ in $L^1(Q_T)$. That estimate will be very important to fulfill the proof of the main result.

Lemma 8

There exists a constant C such that:

- $\|u_m f_m(u_m)\|_{L^1(Q_T)} \leq C$

Proof.

Multiplying the u_m-equation in (7.8) by u_m and integrating over Ω by parts

$$\frac{1}{2}\frac{d}{dt}\int_0^t\int_\Omega u_m^2+\int_0^t\int_\Omega|\nabla u_m|^2+\chi\int_0^t\int_\Omega u_m\nabla(u_m)\nabla v_m=\int_0^t\int_\Omega f(u_m)u_m$$

we end up with

$$\frac{1}{2}\int_0^t\int_\Omega u_m^2-\frac{1}{2}\int_0^t\int_\Omega(u_m^0)^2+\int_0^t\int_\Omega|\nabla u_m|^2+\chi\int_0^t\int_\Omega u_m\nabla(u_m)\nabla v_m=\int_0^t\int_\Omega f(u_m)u_m$$

then

$$\int_0^t\int_\Omega|f(u_m)u_m|=\frac{1}{2}\int_0^t\int_\Omega(u_m^0)^2-\frac{1}{2}\int_0^t\int_\Omega u_m^2-\int_0^t\int_\Omega|\nabla u_m|^2-\chi\int_0^t\int_\Omega u_m\nabla(u_m)\nabla v_m$$

which implies

$$\int_0^t\int_\Omega|f(u_m)u_m|=\frac{1}{2}\int_0^t\int_\Omega(u_m^0)^2-\chi\int_0^t\int_\Omega u_m\nabla(u_m)\nabla v_m \tag{7.12}$$

Multiplying the v_m-equation in (7.8) by u_m^2 and integrating over Ω by parts

$$-\int_\Omega\Delta v_m u_m^2+\int_\Omega v_m u_m^2=\int_\Omega u_m^{\gamma+2}$$

which implies

$$2\int_0^t\int_\Omega u_m\nabla(u_m)\nabla v_m+\int_0^t\int_\Omega v_m u_m^2=\int_0^t\int_\Omega u_m^{\gamma+2}$$

then

$$-\int_0^t\int_\Omega u_m\nabla(u_m)\nabla v_m=\frac{1}{2}\int_0^t\int_\Omega v_m u_m^2-\frac{1}{2}\int_0^t\int_\Omega u_m^{\gamma+2}$$

a simple use of Young's inequality, directly yields that

$$\int_0^t\int_\Omega u_m^2 v_m\leq\frac{2}{\gamma+2}\int_0^t\int_\Omega u_m^{\gamma+2}+\frac{\gamma}{\gamma+2}\int_0^t\int_\Omega v_m^{\frac{\gamma+2}{\gamma}}$$

we deduce

$$-\int_0^t\int_\Omega u_m\nabla(u_m)\nabla v_m \leq -\frac{1}{2}\int_0^t\int_\Omega u_m^{\gamma+2}+\frac{1}{\gamma+2}\int_0^t\int_\Omega u_m^{\gamma+2}+\frac{\gamma}{2(\gamma+2)}\int_0^t\int_\Omega v_m^{\frac{\gamma+2}{\gamma}}$$

then

$$-\int_0^t\int_\Omega u_m\nabla(u_m)\nabla v_m \leq \frac{-\gamma}{2(\gamma+2)}\int_0^t\int_\Omega u_m^{\gamma+2}+\frac{\gamma}{2(\gamma+2)}\int_0^t\int_\Omega v_m^{\frac{\gamma+2}{\gamma}} \tag{7.13}$$

Using (2.5) in (2.8) gives

$$-\int_0^t\int_\Omega u_m\nabla(u_m)\nabla v_m \leq \frac{-4\gamma}{(\gamma+2)^2}\int_0^t\int_\Omega \left|\nabla v_m^{\frac{\gamma+2}{2\gamma}}\right|^2$$

Finally

$$\int_0^t\int_\Omega |f(u_m)u_m| \leq \frac{1}{2}\int_0^t\int_\Omega (u_0)^2$$

Convergence:

The point is to show that (u_m, v_m) solution of the problem (7.8) converge to (u,v) solution of (7.4). Considering the v_m-equation, we already know that $\sup\limits_{0\leq t\leq T}\int_\Omega u_m^\gamma \leq C$ (this can be obtained by testing the v_m-equation by 1) , then by using the compactness theorem [31] we can deduce, up to extracting subsequence if necessary, the following convergences for all $t\in(0,T)$

$$\begin{cases} v_m(t)\to v(t) & \text{in } L^1(\Omega) \text{ and a.e. in } Q_T. \\ \nabla v_m(t)\to \nabla v(t) & \text{in } L^1(\Omega) \text{ and a.e. in } \Omega. \end{cases}$$

Furthermore, we have $\Delta u_m \in L^1(0,T,(H^1(\Omega))')$, $\nabla(u_m\nabla v_m)\in L^1(0,T,(H^1(\Omega))')$ and $f_m(u_m)$ bounded in $L^1(Q_T)$, which yields from Aubin-Simon compactness [165] $\partial_t u_m$ is bounded in $L^1(0,T,(H^1(\Omega))')+L^1(Q_T)$.

Consequently,up to a subsequence also denoted by u_m

$$u_m\to u \text{ in } L^2(Q_T) \text{ strongly, and a.e.}$$

Then,

$$\partial_t u_m-\Delta u_m\to \partial_t u-\Delta u \quad \text{in } D'(Q_T).$$

As ∇v_m is bounded in $L^2(Q_T)$, which is a reflexive space, then $(\nabla v_m)_m$ converges weakly in $L^2(Q_T)$. then,

$$\nabla v_m \to \nabla v \text{ weakly in } L^2(Q_T)$$

Consequently,

$$u_m \nabla v_m \to u \nabla v \text{ weakly in } L^2(Q_T)$$

Then

$$\nabla(u_m \nabla v_m) \to \nabla(u \nabla v) \text{ in } D'(Q_T)$$

Consequently we have $u_m - \Delta u_m - \nabla(u_m \nabla v_m) \to u - \Delta u - \nabla(u \nabla v)$ in $D'(Q_T)$

Thanks to Vitali theorem, to prove that $f_m(u_m)$ converge to $f(u)$ in $L^1(Q_T)$ is equivalent to prove that $f_m(u_m)$ is equi-integrable in $L^1(Q_T)$. We have the following lemma:

Lemma 9

$f_m(u_m)$ is equi-integrable in $L^1(Q_T)$.

Proof.

Let be E a measurable set of Q_T. We have

$$\int_E |f_m(u_m)| \leq \int_{E \cap [u_m \leq k]} |f_m(u_m)| + \frac{1}{k} \int_{E \cap [u_m > k]} u_m |f_m(u_m)|$$

However

$$\int_{E \cap [u_m \leq k]} |f_m(u_m)| \leq \max_{0 \leq |r| \leq k} |f(r)| . |E|$$

$$\ldots \leq C(k) |E|$$

according to Lemma 8

$$\frac{1}{k} \int_{E \cap [u_m > k]} u_m |f_m^n(u_m)| \leq \frac{C(T)}{k}$$

by choosing k sufficiently large, we deduce

$$\int_{E \cap [u_m \leq k]} |f_m(u_m)| \leq \frac{\varepsilon}{2} \text{ and } \frac{1}{k} \int_{E \cap [u_m > k]} u_m |f_m(u_m)| \leq \frac{\varepsilon}{2}$$

consequently, $f_m(u_m)$ is equi-integrable in $L^1(Q_T)$.

Furthermore we have

$$-\Delta v_m + v_m = u_m^\gamma \to -\Delta v + v = u^\gamma \quad \text{in } D'(Q_T).$$

Bibliography

[1] Abdellaoui, B., Attar, A., Miri, S. E. **(2014)**. Nonlinear singular elliptic problem with gradient term and general datum. Journal of Mathematical Analysis and Applications, 409(1), 362-377.

[2] Abramowitz, M., Stegun, I. A. **(1970)**. Handbook of mathematical functions, p. 927ff.

[3] Alaa, N.E. **(1996)**. Contributiona l'étude d'équations elliptiques et paraboliques avec données mesures. These de doctorat d'etat, University "Cadi Ayyad", Faculty of Sciences Semlalia.

[4] Alaa, N. E. **(1989)**. Étude d'équations elliptiques non linéaires à dépendance convexe en le gradient et à données mesures (Doctoral dissertation, Nancy 1).

[5] Alaa, N. E., Iguernane, M. **(2002)**. Weak periodic solutions of some quasilinear parabolic equations with data measures. Journal of Inequalities in Pure and Applied Mathematics, 3(3).

[6] Alaa, N. E., Pierre, M. **(1993)**. Weak solutions of some quasilinear elliptic equations with data measures. SIAM journal on mathematical analysis, 24(1), 23-35.

[7] Amann, H., Crandall, M. G. **(1978)**. On some existence theorems for semi-linear elliptic equations. Indiana University Mathematics Journal, 27(5), 779-790.

[8] Amann, H., Quittner, P. **(1998)**. Elliptic boundary value problems involving measures: existence, regularity, and multiplicity. Advances in Differential Equations, 3(6), 753-813.

[9] Andreianov, B., Bendahmane, M., Karlsen, K. H., Ouaro, S. **(2009)**. Well-posedness results for triply nonlinear degenerate parabolic equations. Journal of Differential Equations, 247(1), 277-302.

[10] Atkinson, L. V., Harley, P. J., Hudson, D. **(1990)**. Numerical methods with Fortran 77: A practical introduction. Addison-Wesley Longman Publishing Co., Inc..

[11] Azzouzi.A, **(2008)**. PhD Thesis, Université de Picardie Jules Verne, Amiens, France.

[12] Bales, G. S., Zangwill, A. **(1990)**. Morphological instability of a terrace edge during step-flow growth. Physical Review B, 41(9), 5500.

[13] Ball, J. M. **(1985)**. VJ Mizel One dimensional minimum problems whose minimizers do not satisfy the Euler Lagrange equation Arch. Rat. Mech. Anal, 90, 325-388.

[14] Ball, J. M., DeVore, R. A. **(2001)**. Foundations of Computational Mathematics. London Mathematical Society Lecture Note Series, DeVore, R., Iserles, A., Süli, E.(Eds.), Cambridge University Press, Cambridge, 284, 1-20.

[15] Ball, J. M., Knowles, G. **(1987)**. A numerical method for detecting singular minimizers. Numerische Mathematik, 51(2), 181-197.

[16] Ball, J. M., Mizel, V. J. **(1984)**. Singular minimizers for regular one-dimensional problems in the calculus of variations. Bulletin of the American Mathematical Society, 11(1), 143-146.

[17] Ball, J. M., Nadirashvili, N. S. **(1993)**. Universal singular sets for one-dimensional variational problems. Calculus of Variations and Partial Differential Equations, 1(4), 429-438.

[18] Baras, P., Pierre, M. **(1984)**. Singularités éliminables pour des équations semi-linéaires. In Annales de l'institut Fourier (Vol. 34, No. 1, pp. 185-206).

[19] Barenblatt, G. I. **(2001)**. Self-similar intermediate asymptotics for nonlinear degenerate parabolic free-boundary problems that occur in image processing. Proceedings of the National Academy of Sciences, 98(23), 12878-12881.

[20] Barenblatt, G. I., Isaakovich, B. G. **(1996)**. Scaling, self-similarity, and intermediate asymptotics: dimensional analysis and intermediate asymptotics (Vol. 14). Cambridge University Press.

[21] Bena, I., Misbah, C., Valance, A. **(1993)**. Nonlinear evolution of a terrace edge during step-flow growth. Physical Review B, 47(12), 7408.

[22] Bensoussan, A. and Boccardo, L., Murat, F. **(1988, July)**. On a non linear partial differential equation having natural growth terms and unbounded solution. In Annales de l'Institut Henri Poincare (C) Non Linear Analysis . Elsevier Masson Vol. 5, No. 4, pp. 347-364.

[23] Bhuiyan, A. K., Dew, S. K., Stepanova, M. **(2011)**. Controlled self-assembly of nanocrystalline arrays studied by 3D kinetic Monte Carlo modeling. The Journal of Physical Chemistry C, 115(40), 19557-19568.

[24] Biagi, S., Misbah, C., Politi, P. **(2014)**. Universality classes for unstable crystal growth. Physical Review E, 89(6), 062114.

[25] Blanchard, D. and Porretta, A. **(2001)**. Nonlinear parabolic equations with natural growth terms and measure initial data. Annali della Scuola Normale Superiore di Pisa-Classe di Scienze, 30(3-4), 583-622.

[26] Bluman, G., Kumei, S. **(1980)**. Bluman, G.,Kumei, S. (1980). $(\partial u/\partial x) - (\partial u/\partial t) = 0$. J. Math. Phys, 21, 1019-1023.J. Math. Phys, 21, 1019-1023.

[27] Braides, A., Dal Maso, G., Garroni, A. **(1999)**. Variational formulation of softening phenomena in fracture mechanics: The one-dimensional case. Archive for Rational Mechanics and Analysis, 146(1), 23-58.

[28] Bray, A. J. **(2002)**. Theory of phase-ordering kinetics. Advances in Physics, 51(2), 481-587.

[29] Brézis, H. and Browder, F. E. **(1982)**. Some properties of higher-order Sobolev spaces. Journal de Mathematiques Pures et Appliquees, 61(3), 245-259.

[30] Brézis, H. and Stampacchia.G., **(1968)**. Sur la régularité de la solution deséquations elliptiques, Bull. Soc. Math. France 96, 153-180.

[31] Brézis, H. and Strauss, W. A. **(1973)**. Semi-linear second-order elliptic equations in L1. Journal of the Mathematical Society of Japan, 25(4), 565-590.

[32] Brodie, B. C. **(1859)**. XIII. On the atomic weight of graphite. Philosophical Transactions of the Royal Society of London, (149), 249-259.

[33] Boccardo, L., Escobedo, M., Porzio, M. M. **(2015)**. Parabolic equations with singular and supercritical reaction terms. Differential and Integral Equations, 28(11/12), 1155-1172.

[34] Boccardo, L. and Gallouët, T. **(1992)**. Strongly nonlinear elliptic equations having natural growth terms and L1 data. Nonlinear Analysis: Theory, Methods and Applications, 19(6), 573-579.

[35] Boccardo, L., Murat, F., Puel, J. P. **(1982)**. Existence de solutions non bornées pour certaines équations quasi-linéaires. Portugaliae Mathematica, 41(1-4), 507-534.

[36] Boccardo, L., Murat, F.,Puel, J. P. **(1989)**. Existence results for some quasilinear parabolic equations. Nonlinear Analysis: Theory, Methods and Applications, 13(4), 373-392.

[37] Boccardo, L., Orsina, L. **(2010)**. Semilinear elliptic equations with singular nonlinearities. Calculus of Variations and Partial Differential Equations, 37(3-4), 363-380.

[38] Bognár, G., Guedda, M., Hriczó, K., Taourirte, L. **(2020)**. Instabilities in certain one-dimensional singular interfacial equation. Physica Scripta, 95(3), 035001.

[39] Caffarelli.L. A.,**(1998)**. The obstacle problem revisited, J. Fourier Anal. Appl. 4, 383-402.

[40] Canino, A., Sciunzi, B., Trombetta, A. **(2016)**. Existence and uniqueness for p-Laplace equations involving singular nonlinearities. Nonlinear Differential Equations and Applications NoDEA, 23(2), 8.

[41] Cao, X., Zheng, S. **(2014)**. Boundedness of solutions to a quasilinear parabolic–elliptic Keller–Segel system with logistic source. Mathematical Methods in the Applied Sciences, 37(15), 2326-2330.

[42] Castellano, C., Krug, J. **(2000)**. Nonmonotonic roughnes evolution in unstable growth. Physical Review B, 62(4), 2879.

[43] Castro Neto. A. H. , F. Guinea, N. M. R. Peres, K. S. Novoselov and A. K. Geim. **(2009)**. Rev. Mod. Phys. 81, 109.

[44] Céa, J. **(1986)**. Conception optimale ou identification de formes, calcul rapide de la dérivée directionnelle de la fonction coût. ESAIM: Mathematical Modelling and Numerical Analysis, 20(3), 371-402.

[45] Chopin, J., Vella, D., Boudaoud, A. **(2008)**. The liquid blister test. Proceedings of the Royal Society A: Mathematical, Physical and Engineering Sciences, 464(2099), 2887-2906.

[46] Cîrstea, F., Motreanu, D., Radulescu, V. **(2001)**. Weak solutions of quasilinear problems with nonlinear boundary condition. Nonlinear Analysis, 43(5), 623-636.

[47] Clarke, F. H., Vinter, R. B. **(1985)**. Regularity properties of solutions to the basic problem in the calculus of variations. Transactions of the American Mathematical Society, 289(1), 73-98.

[48] Clarke, F. H., Vinter, R. B. **(1986)**. Regularity of solutions to variational problems with polynomial Lagrangians. Bull. Polish Acad. Sci. Math, 34(1-2), 73-81.

[49] Crandall, M. G., Rabinowitz, P. H., Tartar, L. **(1977)**. On a Dirichlet problem with a singular nonlinearity. Communications in Partial Differential Equations, 2(2), 193-222.

[50] Cross, M. C., Hohenberg, P. C. **(1993)**. Pattern formation outside of equilibrium. Reviews of modern physics, 65(3), 851.

[51] Cullen, W. G., Yamamoto, M., Burson, K. M., Chen, J. H., Jang, C., Li, L., ... Williams, E. D. **(2010)**. High-fidelity conformation of graphene to SiO 2 topographic features. Physical review letters, 105(21), 215504.

[52] Davie A. M. , Arch. Rat. Mech. **(1988)**.Anal. 190(3), 371 .

[53] Diaz, J. I., Morel, J. M., Oswald, L. **(1987)**. An elliptic equation with singular nonlinearity. Communications in Partial Differential Equations, 12(12), 1333-1344.

[54] Egoroff.D.-Tb. (D. F. Egorov). **(1911)**. Sur les suites des fonctions mesurables, Comptes Rendus Acad. Sci. Paris, 152 244-246.

[55] Ehrlich, G., Hudda, F. G. **(1966)**. Atomic view of surface self-diffusion: tungsten on tungsten. The Journal of Chemical Physics, 44(3), 1039-1049.

[56] Elkinani, I., Villain, J. **(1994)**. Growth roughness and instabilities due to the Schwoebel effect: a one-dimensional model. Journal de Physique I, 4(6), 949-973.

[57] Evans, J. D., Galaktionov, V. A., Williams, J. F. **(2006)**. Blow-up and global asymptotics of the limit unstable Cahn–Hilliard equation. SIAM journal on mathematical analysis, 38(1), 64-102.

[58] Fasolino, A., Los, J. H. Katsnelson, M. I. **(2007)**. Intrinsic ripples in graphene. Nature materials, 6(11), 858-861.

[59] Ferriero, A. **(2012)**. A direct proof of the Tonelli's partial regularity result. Discrete Continuous Dynamical Systems-A, 32(6), 2089.

[60] Friedman, A. **(1969)**. Partial differential equations. Holt, Rinihart and Winston. Inc., New York, 1, 969.

[61] Frisch, T., Verga, A. **(2006)**. Effect of step stiffness and diffusion anisotropy on the meandering of a growing vicinal surface. Physical review letters, 96(16), 166104.

[62] Fujimura, H., Yagi, A. (**2008)**. Dynamical system for BCF model describing crystal surface growth, Vestnik Chelyabinsk Gos. Univ. 10, 75-88.

[63] Fujita, H. **(1952)**. The exact pattern of a concentration-dependent diffusion in a semi-infinite medium, part II. Textile Research Journal, 22(12), 823-827.

[64] Giachetti, D., Martinez-Aparicio, P. J., Murat, F. **(2018)**. Homogenization of a Dirichlet semilinear elliptic problem with a strong singularity at u= 0 in a domain with many small holes. Journal of Functional Analysis, 274(6), 1747-1789.

[65] Gent, A. N., Lindley, P. B. **(1959)**. Internal rupture of bonded rubber cylinders in tension. Proceedings of the Royal Society of London. Series A. Mathematical and Physical Sciences, 249(1257), 195-205.

[66] Golubović, L.,**(1997)**. Interfacial coarsening in epitaxial growth models without slope selection. Phys. Rev. Lett. 78, 90.

[67] Gratwick Richard **(2015)**. Singular sets and the Lavrentiev phenomenon. Proceedings of the Royal Society of Edinburgh: Section A Mathematics, 145(3), 513–533.

[68] Green, M. B. , J. H. Schwarz, and E. Written, **(1987)**. Superstring Theory Cambridge Universiyt Press, New York.

[69] Guedda, M., N. Alaa, and M. Benlahsen. **(2016)**. Analytical results for the wrinkling of graphene on nanoparticles. Physical Review E, 94.4, 042806.

[70] Guedda, M., Kersner, R. **(2003)**. Self-similar solutions to the generalized deterministic KPZ equation. Nonlinear Differential Equations and Applications NoDEA, 10(1), 1-13.

[71] Guedda, M., Trojette, H. **(2010)**. Coarsening in an interfacial equation without slope selection revisited: Analytical results. Physics Letters A, 374(42), 4308-4311.

[72] Guergu,M., Radulescu.V. D., **(2008)**.Singular Elliptic Problems : Bifurcation and Asymptotic Analysis. Oxford lecture series in mathematics and its applications, Vol. 37. Oxford university press, New York.

[73] Guo, Y., Guo, W. **(2013)**. Electronic and field emission properties of wrinkled graphene. The Journal of Physical Chemistry C, 117(1), 692-696.

[74] H. Amann, Ordinary Differential Equations.**(1990)** Walter de Gruyter, Berlin.

[75] Herrero, M. A., **(1989)**. Nonlin. Anal. The. Meth. Appl. 13 (6), 611.

[76] Herrero, M. A., Sastre, L. **(2006)**. Models of aggregation in Dictyostelium discoideum: on the track of spiral waves. Networks Heterogeneous Media, 1(2), 241.

[77] Hestenes, M. R. **(1942)**. The problem of Bolza in the calculus of variations. Bulletin of the American Mathematical Society, 48(2), 57-75.

[78] Ho, C. M., Tai, Y. C. **(1998)**. Micro-electro-mechanical-systems (MEMS) and fluid flows. Annual review of fluid mechanics, 30(1), 579-612.

[79] Horstmann, D. **(2003)**. From 1970 until present: the Keller-Segel model in chemotaxis and its consequences. 105, 103–165.

[80] Hunt, A. W., Orme, C., Williams, D. R. M., Orr, B. G., Sander, L. M. **(1994)**. Instabilities in MBE growth. EPL (Europhysics Letters), 27(8), 611.

[81] Ivanova.N.M., Dyn. PDE 5 (2), 139 **(2008)**.

[82] Ishigami, M., Chen, J. H., Cullen, W. G., Fuhrer, M. S., Williams, E. D. **(2007)**. Atomic structure of graphene on SiO2. Nano letters, 7(6), 1643-1648.

[83] Johnson, M. D., Orme, C., Hunt, A. W., Graff, D., Sudijono, J., Sander, L. M., Orr, B. G. **(1994)**. Stable and unstable growth in molecular beam epitaxy. Physical review letters, 72(1), 116.

[84] Kardar, M., Parisi, G., Zhang, Y. C. **(1986)**. Dynamic scaling of growing interfaces. Physical Review Letters, 56(9), 889.

[85] Keller, E. F., Segel, L. A. **(1970)**. Initiation of slime mold aggregation viewed as an instability. Journal of theoretical biology, 26(3), 399-415.

[86] Kersner, R., Vicsek, M. **(1997)**. Travelling waves and dynamic scaling in a singular interface equation: analytic results. Journal of Physics A: Mathematical and General, 30(7), 2457.

[87] Khalfi, H., Alaa, N. E., Guedda, M. **(2018)**. Period steady-state identification for a nonlinear front evolution equation using genetic algorithms. International Journal of Bio-Inspired Computation, 12(3), 196-202.

[88] Khang, D. Y., Jiang, H., Huang, Y., Rogers, J. A. **(2006)**. A stretchable form of single-crystal silicon for high-performance electronics on rubber substrates. Science, 311(5758), 208-212.

[89] Koenig, S. P., Boddeti, N. G., Dunn, M. L., Bunch, J. S. **(2011)**. Ultrastrong adhesion of graphene membranes. Nature nanotechnology, 6(9), 543.

[90] Kohn, R. V., Yan, X. **(2003)**. Upper bound on the coarsening rate for an epitaxial growth model. Communications on Pure and Applied Mathematics: A Journal Issued by the Courant Institute of Mathematical Sciences, 56(11), 1549-1564.

[91] Krug, J. **(2002)**. Four lectures on the physics of crystal growth. Physica A: Statistical Mechanics and its Applications, 313(1-2), 47-82.

[92] Krug, J. **(1997)**. On the shape of wedding cakes. Journal of statistical physics, 87(3-4), 505-518.

[93] Krug, J., Plischke, M., Siegert, M. **(1993)**. Surface diffusion currents and the universality classes of growth. Physical review letters, 70(21), 3271.

[94] Krug,J., Spohn,H., **(1991)**. Cambridge Univ. Press, 479 .

[95] Kusminskiy, S. V., Campbell, D. K., Neto, A. C., Guinea, F. **(2011)**. Pinning of a two-dimensional membrane on top of a patterned substrate: The case of graphene. Physical Review B, 83(16), 165405.

[96] Ladyzhenskaya, O. A., Ural'tseva, N. N. **(1969)**. Gloval estimates of the gradient of solutions of quasilinear elliptic and parabolic equations. Zapiski Nauchnykh Seminarov POMI, 14, 127-155.

[97] Ladyzhenskaya, O. A., Ural'tseva, N. N. **(1968)**. Certain classes of nonuniformly elliptic equations. In Seminars in Mathematics. Vol. 5, pp. 67-69.

[98] Lair A. V. and Shaker. A. W. **(1997)** Classical and weak solutions of a singular semilinear elliptic problem, Journal of Mathematical Analysis and Applications, vol.211, no. 2, pp. 371-385.

[99] Lankeit, J. **(2015)**. Eventual smoothness and asymptotics in a three-dimensional chemotaxis system with logistic source. Journal of Differential Equations, 258(4), 1158-1191.

[100] Lavrentiev.M, **(1926)**. Ann. Mat. Appli., 4, 7 .

[101] Lazer, A. C., McKenna, P. J. **(1991)**. On a singular nonlinear elliptic boundary-value problem. Proceedings of the American Mathematical Society, 111(3), 721-730.

[102] Lecaros, R., Rosier, L. **(2016)**. ESAIM-Control, Optimisation and Calculus of Variations.

[103] Lee, C., Wei, X., Kysar, J. W., Hone, J. **(2008)**. Measurement of the elastic properties and intrinsic strength of monolayer graphene. science, 321(5887), 385-388.

[104] Lefraich, H., Taourirte, L., Khalfi, H., Alaa, N. E. **(2019)**. On the existence of global weak solutions to a generalized Keller Segel model with arbitrary growth and nonlinear signal production. Annals of the University of Craiova-Mathematics and Computer Science Series, 46(1), 99-108.

[105] Levy, N., Burke, S. A., Meaker, K. L., Panlasigui, M., Zettl, A., Guinea, F., ... Crommie, M. F. **(2010)**. Strain-induced pseudo–magnetic fields greater than 300 tesla in graphene nanobubbles. Science, 329(5991), 544-547.

[106] Li, B. **(2006)**. High-order surface relaxation versus the Ehrlich–Schwoebel effect. Nonlinearity, 19(11), 2581.

[107] Lima, P. M., Morgado, L. **(2009)**. Analytical-numerical investigation of a singular boundary value problem for a generalized Emden–Fowler equation. Journal of computational and applied mathematics, 229(2), 480-487.

[108] Lima, P. M., Oliveira, A. M. **(2003)**. Numerical solution of a singular boundary value problem for a generalized Emden–Fowler equation. Applied numerical mathematics, 45(4), 389-409.

[109] Lions, P. L. **(1980)**. Résolution de problemes elliptiques quasilinéaires. Archive for Rational Mechanics and Analysis, 74(4), 335-353.

[110] Lobkovsky, A. E. **(1996)**. Boundary layer analysis of the ridge singularity in a thin plate. Physical Review E, 53(4), 3750.

[111] Lobkovsky, A., Gentges, S., Li, H., Morse, D., Witten, T. A. **(1995)**. Scaling properties of stretching ridges in a crumpled elastic sheet. Science, 270(5241), 1482-1485.

[112] Luo, J., Zhao, X., Wu, J., Jang, H. D., Kung, H. H., Huang, J. **(2012)**. Crumpled graphene-encapsulated Si nanoparticles for lithium ion battery anodes. The journal of physical chemistry letters, 3(13), 1824-1829.

[113] Manià, B. **(1934)**. Sopra un esempio di Lavrentieff. Zanichelli.

[114] Maz'ya, V. **(2003)**. Lectures on isoperimetric and isocapacitary inequalities in the theory of Sobolev spaces. Contemporary Mathematics, 338, 307-340.

[115] Meirmanov, A. M., Pukhnachov, V. M., Shmarev,**(1997)**. S. I. Evolution equations and Lagrangian coordinates.

[116] Miri, Sofiane. **(2014)**. Existence of solutions to quasilinear elliptic problems with nonlinearity and absorption-reaction gradient term. Electronic Journal of Differential Equations. 1-12.

[117] Mirjalili, S. M., Lewis, A. **(2014)**. Grey wolf optimizer. Advances in engineering software, 69, 46-61.

[118] Mirjalili, S. **(2015)**. How effective is the Grey Wolf optimizer in training multi-layer perceptrons. Applied Intelligence, 43(1), 150-161.

[119] Moldovan, D., Golubovic, L. **(2000)**. Interfacial coarsening dynamics in epitaxial growth with slope selection. Physical Review E, 61(6), 6190.

[120] Mullins, W. W. **(1957)**. Theory of thermal grooving. Journal of Applied Physics, 28(3), 333-339. (1957).

[121] Neek-Amal, M., Peeters, F. M. **(2012)**. Strain-engineered graphene through a nanostructured substrate. II. Pseudomagnetic fields. Physical Review B, 85(19), 195446.

[122] Neto, A. C., Guinea, F., Peres, N. M., Novoselov, K. S., Geim, A. K. **(2009)**. The electronic properties of graphene. Reviews of modern physics, 81(1), 109.

[123] Nicoli, M., Misbah, C., Politi, P. **(2013)**. Coarsening dynamics in one dimension: The phase diffusion equation and its numerical implementation. Physical Review E, 87(6), 063302.

[124] Nirenberg, L. **(1966)**. An extended interpolation inequality. Annali Della Scuola Normale Superiore di Pisa-Classe di Scienze, 20(4), 733-737.

[125] O. Bolza, **(1913)**. Math. Annal. 74, 430.

[126] Oliva, F., Petitta, F. **(2016)**. On singular elliptic equations with measure sources. ESAIM: Control, Optimisation and Calculus of Variations, 22(1), 289-308.

[127] Oliva, F., Petitta, F. **(2020)**. A nonlinear parabolic problem with singular terms and nonregular data. Nonlinear Analysis, 194, 111472.

[128] Oron, A., Davis, S. H., Bankoff, S. G. **(1997)**. Long-scale evolution of thin liquid films. Reviews of modern physics, 69(3), 931.

[129] Osaki, K., Tsujikawa, T., Yagi, A., Mimura, M. **(2002)**. Exponential attractor for a chemotaxis-growth system of equations. Nonlinear Analysis, 51(1), 119-144.

[130] Osborn, D., Madey, R. **(1968)**. The incomplete beta function and its ratio to the complete beta function. Mathematics of Computation, 22(101), 159-162.

[131] Osserman, R. **(2010)**. How the Gateway Arch got its shape. In Recalling Eero Saarinen 1910–2010. Birkhäuser, Basel. pp. 167-189

[132] Pauchard, L., Pomeau, Y., Rica, S. **(1997)**. Déformation des coques élastiques. Comptes Rendus de l'Académie des Sciences-Series IIB-Mechanics-Physics-Chemistry-Astronomy, 324(7), 411-418.

[133] Paulin, S., Gillet, F., Pierre-Louis, O., Misbah, C. **(2001)**. Unstable step meandering with elastic interactions. Physical Review Letters, 86(24), 5538.

[134] Pereira, V. M., Neto, A. C., Liang, H. Y., Mahadevan, L. **(2010)**. Geometry, mechanics, and electronics of singular structures and wrinkles in graphene. Physical review letters, 105(15), 156603.

[135] Pierre-Louis, O. **(2008)**. Adhesion of membranes and filaments on rippled surfaces. Physical Review E, 78(2), 021603.

[136] Pierre-Louis,O., Danker,D., Kassner,K., Misbah,C., **(2005)**. J. Cryst. Grow. 127, 56 .

[137] Pierre-Louis, O., Misbah, C., Saito, Y., Krug, J., Politi, P. **(1998)**. New nonlinear evolution equation for steps during molecular beam epitaxy on vicinal surfaces. Physical review letters, 80(19), 4221.

[138] Pimpinelli, A., Tonchev, V., Videcoq, A., Vladimirova, M. **(2002)**. Scaling and universality of self-organized patterns on unstable vicinal surfaces. Physical review letters, 88(20), 206103.

[139] Politi, P. **(2015)**. Coarsening dynamics at unstable crystal surfaces. Comptes Rendus Physique, 16(3), 280-290.

[140] Politi,P., Grenet,G., Marty,A., Ponchet, A., Villain,J., **(2000)**. Instabilities in crystal growth by atomic or molecular beams Phys. Repo. 324, 271.

[141] Politi, P., Misbah, C. **(2006)**. Nonlinear dynamics in one dimension: A criterion for coarsening and its temporal law. Physical Review E, 73(3), 036133.

[142] Politi, P., Misbah, C. **(2004)**. When does coarsening occur in the dynamics of one-dimensional fronts?. Physical review letters, 92(9), 090601.

[143] Politi, P., Torcini, A. **(2000)**. Coarsening in surface growth models without slope selection. Journal of Physics A: Mathematical and General, 33(8), L77.

[144] Politi, P., Torcini, A. **(2006)**. Asymptotic and effective coarsening exponents in surface growth models. The European Physical Journal B-Condensed Matter and Complex Systems, 53(3), 401-404.

[145] Politi, P., Villain, J. **(1996)**. Ehrlich-Schwoebel instability in molecular-beam epitaxy: A minimal model. Physical Review B, 54(7), 5114.

[146] Ponce, A. C. **(2012)**. Selected problems on elliptic equations involving measures. arXiv preprint arXiv:1204.0668.

[147] Porretta, A. **(2000)**. Existence for elliptic equations in L1 having lower order terms with natural growth. Portugaliae Mathematica, 57(2), 179-190.

[148] Pukhnachev, V. V., Kluwer Acad. Publ. Dordrecht, 75 **(1996)**.

[149] Pukhnachev, V. V. **(2003)**. Exact solutions of the hydrodynamic equations derived from partially invariant solutions. Journal of applied mechanics and technical physics, 44(3), 317-323.

[150] Rădulescu, V. D. **(2007)**. Singular phenomena in nonlinear elliptic problems: from blow-up boundary solutions to equations with singular nonlinearities. In Handbook of differential equations: Stationary partial differential equations (Vol. 4, pp. 485-593). North-Holland.

[151] Rodrigues.J. F., **(1987)**. Obstacle Problems in Mathematical Physics. North Holland Mathematics Studies, North-Holland.

[152] Rosen, G. **(1979)**. Nonlinear heat conduction in solid H 2. Physical Review B, 19(4), 2398.

[153] Rosenau, P. **(2007)**. Compactification of patterns by a singular convection or stress. Physical review letters, 99(23), 234102.

[154] Rost, M., Krug, J. **(1997)**. Coarsening of surface structures in unstable epitaxial growth. Physical Review E, 55(4), 3952.

[155] Rost, M., Šmilauer, P., Krug, J. **(1996)**. Unstable epitaxy on vicinal surfaces. Surface Science, 369(1-3), 393-402.

[156] Samrskii,A. A. , Galaktionov,V.A., Kurdyumov, S. P., Mikhailov,A.P. **(1995)**. Walter de Gruyter, Berlin, New York.

[157] Sato, M., Uwaha, M. **(1995)**. Step bunching as formation of soliton-like pulses in benney equation. EPL (Europhysics Letters), 32(8), 639.

[158] Schwerin, E. **(1929)**. ‹ ber Spannungen und Form‰ nderungen kreisringf^rmiger Membranen. ZaMM, 9(6), 482-483.

[159] Schwoebel, R. L., Shipsey, E. J. **(1966)**. Step motion on crystal surfaces. Journal of Applied Physics, 37(10), 3682-3686.

[160] Seifert, U., Lipowsky, R. **(1990)**. Adhesion of vesicles. Physical Review A, 42(8), 4768.

[161] Serrin, J. **(1969)**. The problem of Dirichlet for quasilinear elliptic differential equations with many independent variables. Philosophical Transactions of the Royal Society of London. Series A, Mathematical and Physical Sciences, 264(1153), 413-496.

[162] Serrin, J. **(1971)**. Gradient estimates for solutions of nonlinear elliptic and parabolic equations. In Contributions to nonlinear functional analysis. pp. 565-601. Academic Press.

[163] Shen, X., Lin, X., Yousefi, N., Jia, J., Kim, J. K. **(2014)**. Wrinkling in graphene sheets and graphene oxide papers. Carbon, 66, 84-92.

[164] Siegert, M., Plischke, M. **(1994)**. Slope selection and coarsening in molecular beam epitaxy. Physical review letters, 73(11), 1517.

[165] Simon, J. **(1986)**. Compact sets in the spacel p (o, t; b). Annali di Matematica pura ed applicata, 146(1), 65-96.

[166] Šmilauer, P., Rost, M., Krug, J. **(1999)**. Fast coarsening in unstable epitaxy with desorption. Physical Review E, 59(6), R6263.

[167] Sokolowski.J. **(1992)**. Shape Sensitivity Analysis of Variational Inequalities, M. C. Delfour and G. Sabidussi (eds.) Shape Optimization and Free Boundaries, 287-319.

[168] Stafford, C. M., Harrison, C., Beers, K. L., Karim, A., Amis, E. J., VanLandingham, M. R., ... Simonyi, E. E. **(2004)**. A buckling-based metrology for measuring the elastic moduli of polymeric thin films. Nature materials, 3(8), 545-550.

[169] Storm, M. L. **(1951)**. Heat conduction in simple metals. Journal of Applied Physics, 22(7), 940-951.

[170] Sun, Y., Choi, W. M., Jiang, H., Huang, Y. Y., Rogers, J. A. **(2006)**. Controlled buckling of semiconductor nanoribbons for stretchable electronics. Nature nanotechnology, 1(3), 201-207.

[171] Sychev, M. A. **(1994)**. Lebesgue measure of the universal singular set for the simplest problems in the calculus of variations. Siberian Mathematical Journal, 35(6), 1220-1233.

[172] Taliaferro,S.D. **(1979)**. Nonlin. Anal. The. Meth. Appl. 3(6), 897.

[173] Tao, Y., Winkler, M. **(2012)**. Boundedness in a quasilinear parabolic–parabolic Keller–Segel system with subcritical sensitivity. Journal of Differential Equations, 252(1), 692-715.

[174] Taourirte, L., Alaa, N. E., Khalfi, H. **(2019)**. Improved GWO algorithm for the determination of the critical wrinkle length of graphene. Annals of the University of Craiova-Mathematics and Computer Science Series, 46(1), 27-40.

[175] Tello, J. I., Winkler, M. **(2007)**. A chemotaxis system with logistic source. Communications in Partial Differential Equations, 32(6), 849-877.

[176] Tonelli, L. **(1923)**. Fondamenti di Calcolo delle Variazioni, Vols. I and II, Zanichelli. Bologna, Italy.

[177] Torcini, A., Politi, P. **(2002)**. Coarsening process in one-dimensional surface growth models. The European Physical Journal B-Condensed Matter and Complex Systems, 25(4), 519-529.

[178] Traub, J. F., Werschulz, A. G. **(1998)**. Complexity and information (Vol. 26862). Cambridge University Press.

[179] Vázquez, Juan Luis. **(1984)**. A strong maximum principle for some quasilinear elliptic equations. Applied Mathematics and Optimization 12.1:191-202.

[180] Villain, J. **(1991)**. Continuum models of crystal growth from atomic beams with and without desorption. Journal de physique I, 1(1), 19-42.

[181] Villain, J., Pimpinelli, A. **(1995)**. Physique de la croissance cristalline, ed. Eyrolles et commissariat à l'énergie atomique.

[182] Wallace, P. R. **(1947)**. The band theory of graphite. Physical review, 71(9), 622.

[183] Wang.F., Eichholz.J., Han,W. **(2018)**. A two level algorithm for an obstacle problem, Appl. Maths. Comp. 330, 65-76.

[184] Wang, L., Mu, C., Zheng, P. **(2014)**. On a quasilinear parabolic–elliptic chemotaxis system with logistic source. Journal of Differential Equations, 256(5), 1847-1872.

[185] Wang, Z. A., Winkler, M., Wrzosek, D. **(2012)**. Global regularity versus infinite-time singularity formation in a chemotaxis model with volume-filling effect and degenerate diffusion. SIAM Journal on mathematical analysis, 44(5), 3502-3525.

[186] Wang, Z. A., Xiang, T. **(2015)**. A class of chemotaxis systems with growth source and nonlinear secretion. arXiv preprint arXiv:1510.07204.

[187] Wen, Y., Zhu, Y., Langrock, A., Manivannan, A., Ehrman, S. H., Wang, C. **(2013)**. Graphene-bonded and-encapsulated Si nanoparticles for lithium ion battery anodes. Small, 9(16), 2810-2816.

[188] Winkler, M. **(2013)**. Finite-time blow-up in the higher-dimensional parabolic–parabolic Keller–Segel system. Journal de Mathématiques Pures et Appliquées, 100(5), 748-767.

[189] Winkler, M. **(2010)**. Aggregation vs. global diffusive behavior in the higher-dimensional Keller–Segel model. Journal of Differential Equations, 248(12), 2889-2905.

[190] Winkler, M. **(2010)**. Boundedness in the higher-dimensional parabolic-parabolic chemotaxis system with logistic source. Communications in Partial Differential Equations, 35(8), 1516-1537.

[191] Winkler, M., Djie, K. C. **(2010)**. Boundedness and finite-time collapse in a chemotaxis system with volume-filling effect. Nonlinear Analysis: Theory, Methods and Applications, 72(2), 1044-1064.

[192] Witten, T. A., Li, H. **(1993)**. Asymptotic shape of a fullerene ball. EPL (Europhysics Letters), 23(1), 51.

[193] Wolpert, D. H.,Macready, W. G. **(1997)**. No free lunch theorems for optimization. IEEE transactions on evolutionary computation, 1(1), 67-82.

[194] Xiang, T. **(2015)**. Boundedness and global existence in the higher-dimensional parabolic–parabolic chemotaxis system with/without growth source. Journal of Differential Equations, 258(12), 4275-4323.

[195] Xue, J., Sanchez-Yamagishi, J., Bulmash, D., Jacquod, P., Deshpande, A., Watanabe, K., ... LeRoy, B. J. **(2011)**. Scanning tunnelling microscopy and spectroscopy of ultra-flat graphene on hexagonal boron nitride. Nature materials, 10(4), 282-285.

[196] Xue.L and X.-L. Cheng. **(2004)**. An algorithm for solving the obstacle problems, Computers Math. Applic. 48, , 1651-1657.

[197] Yamamoto, M. **(2013)**. Two-dimensional crystals on substrates: Morphology and chemical reactivity (Doctoral dissertation).

[198] Yamamoto, M., Pierre-Louis, O., Huang, J., Fuhrer, M. S., Einstein, T. L., Cullen, W. G. **(2012)**. "The princess and the pea" at the nanoscale: wrinkling and delamination of graphene on nanoparticles. Physical Review X, 2(4), 041018.

[199] Zhang, D. B., Seifert, G., Chang, K. **(2014)**. Strain-induced pseudomagnetic fields in twisted graphene nanoribbons. Physical review letters, 112(9), 096805.

[200] Zhang, S., Constantinides, A. G. **(1992)**. Lagrange programming neural networks. IEEE Transactions on Circuits and Systems II: Analog and Digital Signal Processing, 39(7), 441-452.

[201] Zhang, Y. C. **(1992)**. Singular dynamic interface equation from complex directed polymers. Journal de Physique I, 2(12), 2175-2180.

[202] Zhang, Z., Guo, Y., Feng, H. **(2009)**. Boundary behaviour of the unique solution to a singular Dirichlet problem with a convection term. Journal of mathematical analysis and applications, 352(1), 77-84.

[203] Zhang, Z., Yu, J. **(2000)**. On a singular nonlinear Dirichlet problem with a convection term. SIAM Journal on Mathematical Analysis, 32(4), 916-927.

[204] Zhao, X., Liu, B., Duan, N. **(2013)**. Time-periodic solution for a fourth-order parabolic equation describing crystal surface growth. Electronic Journal of Qualitative Theory of Differential Equations, 2013(7), 1-15.

[205] Zhao, X., Liu, F., Liu, B. **(2014)**. Finite element method for a nonlinear differential equation describing crystal surface growth. Mathematical Modelling and Analysis, 19(2), 155-168.

[206] Zhao, X., Liu, F., Liu, B. **(2015)**. Finite difference discretization of a fourth-order parabolic equation describing crystal surface growth. Applicable Analysis, 94(9), 1964-1975.

[207] Zheng, J. **(2015)**. Boundedness of solutions to a quasilinear parabolic–elliptic Keller–Segel system with logistic source. Journal of Differential Equations, 259(1), 120-140.

[208] Zhou, Y. et al. **(2014)**. Carbon 84, 263 .

[209] Zhu, J., Duan, R., Zhang, S., Jiang, N., Zhang, Y., Zhu, J. **(2014)**. The application of graphene in lithium ion battery electrode materials. SpringerPlus, 3(1), 585.

[210] Zhu, S., Galginaitis, J.,Li, T. **(2012)**. Critical dispersion distance of silicon nanoparticles intercalated between graphene layers. Journal of Nanomaterials.

[211] Zhu, S., Li, T. **(2014)**. Wrinkling instability of graphene on substrate-supported nanoparticles. Journal of Applied Mechanics, 81(6).

Chapter 8

Conclusion and Perspectives

Using the Grey Wolf Optimizer algorithm, we were able to obtain good results in comparison with the results found in the literature, which insures the efficiency of the algorithm for our problem. However, the obtained critical wrinkle length is still not satisfying enough, and based on the analytical analysis in the second chapter, we ensure that unlike what the physicians may think, the difference in the nanoparticle's sizes is not the only reason behind the discrepancy between the experimental and theoretical results, and other physical mechanisms such as the thermal fluctuations and the impurites that might exist on the substrate surface, can have an effect on the observed results. We have also presented a detailed analysis of similarity solutions to the one-dimensional singular interfacial equation. This equation was used, for large slope, to describe the mound-type structures on the growing surfaces, where the destabilizing current is of the form suggested by Villain. A central result of the similarity assumption is that the singular interfacial equation is reduced to a singular ordinary differential equation satisfied by the shape or the similarity profile f. Although the mathematical and numerical results proved the local existence of the profile which is singular at some point, our first approach could not be directly used to understand the coarsening phenomenon. An additional analysis, based on periodic steady states, showed that the singularity is incomplete; The steady state solutions of the generalized phenomenological equation have been analytically analyzed. It is found that the equation has periodic and not periodic solutions as well. Besides all these results, we gathered in this thesis various mathematical techniques that are used for proving the existence and uniqueness of solutions for the proposed various quasilinear elliptic equations with singular nonlinearities. For the perspectives, we are now working on creating a new mathematical model that takes into account the different physical mechanisms that affect the energy, as well as the energies at the point of equilibrium which were neglected as mentioned in the first chapter. Another

important task for the future is to study the model in which the graphene layer is put between a group of silica nanoparticles instead of two.

We also started to investigate the energy functional with the exact expression of the stretching strain ε_x given by:

$$\varepsilon_x = \sqrt{1+(\zeta_x)^2} - 1,$$

instead of its approximation near the center given by $\varepsilon_x \approx \frac{|\zeta_x|^2}{2}$.

Another perspective is the study of the global existence in $L^1(\Omega)$ instead of $L^2(\Omega)$, of weak global solutions to a class of parabolic-elliptic chemotaxis systems.

Furthermore, we aim to study the parabolic equation

$$(P_\lambda)\begin{cases} \dfrac{\partial u}{\partial t} - \triangle_p u = \dfrac{a(t,x)}{u^\gamma} + b(t,x)|\nabla u|^p \ \ in \ \ (0,T)\times\Omega \\ u(0,x) = \lambda f \quad in \ \ \Omega \\ u = 0 \qquad\qquad on \ \ (0,T)\times\partial\Omega \end{cases} \tag{8.1}$$

Last but not least, we are very concerned with the finite elements approximation and the resolution by penalization-duality, of the nonlinear Dirichlet problem

$$\begin{cases} -div\left(|\nabla u|^{p-2}\nabla u\right) = u^{-\gamma} + f \ \ in \ \ \Omega \\ u = 0 \qquad\qquad\qquad\qquad on \ \ \partial\Omega \end{cases} \tag{8.2}$$

List of Papers and Communications

Papers

- Bognár, G., Guedda, M., Hriczó, K. and Taourirte, L. **(2020)**. Instabilities in certain one-dimensional singular interfacial equation. Physica Scripta, 95(3), 035001.
- Taourirte, L., Alaa, N. E., Khalfi, H. **(2019)**. Improved GWO algorithm for the determination of the critical wrinkle length of graphene. Annals of the University of Craiova-Mathematics and Computer Science Series, 46(1), 27-40.
- Lefraich, H.,Taourirte, L., Khalfi, H., Alaa, N. E. **(2019)**. On the existence of global weak solutions to a generalized Keller Segel model with arbitrary growth and nonlinear signal production. Annals of the University of Craiova-Mathematics and Computer Science Series, 46(1), 99-108.
- Taourirte, L., Aqel.F. and Alaa.N. E. **(2020)**. On singular quasilinear elliptic equations with data measures. Accepted in the journal Advances in Nonlinear Analysis.
- Taourirte, L., Guedda.M and Alaa.N. E. **(2020)**. Analytical results for the wrinkling of graphene on nanoparticles of different diameters. Submitted to the journal Surface Science.
- Taourirte, L., Alaa N. E. and Guedda M. **(2020)**.An obstacle problem for a graphene wrinkle model-type, submitted to the journal Mathematical Modeling and Computing.
- Taourirte, L., Bognar.G, Hriczo.K, Alaa.N and Guedda.M, Scaling properties for one-dimensional singular interfacial equations, in preparation (Second section of Chapter 4 of the thesis).

Oral Communications

- Taourirte, L., Alaa. N. E., Guedda.M and Khalfi.H.: «Wrinkle Shape Analysis of the Graphene on Nano-particles». international congress "Modélisation et Calcul Scientifique pour l'Ingénierie Mathématique" (MOCASIM), in the Faculty of Sciences and Techniques of Marrakech from 17 to 20 April 2017.

- Taourirte, L., Alaa. N. E. and Guedda.M. : «Mathematical and numerical study of the effect of the nanoparticles diameters on the graphene wrinkling ». Seminary in the Laboratory LAMFA of Pi cardie Jules Verne University Amiens, France, 13 November 2017.

- Taourirte, L., Alaa, N. E. and Guedda.M. : «The Mathematical and Numerical Analysis of the effect of the nanoparticles diameters on the grapheme wrinkling ». Second International Workshop on Complex Systems and applications », in the Superior school of Technology, Essaouira, from 12 to 13 December 2017.

- Taourirte, L., Alaa.N. E. and Pierre.M. «Mathematical Analysis of a quasilinear elliptic equation with singular nonlinearity». international congress "Modélisation et Calcul Scientifique pour l'Ingénierie Mathématique" (MOCASIM), in the Faculty of Sciences and Techniques of Marrakesh from 26 to 27 November 2018.

- Taourirte, L. and Alaa.N. E: «Characterization of the Critical Diameter for the Graphene Wrinkle Model ». International Workshop : Modélisation et Calcul numérique pour la Biomathématique, in the Superior school of Technology, Essaouira, from 08 to 10 July 2019.

- Taourirte, L. and Alaa.N. E: «Weak Solutions of some Quasilinear Singular Elliptic Equations with Data Measures». Journées Scientifiques in Mohamed V University, Rabat, from 24 to 25 December 2019.

Abstract

In this thesis, we analytically and numerically examine a class of partial differential equations that appear in different physical contexts: 1) wrinkling of graphene, 2) coarsening of growing interfaces, and 3) chemotaxis phenomenon.

In part 1), we firstly investigate the critical wrinkle length (or the critical distance between two nanoparticles), and the electronic property of the wrinkling of graphene. We also propose an algorithm for determining the critical length, introduce an obstacle problem, derive an example for the so-called Lavrentiev GAP phenomena, and study some quasilinear problems with gradient and singular terms. In part 2), we analyze two phenomenological equations for the height of the surface above a plane substrate. This study deals with properties of similarity solutions and with the coarsening process by inspecting the behavior of a branch of the steady state periodic solutions.

Finally, in part 3), we investigate the existence result of weak time-global solutions for Keller-Segel type models.

Keywords: wrinkling, graphene, silicium, nanoparticles, critical, obstacle problem, Lavrentiev, quasilinear, singular, similarity, scaling, coarsening, Keller-Segel.

Résumé

Le but de cette thèse est d'examiner analytiquement et numériquement une classe d'équations aux dérivées partielles qui apparaissent dans différents problèmes physiques: 1) froissement du graphène, 2) instabilité ou croissance de surfaces et 3) phénomène de chemotaxis.

Au point 1), l'étude porte d'abord sur la longueur critique des rides (ou distance critique entre deux nanoparticules), et sur certaines propriétés électroniques dues au froissement du graphène. Nous avons également proposé un algorithme pour déterminer le longueur critique, étudié un problème d'obstacle, dérivé un exemple pour le phénomène de GAP de Lavrentiev, et analysé certains problèmes quasilinéaires contenant gradient et des termes singuliers. Au point 2), nous analysons deux équations phénoménologiques pour la morphologie d'une surface. Les solutions autosimilaires et des résultats sur le processus de murissement (coarsening) sont concernés par cette étude. Enfin, au point 3), nous étudions l'existence de solutions faibles globales en temps pour les modèles de type Keller-Segel.

Mots clé: froissement, graphène, silicium, nano-particules, critique, problème d'obstacle, Lavrentiev, quasilinéaire, singulière, auto-similaire, scaling, mûrissement, solution stationnaire, Keller-Segel.